UNIVERSIDADE ESTADUAL DE CAMPINAS

FACULDADE DE ENGENHARIA DE ALIMENTOS

DEPARTAMENTO DE ENGENHARIA DE ALIMENTOS

EMPREGO DE MÉTODOS DE CONTRIBUIÇÃO DE GRUPOS NO CÁLCULO E PREDIÇÃO DE PROPRIEDADES FÍSICO-QUÍMICAS

Luciana Ninni
Engenheira de Alimentos
Mestre em Engenharia de Alimentos

Prof. Dr. Antonio José de Almeida Meirelles
Orientador

Tese apresentada à Faculdade de Engenharia de Alimentos da Universidade Estadual de Campinas para a obtenção do título de doutor em Engenharia de Alimentos.

Campinas/SP
Novembro de 2003

BANCA EXAMINADORA

Prof: Dr. Antonio José de Almeida Meirelles (FEA/UNICAMP)

Prof^{a}. Dr^{a}. Maria Alvina Krähenbühl (FEQ/UNICAMP)

Prof. Dr. Pedro de Alcântara Pessôa Filho (POLI/USP)

Prof. Dr. Martín Aznar (FEQ/UNICAMP)

Prof. Dr. Fernando Antonio Cabral (FEA/UNICAMP)

Prof. Dr. Eduardo Augusto Caldas Batista (DZT/UEPG)

Prof^{a}. Dr^{a}. Maria Ângela de Almeida Meireles (FEA/UNICAMP)

Aos meus dois amores,
Dirk e nosso filho.

AGRADECIMENTOS

Ao Prof. Dr. Antonio José de Almeida Meirelles, pela orientação, incentivo e presença sempre.

Ao Prof. Dr. Gerd Maurer pela orientação em parte deste trabalho e auxílio para a realização do mesmo.

Ao CNPq pela bolsa de estudos e pelo financiamento da pesquisa no Brasil e ao convênio CNPq/DAAD pelo financiamento da bolsa de estudos na Alemanha.

Aos membros da banca examinadora pelas observações e sugestões feitas para a melhor elaboração da versão final deste trabalho.

Aos meus pais e minhas irmãs que sempre me incentivam e apóiam.

Às minhas amigas Cíntia, Sueli, Christiane, Cristina e Roberta pelos bons momentos que passamos juntas.

À Melissa, Wong e Helcio pela ajuda nos trabalhos experimentais.

À minha vó que me faz rir e que tanto amo.

À Silke Lammertz e Viktor Ermatchkov pela ajuda inicial nos laboratórios na Universidade Kaiserslautern.

Aos meus amigos Raquel, Vanderlei e Hicham, que estão na Alemanha, pelas conversas alegres e apoio quando precisei.

ÍNDICE GERAL

CAPÍTULO 1

CAPÍTULO 2

CAPÍTULO 3

CAPÍTULO 4

CAPÍTULO 5

CAPÍTULO 6

ANEXOS

Índice de Tabelas

CAPÍTULO 2

CAPÍTULO 3

CAPÍTULO 4

CAPÍTULO 5

CAPÍTULO 6

ANEXO 1

Índice de Figuras

CAPÍTULO 1

CAPÍTULO 2

CAPÍTULO 3

CAPÍTULO 4

CAPÍTULO 5

CAPÍTULO 6

ANEXO 1

RESUMO

Métodos de contribuição de grupos têm sido ferramenta útil no cálculo de coeficientes de atividade nos mais variados sistemas. Em sistemas aquosos, e mais especificamente naqueles que possuem compostos biológicos como açúcares, aminoácidos, sais orgânicos, polímeros, etc., o uso de métodos de contribuição de grupos para a correlação e predição do equilíbrio de fases tem crescido nos últimos anos. Em alimentos e em biotecnologia, os sistemas são geralmente multicomponentes e por essa razão, a aplicação de métodos de contribuição de grupos torna-se atraente partindo-se do princípio que, de posse dos parâmetros de interação entre grupos, é possível calcular propriedades de sistemas mais complexos a partir de parâmetros obtidos da correlação a dados experimentais de sistemas mais simples. Neste trabalho, os métodos de contribuição de grupos ASOG, UNIFAC, VERS e UNIMOD foram empregados em diferentes sistemas para a correlação e predição de propriedades físico-químicas. Os compostos estudados foram: polióis, aminoácidos, maltodextrinas e polietileno glicóis (PEG)s, sendo os três primeiros compostos geralmente encontrados em sistemas alimentícios, e o PEG é bastante utilizado em sistemas aquosos bifásicos para o estudo do equilíbrio e separação de biomoléculas. Propriedades físico-químicas como atividade de água, solubilidade, depressão do ponto de congelamento, pH, espalhamento de luz, entalpia de diluição e viscosidade, são algumas das propriedades determinadas e/ou retiradas da literatura usadas para a correlação e predição empregando os modelos acima citados. A intenção deste trabalho foi então, testar os métodos de contribuição de grupos para o cálculo de propriedades físico-químicas tratando também das particularidades de cada sistema estudado, como a dissociação parcial dos aminoácidos, o efeito de proximidade dos grupamentos hidroxilas nos polióis e a polidispersão das maltodextrinas. Também são apresentados resultados da correlação e predição de viscosidades de sistemas aquosos contendo PEGs por um modelo semi-empírico que não trata da contribuição de grupos mas considera a hidratação das moléculas desses polímeros em meio aquoso.

ABSTRACT

Group contribution methods have been used as a useful tool for calculating activity coefficients in different types of systems. In aqueous systems, specifically those containing biological compounds such as sugars, amino acids, organic salts, polymers, etc., the use of group contribution models for correlating and predicting phase equilibrium has increased in the last years. In the food and in the biotechnology areas, the systems are generally multicomponent, and for this reason, the use of group-contribution methods becomes an attractive tool considering the possibility of calculation of properties in complex systems with parameters adjusted for simple ones. In this work, the group-contribution models ASOG, UNIFAC, VERS and UNIMOD were utilized in different types of systems for the correlation and prediction of physical chemical properties. The studied compounds were: polyols, amino acids, maltodextrins and polyethylene (glycols) (PEG)s, which the first three compounds are found in food systems, and PEGs are wide used in aqueous-two-phase systems to study equilibrium and separation of biomolecules. Physical-chemical properties such as water activity, solubility, freezing point depression, pH, light scattering, enthalpy of dilution and viscosity are some of the properties experimentally determined and/or found in literature used in this work for the correlation and prediction using the above cited models. Thus, the objective of this work was to test the group-contribution models for calculating physical-chemical properties considering the particularities of each system such as partial dissociation phenomena in aqueous amino acid systems, proximity effect of hydroxyl groups in polyols, and polydispersity of maltodextrins. It is also presented in this work, the results of viscosity correlation and prediction in aqueous PEG solutions by a semi-empirical equation that does not consider group contributions but take into account the hydration of the polymer molecules in aqueous media.

Capítulo 1

REVISÃO BIBLIOGRÁFICA

Introdução

Métodos de contribuição de grupos são ferramentas úteis na modelagem e predição do equilíbrio de fases em variados sistemas. Por essa razão, têm sido empregados em simulação de processos industriais como a destilação e na modelagem de propriedades termodinâmicas de sistemas mais complexos contendo compostos orgânicos. Dentre os modelos de contribuição de grupos descritos na literatura, pode-se citar os modelos UNIFAC, ASOG e VERS que são baseados em expressões para a energia livre de Gibbs. Esses modelos possuem vantagens, como por exemplo, a de necessitar apenas de um pequeno número de parâmetros ajustáveis a serem conhecidos, além de parâmetros estruturais que podem ser prontamente calculados ou retirados de tabelas na literatura. Dessa forma, se existem parâmetros disponíveis para os grupos presentes em uma mistura, é possível realizar a predição dos coeficientes de atividade dos compostos nessa mistura ou de sistemas mais complexos. Métodos de contribuição de grupos vêm sendo bastante empregados para descrever as propriedades termodinâmicas de misturas de compostos de interesse da indústria alimentícia, farmacêutica e de processos biotecnológicos, como por exemplo: açúcares, sais orgânicos, polímeros e aminoácidos.

Apesar de serem encontrados na literatura valores de parâmetros desses modelos para vários grupos que formam as moléculas de compostos orgânicos e inorgânicos, o emprego desses parâmetros em sistemas contendo compostos biológicos muitas vezes não gera bons resultados por causa da complexidade dos sistemas envolvidos, da presença de compostos muito diferentes nas misturas, e também das particularidades dos compostos biológicos, como hidratação, dissociações, efeitos de proximidade de grupos polares, diferenças de tamanhos de moléculas entre compostos homólogos, etc. Por isso, um ajuste dos parâmetros dos modelos torna-se muitas vezes necessário para uma melhor descrição das propriedades físico-químicas de tais sistemas. A proposta deste trabalho foi justamente aplicar métodos de contribuição de grupos para descrever propriedades de sistemas aquosos contendo compostos presentes em alimentos (polióis, aminoácidos e maltodextrinas), bem como polímeros empregados em separação de compostos biológicos através de sistemas aquosos bifásicos (polietileno glicóis e maltodextrinas). A seguir, são apresentados os resumos dos capítulos deste trabalho que se referem a trabalhos publicados e a serem submetidos a revistas científicas da área. Também segue o resumo de um anexo com alguns resultados que não foram publicados mas que são também parte deste trabalho.

1. Capítulo 1. Revisão Bibliográfica, apresentando os fundamentos termodinâmicos do equilíbrio de fases e de outras propriedades físico-químicas, e os modelos de coeficiente de atividade e de outras propriedades de interesse neste trabalho.

2. Capítulo 2. Determinação experimental e modelagem da atividade de água em sistemas contendo quatro diferentes polióis. O trabalho apresenta resultados de correlações empregando os modelos ASOG e UNIFAC, sendo que para o modelo UNIFAC foram testadas duas diferentes formas de divisão de grupos para as moléculas envolvidas. A justificativa de reajuste de parâmetros é que a presença de grupos polares muito próximos (grupos hidroxilas consecutivos ligados à cadeia de carbonos da molécula) podem provocar um efeito de proximidade intramolecular. Na correlação, dados de solubilidade dos poliálcoois foram também utilizados. As atividades de água de misturas ternárias foram empregadas em teste para avaliar a capacidade preditiva dos modelos com os novos parâmetros ajustados.

3. Capítulo 3. Algumas propriedades de soluções aquosas contendo aminoácidos como atividade de água, pH e densidade foram determinadas em três diferentes tipos de solventes. O modelo UNIFAC-Lyngby de contribuição de grupos combinado com a equação de Debye-Hückel foram empregados na correlação e modelagem das propriedades determinadas neste trabalho, assim como outros dados de equilíbrio apresentados na literatura. A dissociação parcial desses compostos em água e em dois tampões foi considerada nas correlações.

4. Capítulo 4. Correlação e predição, pelo modelo GC-UNIMOD, de viscosidades cinemáticas de misturas contendo polietileno glicóis, determinadas neste trabalho como função da temperatura. As viscosidades de misturas binárias foram também empregadas no cálculo da energia de ativação para o escoamento viscoso.

5. Capítulo 5. Determinação de viscosidades cinemáticas de misturas aquosas contendo polietileno glicóis numa ampla faixa de massas molares, temperatura e concentração. Na correlação, ao contrário dos outros capítulos, não foi empregado um modelo de contribuição de grupos, mas sim uma correlação semi-empírica que descreveu bem as viscosidades considerando o grau de hidratação das diferentes moléculas estudadas

(correlação de Kumar). A predição das viscosidades de misturas com até cinco componentes foi satisfatória.

6. Capítulo 6. Determinação de atividade de água, espalhamento de luz e entalpia de diluição em sistemas contendo três diferentes maltodextrinas e correlação dos dados por equação osmótica virial e o modelo VERS (Virial Equation with Relative Surface Fractions). Os parâmetros do modelo VERS foram também empregados na predição da atividade de água, depressão do ponto de congelamento e de ebulição em sistemas contendo sacarídeos como glicose, maltose, maltotriose, etc.

7. Anexo 1. Resultados da correlação e predição das viscosidades cinemáticas de misturas aquosas, contendo polietileno glicóis, pelo modelo GC-UNIMOD. Apesar das diversas tentativas para melhorar os resultados de correlação e predição, o resultado geral foi insatisfatório. Por esse motivo, optou-se por outra abordagem, apresentada no Capítulo 5, que gerou resultados consideravelmente melhores.

Objetivos

Este trabalho tem por objetivos determinar, modelar e predizer propriedades físico-químicas como atividade de água (a_w), pH, solubilidade, depressão do ponto de congelamento, entalpia de diluição, elevação do ponto de ebulição e viscosidade de soluções contendo componentes presentes em alimentos e empregados em processos biotecnológicos. Foi estudado o comportamento de sistemas contendo polióis, aminoácidos e polímeros naturais em misturas com dois ou mais componentes. Esses compostos possuem diversas aplicações industriais, incluindo usos como modificadores de textura, umectantes, plasticizantes e outros, além de suas propriedades em solução serem importantes no projeto de equipamentos e processos. Apesar de importantes, poucos dados físicos e termodinâmicos para esses compostos estão disponíveis na literatura. Com base em um banco de dados que incluiu os dados experimentais determinados neste trabalho e obtidos na literatura, os métodos de contribuição de grupos UNIFAC, ASOG e o modelo VERS foram utilizados na modelagem de propriedades termodinâmicas através do ajuste de parâmetros dos modelos – quando necessário – e tratamento matemático adequado para cada conjunto de dados.

1. Revisão Bibliográfica

1.1 Fundamentos e modelos termodinâmicos

Neste capítulo serão comentados os fundamentos termodinâmicos e modelos que neles se baseiam para melhor compreensão da modelagem, assim como do cálculo do equilíbrio de fases dos sistemas aquosos estudados. Como foram estudados diferentes compostos – poliálcoois, aminoácidos e polímeros – os procedimentos no tratamento e cálculo das propriedades serão apresentados em detalhe para cada sistema nos itens abaixo, e nos capítulos correspondentes a cada composto.

1.1.1 Bases Termodinâmicas

Os modelos baseados na energia livre de Gibbs de excesso são normalmente empregados para a descrição do equilíbrio de fases.

A energia livre de Gibbs G depende das variáveis temperatura, pressão e número de mol dos componentes que formam a mistura.

$$G = G(T, P, n_1, n_{2,} ... n_N) \tag{1.1}$$

Na forma diferencial a equação fundamental de Gibbs é dada por:

$$dG = -SdT + VdP + \sum_{i=1}^{N} \mu_i dn_i \tag{1.2}$$

em que S é a entropia, uma quantidade de estado extensiva do sistema:

$$-S = \left(\frac{\partial G}{\partial T} \right)_{P,n_j} \tag{1.3}$$

e o volume, também uma quantidade extensiva é dado por:

$$V = \left(\frac{\partial G}{\partial p} \right)_{T,n_j} \tag{1.4}$$

e o potencial químico μ_i é a energia livre de Gibbs parcial molar do componente i:

$$\mu_i = \left(\frac{\partial G}{\partial n_i}\right)_{T,P,n_{j\neq i}} \tag{1.5}$$

Já que a função G é homogênea de primeira ordem em massa ou número de mol, pode-se aplicar o teorema de Euler para obter a seguinte função:

$$\sum_{i=1}^{N} n_i \left(\frac{\partial G}{\partial n_i}\right)_{T,P,n_{j\neq i}} = \sum_{i=1}^{N} n_i \mu_i = G \tag{1.6}$$

e,

$$dG = \sum_{i=1}^{N} \mu_i dn_i + \sum_{i=1}^{N} n_i d\mu_i \tag{1.7}$$

Das equações 1.2 e 1.7 obtém-se a equação de Gibbs-Duhem, uma relação fundamental da termodinâmica:

$$SdT - VdP + \sum_{i=1}^{N} n_i d\mu_i = 0 \tag{1.8}$$

e considerando um sistema a temperatura e pressão constantes, a equação 1.8 resume-se a:

$$\sum_{i=1}^{N} n_i d\mu_i = 0 \tag{1.9}$$

Existe equilíbrio termodinâmico de fases em um sistema – que não possui interações com a vizinhança – quando não se observa macroscopicamente mudanças nas suas variáveis num determinado período e a inexistência de fluxos líquidos. A condição para o equilíbrio de fases de um sistema à temperatura e pressão constantes pode ser escrita com o auxílio da segunda lei da termodinâmica como:

$$T,P = \text{constante} \qquad \Rightarrow \qquad G = \text{mínima} \tag{1.10}$$

Partindo-se da condição de equilíbrio de fases apresentada na equação 1.10 acima, tem-se que:

$$dG = 0 \qquad \text{e} \qquad d^2G > 0 \tag{1.11, 1.12}$$

que permite concluir que o equilíbrio corresponde a:

$$\begin{aligned} &T' = T'' = T''' = \ldots = T^{\pi} \\ &P' = P'' = P''' = \ldots = P^{\pi} \\ &\mu_i' = \mu_i'' = \mu_i''' = \ldots = \mu_i^{\pi} \end{aligned} \tag{1.13}$$

em que o sobrescrito refere-se a fase e o subescrito ao componente do sistema.

1.1.2 Modelos para energia livre de Gibbs

Como foi apresentado na equação 1.2, a energia de Gibbs é função do potencial químico. Numa solução ideal, o potencial químico do componente *i* é dado por:

$$\mu_i^{\text{id}} = \mu_i^{\text{o}} + RT \ln x_i \tag{1.14}$$

onde μ_i^{o} é o potencial químico do componente *i* puro, à mesma temperatura e pressão da solução e x_i é a fração molar do componente *i*.

Já o potencial químico de um componente *i* numa solução real é calculado como a soma de duas contribuições, uma ideal e outra de excesso, como a seguir:

$$\mu_i = \underbrace{\mu_i^{\text{o}} + RT \ln x_i}_{\mu_i^{\text{id}}} + \underbrace{RT \ln \gamma_i}_{\mu_i^{\text{E}}} \tag{1.15}$$

em que γ_i é o coeficiente de atividade do componente *i* e $\mu_i^{\text{E}} = \left(\partial G^{\text{E}} / \partial n_i\right)_{P,T,n_j}$ o termo de excesso.

O termo de excesso – que inclui os coeficientes de atividade – descreve o comportamento real do componente. Dessa forma, os coeficientes de atividade possuem um significado decisivo na modelagem do equilíbrio de fases. Neste trabalho serão investigados alguns modelos que relacionam a energia livre em excesso para o cálculo de propriedades físico-químicas em sistemas aquosos contendo diferentes componentes. Por isso será apresentado a seguir, um resumo sobre os modelos para o cálculo de coeficientes de atividade.

Os modelos de energia livre de Gibbs em excesso podem ser divididos entre empíricos e teóricos, de acordo com suas abordagens fundamentais.

1. Abordagem empírica

Com relação à abordagem empírica poder-se-ia citar uma série de trabalhos que se utilizaram de ajuste polinomial aos dados experimentais para obter uma equação simples que estime os coeficientes de atividade. Um exemplo desse tipo de ajuste é a abordagem de Porter (1920) que leva ao cálculo de coeficientes de atividade de compostos bem semelhantes numa mistura. Extensões desse tipo de abordagem são as equações de Margules (Prausnitz, 1969) e de Redlich e Kister (Redlich and Kister, 1948).

2. Abordagem teórica

Aqui pode-se citar três diferentes grupos de modelos: um que emprega a teoria da solução regular; outro a teoria da solução atérmica e um terceiro grupo que se utiliza das duas teorias anteriores como base para compor os modelos.

(a) Teoria da solução regular

A energia livre de Gibbs pode também ser escrita – com base nas tranformadas de Legendre – da seguinte forma:

$$G^E = H^E - TS^E = U^E + PV^E - TS^E \tag{1.16}$$

De acordo com a experiência, o volume e a entropia de excesso podem ser considerados desprezíveis em misturas apolares constituídas por compostos semelhantes. Essas são considerações da teoria da solução regular.

$$\underbrace{\begin{array}{l} V^E = 0 \\ S^E = 0 \end{array}}_{\Downarrow} \\ G^E = U^E \tag{1.17}$$

A teoria de soluções regulares chamada também teoria de Scatchard-Hildebrand (Prausnitz, 1986) fornece coeficientes de atividade maiores ou iguais a 1, isto é, uma solução regular pode exibir apenas desvio positivo da idealidade segundo a Lei de Raoult. Nessa abordagem considera-se que a interação entre duas moléculas em solução depende apenas da distância entre essas moléculas sendo aleatória a distribuição das moléculas em posição e orientação.

(b) Teoria da solução atérmica

Ao contrário da teoria de soluções regulares, a teoria da solução atérmica não considera interações entre moléculas ou espécies químicas em soluções e sim efeitos de configuração. É denominada atérmica, pois o excesso de entalpia é desprezado, e dessa forma, os coeficientes de atividade são independentes da temperatura.

$$H^E = 0 \;\Rightarrow\; G^E = -TS^E \tag{1.18}$$

$$\left(\frac{\partial G^E / RT}{\partial T}\right)_{p,n_j} = -\frac{H^E}{RT^2} \tag{1.19}$$

$$H^E = 0 \Rightarrow \frac{G^E}{RT} = \sum_{i=1}^{N} n_i \ln \gamma_i \neq f(T) \tag{1.20}$$

A entropia de excesso pode ser calculada com o auxílio de modelos que consideram as diferenças de tamanho entre as moléculas num sistema. Um exemplo desse tipo de abordagem é o modelo de Flory-Huggins (Flory, 1941) que prediz desvios negativos da idealidade segundo a lei de Raoult.

(c) Abordagem combinada

Essa abordagem utiliza-se das teorias das soluções regulares e atérmicas, considerando então efeitos de interação e configuração nos modelos para o cálculo dos coeficientes de atividade. Um exemplo típico desse grupo é o modelo UNIQUAC (Universal Quasi-Chemical Equation) proposto por Abrams and Prausnitz (1975). Alguns desses modelos foram estendidos para compor os chamados modelos de contribuição de grupos. Tais modelos consideram que o comportamento dos compostos em solução é o resultado das interações e das diferenças de tamanho e forma dos grupos funcionais dessas substâncias. Os modelos desse tipo mais conhecidos são o ASOG (Analytical Solution Of Groups) de Kojima and Tochigi (1979) e o modelo UNIFAC (UNIQUAC Functional-Group Activity Coefficient) de Fredenslund and Jones (1975). Pode-se citar também nesse grupo o modelo VERS (Virial

Equation with Relative Surface Fractions) desenvolvido por Großmann (1994) e baseado no desenvolvimento virial da equação de Pitzer (Pitzer, 1991) para soluções de eletrólitos. A seguir, estão apresentadas as equações dos modelos de contribuição de grupos empregados neste trabalho: UNIFAC, ASOG, VERS e GC-UNIMOD (esse último baseado no modelo de contribuição de grupos UNIFAC, utilizado para o cálculo de viscosidades de misturas e desenvolvido por Cao *et al.*, 1993).

1.2 Métodos de contribuição de grupos

1.2.1 Para cálculo de coeficientes de atividade

O cálculo de coeficientes de atividade por contribuição de grupos foi primeiramente sugerido em 1925 por Langmuir (Prausnitz, 1986) mas o emprego de tais métodos expandiu-se com o aumento do número de dados experimentais e o surgimento de modelos como o ASOG (Analytical Solutions of Groups) e o UNIFAC (Universal Functional Activity Coefficient). Abaixo, são apresentadas as equações desses modelos e também do modelo VERS (Virial Equation with Relative Surface Fractions).

Modelo UNIFAC

Nesse modelo, o cálculo do coeficiente de atividade de um componente é dividido em duas partes, como no modelo UNIQUAC: uma parte fornece a contribuição devido às diferenças no tamanho e na forma molecular e a outra está relacionada às interações energéticas entre grupos como mostrado abaixo, para o componente *i* de uma mistura:

$$\ln\gamma_i = \underset{\text{combinatorial}}{ln\gamma_i^C} + \underset{\text{residual}}{ln\gamma_i^R} \tag{1.21}$$

I. Parte combinatorial

No modelo UNIFAC, o termo combinatorial da equação UNIQUAC é usado diretamente. Apenas propriedades dos compostos puros entram nesta parte da equação:

$$\ln\gamma_i^C = \ln\frac{\phi_i}{x_i} + \frac{z}{2} q_i \, ln\frac{\theta_i}{\phi_i} + l_i - \frac{\phi_i}{x_i}\sum_j x_j l_j \tag{1.22}$$

$$l_i = \frac{z}{2}(r_i - q_i) - (r_i - 1) \tag{1.23}$$

onde z é chamado de número de coordenação e representa o número de locais nos quais pode haver interação entre moléculas. Geralmente, para líquidos em condições moderadas, o valor de z é próximo de 10.

$$\theta_i = \frac{q_i x_i}{\sum_j q_j x_j} \qquad \phi_i = \frac{r_i x_i}{\sum_j r_j x_j} \tag{1.24, 1.25}$$

em que θ_i e ϕ_i são frações de área e volume do componente i, respectivamente.

Os parâmetros r_i e q_i do componente puro são calculados como a soma dos parâmetros de volume (R_k) e de área (Q_k) do grupo k na molécula i. Estes, por sua vez, são obtidos a partir do volume e área de van der Waals V_k e A_k, dados por Bondi (1968):

$$r_i = \sum_k v_k^i R_k \qquad q_i = \sum_k v_k^i Q_k \tag{1.26, 1.27}$$

$$R_k = V_k / 15{,}17 \qquad Q_k = A_k / 2{,}5\times10^9 \tag{1.28, 1.29}$$

em que v_k^i é um número inteiro que representa o número de grupos do tipo k na molécula i. Os fatores de normalização 15,17 e $2{,}5\times10^9$ são dados por Abrams and Prausnitz (1975).

II. Parte Residual

A parte residual do modelo UNIQUAC é substituída no modelo UNIFAC pelo conceito de solução de grupos. A solução é tratada como uma mistura de grupos funcionais com interações energéticas (Wilson and Deal, 1962):

$$\ln\gamma_i^R = \sum_k v_k^i [\ln\Gamma_k - \ln\Gamma_k^i] \tag{1.30}$$

Γ_k é o coeficiente de atividade residual do grupo k e Γ_k^i o coeficiente de atividade residual do grupo k numa solução referência contendo apenas moléculas do tipo i. Γ_k pode ser calculado como:

$$ln\Gamma_k = Q_k\left[1 - ln\left(\sum_m \theta_m \Psi_{mk}\right) - \sum_m\left(\theta_m \Psi_{km} \Big/ \sum_n \theta_m \Psi_{nm}\right)\right] \tag{1.31}$$

$$\theta_m = \frac{Q_m X_m}{\sum_n Q_n X_n} \qquad X_m = \frac{\sum_i v_m^i x_i}{\sum_i \sum_k v_k^i x_i} \tag{1.32, 1.33}$$

em que θ_m é a fração de área do grupo *m*, X_m é a fração do grupo *m* na mistura e ψ_{nm} é o parâmetro de interação entre os grupos *m* e *n*, e é dado por:

$$\psi_{nm} = \exp\left[-\left(\frac{Umn - Unn}{RT}\right)\right] = exp\left[(-a_{nm}/T)\right] \tag{1.34}$$

U_{mn} é uma medida da energia de interação entre os grupos *m* e *n*, e a_{mn} representa os parâmetros binários de interação de grupos com unidades em Kelvin e $a_{mn} \neq a_{nm}$.

Modelo ASOG

No modelo ASOG o coeficiente de atividade de um componente *i* na solução é calculado pela soma das contribuições devido às diferenças nos tamanhos moleculares (γ_i^{FH}) e das interações entre grupos (γ_i^{G}) que descrevem as diferenças de forças intermoleculares:

$$\ln\gamma_i = ln\,\gamma_i^{FH} + \ln\gamma_i^{G} \tag{1.35}$$

A contribuição devido às diferenças nos tamanhos das moléculas é calculada aplicando-se equação similar à equação de Flory e Huggins citados por Prausnitz *et al.* (1986).

$$ln\,\gamma_i^{FH} = 1 + ln\left(\frac{\mathrm{v}_i^{FH}}{\sum_{j=1}^{n} x_j v_j^{FH}}\right) - \frac{v_i^{FH}}{\sum_{j=1}^{n} x_i v_i^{FH}} \tag{1.36}$$

A parte residual, que também contribui para o cálculo do coeficiente de atividade, é dada por:

$$ln\gamma_i^G = \sum_k v_k^i [ln\Gamma_k - ln\Gamma_k^i] \tag{1.37}$$

O coeficiente de atividade do grupo k (Γ_k) é função da temperatura e da fração de cada grupo na solução; ele é definido analiticamente pela equação de Wilson (1964), como a seguir:

$$ln\Gamma_k = -ln\sum_n X_n a_{kn} + 1 - \sum_n \frac{X_n a_{nk}}{\sum_m X_m a_{nm}} \tag{1.38}$$

$$X_n = \frac{\sum_j x_j v_n^j}{\sum_j x_j \sum_k v_k^i} \tag{1.39}$$

$$ln\, a_{kn} = m_{kn} + \frac{n_{kn}}{T} \tag{1.40}$$

em que v_i^{FH} é o número de átomos não hidrogênio na molécula i; v_k^i o número de átomos não hidrogênio no grupo k da molécula i; x_j a fração molar do componente j; Γ_k e Γ_k^i são os coeficientes de atividade do grupo k no sistema e no estado padrão (componente i puro), respectivamente. O parâmetro a_{kn} representa as interações energéticas entre os grupos k e n ($a_{kn} \neq a_{nk}$); m_{kn} e n_{kn} são parâmetros independentes da temperatura característicos das interações entre os grupos k e n.

Modelo VERS

Neste trabalho, um modelo semi-empírico é empregado para descrever os dados de atividade de água e entalpia de diluição.

Como de costume, o modelo começa com a energia livre de Gibbs em excesso G^E. O excesso é definido pela normalização assimétrica como mostrado abaixo:

$$x_w \rightarrow 1 \qquad \gamma_w \rightarrow 1 \quad \text{para o solvente} \tag{1.41}$$

$$x_i \rightarrow 0 \qquad \gamma_i \rightarrow 1 \quad \text{para os solutos} \tag{1.42}$$

A influência da pressão sob G^E é desprezível. Então, quando um componente 1 não iônico é dissolvido em água, o excesso da energia livre de Gibbs é expressa da maneira mais simples:

$$\frac{G^E}{n_w RT} = A_{11}[conc.(1)]^2 \tag{1.43}$$

A_{11} representa a interação entre duas moléculas do componente 1 dissolvidas em água. Esse coeficiente é multiplicado pela probabilidade dessa interação, que é considerada como sendo o quadrado da concentração de soluto. A concentração do soluto é expressa como:

$$conc.(1) = \frac{1000}{M_w}\frac{\Theta_1}{\Theta_w} \tag{1.44}$$

$$\Theta_i = \frac{m_i q_i}{\sum\limits_{\substack{\text{todos os}\\ \text{componentes}\\ j}} m_j q_j} \tag{1.45}$$

em que Θ_1 é a fração de área do componente 1, Θ_w a fração de área da água, m_i a molalidade do componente i e q_i o parâmetro de área do componente i. Das equações (1.43)-(1.44) resulta:

$$\frac{G^E}{n_w RT} = \left(\frac{1000}{M_w}\frac{\Theta_1}{\Theta_w}\right)^2 A_{11} \tag{1.46}$$

A expressão (1.46) pode ser facilmente estendida para interações ternárias assim como para mais solutos, da seguinte forma:

$$\frac{G^E}{n_w RT} = \left(\frac{1000}{M_w}\right)^2 \sum_{i \neq w}\sum_{j \neq w} \frac{\Theta_i}{\Theta_w}\frac{\Theta_j}{\Theta_w} A_{ij} + \left(\frac{1000}{M_w}\right)^3 \sum_{i \neq w}\sum_{j \neq w}\sum_{k \neq w} \frac{\Theta_i}{\Theta_w}\frac{\Theta_j}{\Theta_w}\frac{\Theta_k}{\Theta_w} B_{ijk} \tag{1.47}$$

As somas na equação (1.47) devem ser feitas para todas as espécies de solutos presentes. Para considerar a influência da massa molar do soluto, o parâmetro de área q_i é calculado por método de contribuição de grupos:

$$q_i = \sum_{\substack{\text{todos os} \\ \text{grupos } l}} v_l^{(i)} Q_l \tag{1.48}$$

e para os parâmetros A_{ij} e B_{ijk}:

$$A_{ij} = \sum_{\substack{\text{todos grupos} \\ l}} \; \sum_{\substack{\text{todos grupos} \\ m}} \Theta_l^{(i)} \Theta_m^{(j)} a_{lm} \tag{1.49}$$

$$B_{ijk} = \sum_{\substack{\text{todos grupos} \\ l}} \; \sum_{\substack{\text{todos grupos} \\ m}} \; \sum_{\substack{\text{todos grupos} \\ n}} \Theta_l^{(i)} \Theta_m^{(j)} \Theta_n^{(k)} b_{lmn} \tag{1.50}$$

$$\Theta_l^{(i)} = \nu_l^{(i)} \frac{Q_l}{q_i} \tag{1.51}$$

O parâmetro $v_l^{(i)}$ representa o número de grupos l na molécula de soluto i. Q_t é o parâmetro de área do grupo l, a_{lm} e b_{lmn} são parâmetros de interação de grupos. Esse modelo foi denominado VERS (Virial Equation with Relative Surface Fractions).

Para descrever os dados calorimétricos e a influência da temperatura na atividade de água, a seguinte expressão empírica, que apresenta a influência da temperatura nos parâmetros de interação binários a_{lm} foi empregada:

$$a_{lm} = \beta_{lm}^{(0)} + \beta_{lm}^{(1)} (T/K)(1-(T_0/T)) + \beta_{lm}^{(2)} \ln(T/T_0) \tag{1.52}$$

em que T_0 é a temperatura de referência igual a 25 °C. Assume-se que todos os parâmetros são simétricos, ou seja, que $\beta_{lm}^{(j)} = \beta_{ml}^{(j)}$ e $b_{lmn} = b_{lnm} = b_{mln} = b_{mnl} = b_{nlm} = b_{nml}$.

A partir das equações acima, pode-se então escrever equações para a atividade de água (a_w) e atividade do soluto ($a_{i,m}^{*}$):

$$ln\, a_w = -\frac{M_1}{1000}\sum_i m_i - \frac{1000}{M_1}\sum_{i \neq 1}\sum_{j \neq 1}\frac{\Theta_i}{\Theta_1}\frac{\Theta_j}{\Theta_1}A_{ij} - 2\left(\frac{1000}{M_1}\right)^2\sum_{i \neq 1}\sum_{j \neq 1}\sum_{k \neq 1}\frac{\Theta_i}{\Theta_1}\frac{\Theta_j}{\Theta_1}\frac{\Theta_k}{\Theta_1}B_{ijk} \tag{1.53}$$

$$\ln a_{i,m}^{*} = \ln m_i + 2\left(\frac{1000}{M_1}\right)\frac{q_i}{q_1}\sum_{j \neq 1}\frac{\Theta_j}{\Theta_1}A_{ij} + 3\left(\frac{1000}{M_1}\right)^2\frac{q_i}{q_1}\sum_{j \neq 1}\sum_{k \neq 1}\frac{\Theta_j}{\Theta_1}\frac{\Theta_k}{\Theta_1}B_{ijk} \tag{1.54}$$

assim como para a entalpia molar de excesso da água:

$$h_w^E = -T^2\left(\frac{\partial(\mu_i^E/T)}{\partial T}\right)_{p,n_j} \tag{1.55}$$

$$\frac{h_w^E}{RT} = T\left(\frac{1000}{M_w}\right)^2\sum_{i \neq w}\sum_{j \neq w}\frac{\Theta_i}{\Theta_w}\frac{\Theta_j}{\Theta_w}\frac{\partial A_{ij}}{\partial T} \tag{1.56}$$

e do soluto:

$$\frac{h_{i \neq w}^E}{RT} = -2T\left(\frac{1000}{M_w}\right)^2\frac{q_i}{q_w}\sum_{j \neq w}\frac{\Theta_j}{\Theta_w}\frac{\partial A_{ij}}{\partial T} \tag{1.57}$$

com:

$$\frac{\partial A_{ij}}{\partial T} = \sum_{\substack{\text{todos grupos}\\ l}}\ \sum_{\substack{\text{todos grupos}\\ m}}\Theta_l^{(i)}\Theta_m^{(j)}\left(\beta_{lm}^{(1)} + \frac{\beta_{lm}^{(2)}}{T}\right) \tag{1.58}$$

1.2.2 Para cálculo de viscosidade de misturas

Modelo GC-UNIMOD

O modelo GC-UNIMOD proposto por Cao *et al.* (1993) é baseado no método de contribuição de grupos UNIFAC. O GC-UNIMOD é também um modelo de contribuição de grupos funcionais empregado no cálculo da viscosidade de misturas líquidas multicomponentes. Nesse modelo, a viscosidade de uma mistura pode ser calculada como a soma de duas partes como no modelo UNIFAC: uma combinatorial e uma residual. Para os cálculos, são normalmente utilizados parâmetros do UNIFAC para o equilíbrio líquido-vapor (UNIFAC-VLE). Segue abaixo uma apresentação das equações matemáticas correspondentes ao modelo GC-UNIMOD para o cálculo da viscosidade cinemática em que: ν corresponde à viscosidade cinemática da mistura, ξ_i^C à contribuição combinatorial e ξ_i^R à residual do componente i.

$$ln(\nu) = \sum_{i=1}^{n}(\xi_i^C + \xi_i^R) \tag{1.59}$$

I. Parte Combinatorial

$$\xi_i^C = \phi_i \ln\left(\nu_i \frac{M_i}{M}\right) + 2\phi_i \, ln\left(\frac{x_i}{\phi_i}\right) \tag{1.60}$$

$$r_i = \sum_k v_k^i R_k \tag{1.61}$$

$$\phi_i = \frac{x_i r_i}{\sum_{j=1}^{n} x_j r_j} \tag{1.62}$$

em que M_i, M, r_i, x_i, R_k, v_k^i, v_i e ϕ_i são respectivamente, massa molar do componente i, massa molar da mistura, número de segmentos na molécula i, fração molar do componente i na mistura, parâmetro de volume do grupo k, número de grupos k na molécula i, viscosidade cinemática do líquido i e fração de volume do componente i.

II. Parte Residual

$$\xi_i^R = \sum_k v_k^i [\Xi_{ki} - \Xi_{ki}^i] \tag{1.63}$$

Ξ_{ki} e Ξ^i_{ki} correspondem respectivamente à viscosidade residual do grupo k para o componente i quando numa mistura e à viscosidade residual do grupo k no componente i quando em uma solução contendo apenas o componente i.

$$\Xi_{mi} = -\frac{Q_m}{R_m} N_{mi}^{visc} \phi_i \sum_k \theta_{km} \ln\left(\psi_{km}\right) \tag{1.64}$$

$$\theta_{mn} = \frac{\theta_m \Psi_{mn}}{\sum\limits_k \theta_k \Psi_{kn}} \tag{1.65}$$

$$\Psi_{mn} = \exp\left(\frac{\mathrm{a}_{mn}}{T}\right) \tag{1.66}$$

$$\theta_m = \frac{X_m Q_m}{\sum\limits_k X_k Q_k} \tag{1.67}$$

$$N_{ki}^{visc} = Q_k\left(\frac{q_i - r_i}{2} - \frac{1 - r_i}{z}\right) \tag{1.68}$$

$$q_i = \sum_k v_k^i Q_k \tag{1.69}$$

a_{mn}, q_i, Q_k, X_k ψ_{mn}, θ_k, θ_{mn} correspondem a: parâmetro de interação binária entre os grupos *m* e *n*; parâmetro de área para molécula *i*; parâmetro de área superficial para o grupo *k*; fração molar do grupo *k*; parâmetro de interação binária entre os grupos *m* e *n*; fração de área do grupo *k* e composição local dos grupos.

A equação abaixo representa o cálculo global da viscosidade, com as expressões matemáticas para as contribuições combinatorial e residual.

$$\ln(\nu) = \sum_{i=1}^{n}\left[\phi_i \ln\left(\nu_i \frac{M_i}{M}\right) + 2\phi_i \ln\left(\frac{x_i}{\phi_i}\right) + \sum_k v_k^i\left(\Xi_{ki} - \Xi_{ki}^i\right)\right] \tag{1.70}$$

As viscosidades dos compostos puros requeridas pelo modelo GC-UNIMOD podem ser retiradas da literatura (quando houver dados) ou calculadas por modelos do tipo proposto por Joback and Reid (1987). Alguns trabalhos do grupo de pesquisa em que esta fase foi realizada estão relacionados com a determinação experimental e modelagem de propriedades físicas, como por exemplo: Valeri and Meirelles (1997); Chumpitaz *et al.* (1999) e Cruz *et al.* (2000). Trata-se agora de estender tal abordagem a misturas multicomponentes que de fato são encontradas na prática industrial.

Equação de Kumar

Apesar de não se tratar de um modelo de contribuição de grupos, as equações da correlação de Kumar, empregadas nas investigações da viscosidade de misturas de polietileno glicóis no Capítulo 5, são apresentadas neste item. Primeiramente a correlação foi proposta para o cálculo de viscosidades de soluções de sais (Kumar, 1993) e posteriormente, também empregada no cálculo de viscosidades de misturas de sais e açúcares (Pereira, 2001).

A equação de Kumar para viscosidade foi desenvolvida assumindo que um sal *AB*, quando dissolvido em um solvente *S*, forma um complexo solvatado como, a seguir:

$$AB + h\,S \Leftrightarrow AB \cdot hS \tag{1.71}$$

em que *h* é o número de moléculas de solvente.

Se N_1, N_2 e N_c são, respectivamente, o número de moles de sal, solvente e complexo solvatado, as frações molares do sal (x_1) e do complexo solvatado (x_c) podem ser escritas como:

$$x_1 = N_1 / (N_1 + N_2) \tag{1.72}$$

$$x_c = N_c / \left[N_c + (N_2 - h\,N_c) \right] \tag{1.73}$$

Assumindo que N_1=N_c, pode-se obter N_2 da equação 1.72 como:

$$N_2 = N_c (1\text{-}\,x_1)/x_1 \tag{1.74}$$

Substituindo N_2 da equação 1.74 na equação 1.73:

$$x_c = x_1 / (1 - x_1\,h) \tag{1.75}$$

Seguindo a proporcionalidade entre viscosidade e concentração proposta por Harned and Owen (1965):

$$(\eta_{rel}\ \text{-}1) \propto x_c = \mathrm{B}\, x_1/(1\text{-}\,x_1 h) \tag{1.76}$$

em que, $\eta_{rel}=\eta/\eta_0$; η e η_0 são as viscosidades da solução e do solvente, respectivamente e B é uma constante. A equação 1.76 pode também ser reescrita como:

$$1/(\eta_{rel}-1) = -h/\mathrm{B} + 1/(\mathrm{B}\,x_1) \tag{1.77}$$

A equação acima é a expressão proposta para correlacionar viscosidade com fração molar do sal na solução. O parâmetro h indica a solvatação ou hidratação, se o solvente é água e o outro parâmetro, B, representa as interações entre íon e solvente como discutido por Feakins and Laurence (1966).

1.3 Compostos orgânicos de interesse na área de alimentos e biotecnologia

O crescente avanço tecnológico tem despertado interesse para o desenvolvimento de processos eficientes na indústria, em particular na área biotecnológica e na indústria de alimentos. Para o projeto de processos de purificação, recuperação de biomoléculas ou mesmo desenvolvimento de produtos é geralmente necessário o conhecimento de propriedades físicas dos mesmos para a otimização de operações na indústria.

Dentro desse contexto, o estudo do equilíbrio de fases desempenha papel importante em processos de extração líquido-líquido como nos sistemas aquosos bifásicos, SABs (técnica comumente empregada para separação e purificação de biomoléculas), processos de cristalização e crioconcentração que envolvem equilíbrio sólido-líquido, estudos da atividade de água (equilíbrio líquido-vapor) como parâmetro de controle de qualidade em alimentos, e também na tecnologia de alimentos já que tanto os produtos naturais quanto os processados apresentam microestrutura complexa e multifásica.

Dessa forma, deve-se enfatizar a importância do estudo do comportamento de compostos alimentícios em soluções aquosas. O conhecimento de propriedades termodinâmicas de sistemas aquosos simples pode levar a uma melhor compreensão de biomoléculas em seus ambientes naturais. Além de compostos orgânicos, outro material estudado neste trabalho, também interessante e muito utilizado nas mais diversas áreas industriais e investigações científicas – como, por exemplo, em sistemas aquosos bifásicos – são os polietileno glicóis.

Dentre muitos materiais comumente encontrados em biotecnologia e na indústria de alimentos estão polímeros, aminoácidos, triglicerídeos, açúcares, ácidos orgânicos, etc. O conhecimento de propriedades físico-químicas tais como solubilidade, atividade de água, ponto de congelamento, pH, massa molar e parâmetros de interação soluto-solvente de misturas que incluem esses compostos é necessário sob o ponto de vista de projeto de equipamentos e processos e também para o melhor entendimento da formação da estrutura no alimento. Do ponto de vista da simulação de processos, o uso de modelos matemáticos existentes e consolidados na literatura torna-se uma ferramenta útil para o cálculo das propriedades de interesse. Nos próximos itens, segue-se uma descrição rápida dos compostos que são utilizados neste trabalho – polióis, aminoácidos, polietileno glicóis e maltodextrinas – para esclarecimento de suas estruturas químicas, propriedades físico-químicas e empregos na indústria e pesquisa. A seguir, são também descritos os métodos de cálculo das propriedades físico-químicas que se deseja estudar.

1.3.1 Polióis

Polióis são polihidróxi-álcoois empregados em diversas áreas, incluindo a de alimentos, a farmacêutica e a de cosméticos. Na indústria de alimentos, por exemplo, soluções de sorbitol são usadas como umectantes e plasticizantes em algumas formulações de alimentos e filmes comestíveis (Moreton and Armstrong, 1998). O poder adoçante é outra importante característica desses compostos, que são utilizados na confecção de doces dietéticos, produtos de higiene e fármacos (Kirk and Othmer, 1983). Em geral, são produzidos industrialmente a partir da hidrogenação catalítica de carboidratos comestíveis ou são produzidos por processos biológicos (Billaux *et al.*, 1991). Existe atualmente um grande interesse em se produzir xilitol (poliálcool) por via microbiológica (Azuma *et al.*, 2000; Silva *et al.*, 1998). Dessa forma, o emprego de métodos para a estimativa de dados como solubilidade apresenta-se como uma ferramenta útil no planejamento de processos de recuperação de compostos - como xilitol – produzidos por fermentação.

1.3.2 Aminoácidos

Dentre vários compostos bioquímicos, os aminoácidos são de grande interesse para a pesquisa devido à sua simplicidade e importância para o entendimento do comportamento de moléculas como peptídeos e proteínas em soluções mais complexas. Em geral, os aminoácidos são produzidos por microorganismos em meio aquoso contendo solutos como sais, ácidos orgânicos, etc.

Processos de separação baseados na precipitação e cristalização têm sido largamente utilizados para concentração e purificação de biomoléculas (Cussler *et al.*, 1989). De acordo com Eyal and Bressler (1993), o custo de separação e concentração de biomoléculas a partir de meios aquosos diluídos, nos quais eles são geralmente produzidos, pode alcançar 90% do custo total de obtenção de bioprodutos. No projeto de equipamentos e processos é necessário o conhecimento de algumas propriedades físico-químicas como solubilidade, atividade de água e a influência do pH sobre essas propriedades em misturas contendo biomoléculas. Dessa forma, é interessante o estudo de propriedades físico-químicas de sistemas contendo tais compostos a várias concentrações e pHs.

1.3.3 Polietileno glicóis

Polietileno glicóis (PEGs) são polímeros de cadeia linear formados por unidades de oxietileno, cujas características principais são alta solubilidade em água, baixa toxicidade e boa estabilidade. Dependendo do tamanho da cadeia, apresentam-se sólidos (MM 3000 a 20000), semi-sólidos (MM 1000 a 2000) ou líquidos viscosos (MM 200 a 700) à temperatura ambiente (Davidson, 1980). Estas propriedades têm favorecido o uso dos PEGs em diversas aplicações comerciais das indústrias farmacêuticas, cosmética, química e de alimentos. Na área biotecnológica são empregados em sistemas aquosos bifásicos para a separação e purificação de biomoléculas em meios biocompatíveis, já que o PEG possui baixa toxicidade (Chirife e Ferro Fontan, 1980; Coimbra *et al.*, 1995; Silva e Meirelles, 2000a, b; Alves *et al.*, 2000, Sé e Aznar, 2002). Dessa forma, o conhecimento do comportamento reológico de sistemas contendo PEGs é importante para avaliação, otimização e também projeto de equipamentos.

A estrutura química dos PEGs é representada por:

$$\mathrm{HO}-(\mathrm{CH_2CH_2O})_n-\mathrm{H}$$

onde *n* representa o grau de polimerização.

O polímero de mais alta massa molar produzido comercialmente como um composto puro é o tetraetilenoglicol com *n*=4. À medida que o grau de polimerização aumenta, não é mais possível a separação de compostos puros por destilação devido à baixa volatilidade dos mesmos e, dessa forma, são produzidas misturas de moléculas com várias massas molares. O polímero é então caracterizado por um grau de polimerização médio. Comercialmente são identificados por números que indicam suas massas molares aproximadas, como por exemplo, PEG 400, PEG 1000, etc.

1.3.4 Maltodextrinas (MD)

Maltodextrinas são polissacarídeos solúveis em água que têm sido empregados numa ampla variedade de produtos industriais nas áreas de alimentos e farmacêutica. Atualmente, a necessidade de proteção do meio ambiente coloca os polímeros biodegradáveis, como os polissacarídeos, em vantagem para fins industriais (Swift, 1998). Os polissacarídeos apresentam distribuição de massa molar, geralmente representada pelas massas molares médias: nominal (M_n) ou mássica (M_w). Essas massas molares são calculadas como:

$$M_\text{n} = \frac{\sum_i n_i M_i}{\sum_i n_i} \tag{1.78}$$

$$M_\text{w} = \frac{\sum_i m_i M_i}{\sum_i m_i} \tag{1.79}$$

em que n_i é número de moles e m_i a massa da espécie i. A partir desses valores pode-se também definir o quociente M_w/M_n denominado índice de polidispersão que é uma medida da amplitude da distribuição.

As MD apresentam-se como uma mistura de sacarídeos com uma ampla distribuição de massas molares entre polissacarídeos e oligossacarídeos. Suas massas molares variam de 900 a 18000 g/mol. A ampla distribuição de massas molares confere às maltodextrinas variadas características relacionadas com propriedades físico-químicas como viscosidade, pressão de vapor, capacidade de formação de gel, etc. (Kasapis *et al.*, 1993; Mothé e Rao, 1999).

Dentre os polissacarídeos, as maltodextrinas são polímeros de grande interesse comercial devido à sua alta solubilidade em água (Gliksmann, 1986; Marchal, 1999) e aplicação potencial em sistemas aquosos bifásicos (Silva e Meirelles, 2000 a,b). A estrutura química da maltodextrina é apresentada a seguir:

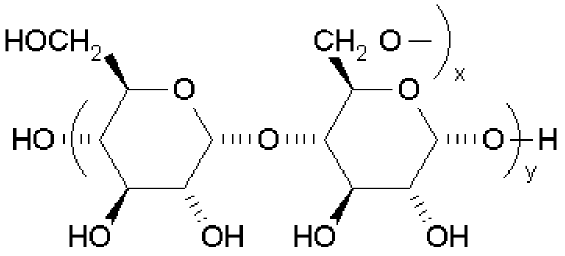

Figura 1.1 Estrutura química da maltodextrina (x=ligação α-1,6 com possibilidade de ramificação; y= ligação α-1,4 para a formação de cadeia linear).

1.4 Propriedades físico-químicas estudadas

No presente trabalho, métodos de contribuição de grupos foram empregados para a estimativa de propriedades como atividade de água, solubilidade, depressão do ponto de congelamento, elevação do ponto de ebulição, pH, espalhamento de luz, entalpia de diluição e viscosidade. As equações termodinâmicas para o cálculo dessas propriedades são apresentadas a seguir, e o tratamento termodinâmico mais detalhado nos capítulos seguintes referentes a cada um dos compostos estudados.

1.4.1 Atividade de água

O conceito termodinâmico de atividade de água pode ser relacionado à razão entre a fugacidade da água numa amostra (f_w) e a fugacidade da água pura (f_w^o) à mesma temperatura e pressão:

$$a_w = x_w \gamma_w = \frac{f_w(T,P,x_w)}{f_w^o(T,P)} = \frac{P_w}{P_w^o} \tag{1.80}$$

Em condições moderadas de temperatura e pressão, a fase vapor comporta-se como um gás ideal e a razão de fugacidades pode então ser aproximada pela razão entre a pressão parcial da água numa amostra (P_w) e a pressão de vapor da água pura na mesma temperatura (P_w^o). O produto $\gamma_w x_w$ é a atividade da água numa mistura, em que o coeficiente de atividade γ_w pode ser calculado pelos métodos de contribuição de grupos.

1.4.2 Solubilidade

O critério de cálculo da solubilidade de um componente sólido *i* em solução é a igualdade de fugacidades de *i* nas fases líquida (*L*) e sólida (*S*) no equilíbrio. Considerando que não há solubilidade do solvente na fase sólida, pode-se escrever:

$$f_i^S(T,P) = f_i^L(T,P,x_i) \tag{1.81}$$

em que, x_i é a fração molar do soluto, e T a temperatura do sistema. Assumindo que a temperatura do ponto triplo é aproximadamente a temperatura de fusão do sólido (T_f) e que ΔC_p apresenta dependência linear com a temperatura numa faixa entre T e T_f, a equação resultante para predizer a concentração de saturação do sólido *i* num líquido pode ser expressa como:

$$ln\gamma_i x_i = -\frac{\Delta H_f}{RT_f}\left(\frac{T_f}{T}-1\right)+\frac{\Delta C_p}{R}\left(\frac{T_f}{T}-1\right)-\frac{\Delta C_p}{R}ln\left(\frac{T_f}{T}\right) \tag{1.82}$$

A consideração que ΔC_p é uma função linear da temperatura já foi utilizada em trabalhos prévios (Catté *et al.*, 1994; Peres and Macedo, 1996, 1997) para sistemas contendo açúcares. A expressão representando a diferença entre os calores específicos do líquido e do sólido (ΔC_p) é dada por:

$$\Delta C_p = \Delta A + \Delta B(T - T_{ref}) \tag{1.83}$$

em que T_{ref} é uma temperatura de referência, ΔA e ΔB são dois parâmetros ajustáveis e ΔH_f a entalpia de fusão do sólido. Considerando a dependência linear de ΔC_p com a temperatura pode-se calcular a atividade do soluto como:

$$\begin{aligned} ln\gamma_i x_i = &\left[-\frac{\Delta H_f}{R}+\frac{\Delta A-\Delta BT_{ref}}{R}T_f+\frac{\Delta B}{2R}T_f^2\right]\left(\frac{1}{T}-\frac{1}{T_f}\right)+ \\ &\frac{\Delta A-\Delta BT_{ref}}{R}ln\left(\frac{T}{T_f}\right)+\frac{\Delta B}{2R}(T-T_f) \end{aligned} \tag{1.84}$$

Com a equação 1.84 calcula-se a solubilidade x_i, sabendo-se as propriedades do componente *i* puro e o coeficiente de atividade de *i* em solução. Esse cálculo requer um procedimento iterativo para a estimativa simultânea da solubilidade e do coeficiente de atividade, que neste trabalho será obtido dos métodos de contribuição de grupos.

1.4.3 Depressão do ponto de congelamento

Pode-se calcular a depressão do ponto de congelamento de uma mistura empregando a seguinte expressão (Ferro Fontan and Chirife, 1981):

$$\ln a_w = \ln(x_w \gamma_w) = \frac{\Delta H_{f,w}}{R}\left(\frac{1}{T_w} - \frac{1}{T_{mist}}\right) - \frac{\Delta C_{p,w}}{R}\ln\left(\frac{T_w}{T_{mist}}\right) - \frac{\Delta C_{p,w}}{R}\left(1 - \frac{T_w}{T_{mist}}\right) \tag{1.85}$$

em que a_w é a atividade de água, R a constante dos gases, T_w e T_{mist} os pontos de congelamento da água pura e da mistura com concentração conhecida, respectivamente, $\Delta H_{f,w}$ é a entalpia de fusão da água na temperatura T_w, e $\Delta C_{p,w}$ é a diferença entre os calores específicos da água líquida e do gelo à temperatura T_{mist}, assumindo que $\Delta C_{p,w}$ é independente da temperatura entre T_w e T_{mist}.

Dessa forma, sabendo-se a concentração da mistura, o coeficiente de atividade da água (calculado por método de contribuição de grupos) e as propriedades da água pura, pode-se estimar a temperatura de congelamento da mistura (T_{mist}).

Um parâmetro geralmente estudado em equilíbrio sólido-líquido de soluções é o ponto eutético. Nesse ponto, existem em equilíbrio uma fase líquida com o(s) componente(s) sólido(s), ou seja, no ponto eutético, uma solução de composição x_e formada por exemplo por dois componentes A e B, está simultâneamente em equilíbrio com o sólido puro A e o sólido puro B.

1.4.4 Elevação do ponto de ebulição

Em um sistema soluto-solvente em equilíbrio líquido-vapor, assumindo que a fase de vapor tem o comportamento de um gás ideal, a relação básica para o cálculo da temperatura de ebulição deste sistema é:

$$P = \gamma_w x_w P_w^o \tag{1.86}$$

em que P é a pressão total do sistema, γ_w o coeficiente de atividade da água, x_w a fração molar da água e P_w^o a pressão de vapor da água pura que pode ser calculada usando a equação de Antoine com as constantes dadas por Gmehling (1977).

A temperatura de ebulição (T_{eb}) pode então ser calculada iterativamente empregando a equação 1.86 e conhecendo-se a composição da mistura (x_w), uma estimativa inicial para a T_{eb} e o coeficiente de atividade da água que pode ser calculado por método de contribuição de grupos. Dessa forma, um novo valor para a T_{eb} pode ser obtido e comparado ao valor inicial estimado.

1.4.5 pH

O *pH* de uma solução contendo eletrólitos fracos pode ser estimado pela seguinte equação que considera a não idealidade do sistema:

$$pH = -\log\left[\gamma^{c}_{H^+} c_{H^+}\right] \tag{1.87}$$

O procedimento numérico desenvolvido por Achard *et al.* (1994) que considera o fenômeno de dissociação parcial das espécies em solução apresenta-se como uma metodologia eficiente para o cálculo da concentração de íons H^+ (c_{H^+}) e do coeficiente de atividade ($\gamma^{c}_{H^+}$), simultaneamente. Este procedimento é apresentado em detalhe no capítulo sobre soluções de aminoácidos (Capítulo 3).

1.4.6 Espalhamento de luz

Em vários livros-texto pode-se encontrar a derivação da equação básica para a avaliação dos dados de espalhamento de luz laser (Kurata, 1982). Segundo essa derivação pode-se encontrar uma expressão que relaciona os dados medidos nos experimentos de espalhamento de luz laser com a concentração do soluto (c_s) e o potencial químico do solvente (μ_1).

$$\frac{Kc_s}{R_E} = -\frac{\rho_1}{RT}\frac{\partial \mu_1}{\partial c_s} \tag{1.88}$$

Os termos da parte esquerda da equação 1.88 são experimentais. A constante *K* é dada por:

$$K = \frac{4\pi^2 n_1^2 \left(\partial n / \partial c_s\right)^2}{N_A \lambda^4} \tag{1.89}$$

em que n é o índice de refração do solvente puro, N_A é o número de Avogrado e λ é o comprimento de onda do laser. O incremento ($\partial n/\partial c$) é determinado por refratômetro interferométrico para cada polímero e temperatura de trabalho. O excesso Rayleigh (R_E) considera a diferença entre a intensidade de luz espalhada pela solução polimérica e a intensidade espalhada pelo solvente puro.

1.4.7 Entalpia de diluição

A entalpia parcial de excesso de um componente i está relacionada com o coeficiente de atividade da seguinte maneira:

$$-\frac{h_i^E}{RT^2} = \left(\frac{\partial \ln \gamma_i}{\partial T}\right)_{p,n_j} \tag{1.90}$$

em que h_i^E é a entalpia parcial molar do componente i menos a entalpia molar do componente i puro a mesma temperatura e pressão.

1.5 Nomenclatura

Símbolos latinos

A	Área de van der Waals
A	Coeficiente virial
a	Atividade
a	Parâmetro de interação
B	Coeficiente virial
b	Parâmetros de interação
c	concentração molar (g mol^{-1})
Cp	Capacidade calorífica

f	Fugacidade
G	Energia de Gibbs
H	Entalpia
h	Entalpia
K	Constante ótica
M	Massa molar
m	Parâmetros de interação independente da temperatura
n	Índice de refração
N_A	Número de Avogrado
N	Número de componentes
N	Número de viscosidade
n	Número de moles
n	Parâmetros de interação independente da temperatura
P	Pressão
q	Parâmetro de área de componente
Q	Parâmetro de área de grupo
r	Parâmetro de volume de componente
R	Constante universal dos gases (R=8.31441 J (mol K)$^{-1}$)
R	Parâmetro de volume
R	Relação de Rayleigh
S	Entropia

T	Temperatura
U	Energia de interação
U	Energia interna
v	Número de grupos
V	Volume
V	Volume de van der Waals
X	Fração de grupo
x	Fração molar
z	Número de coordenação

Símbolos gregos

β	Parâmetro de interação entre grupos no modelo VERS
γ	Coeficiente de atividade
Δ	Medida de variação
θ	Ângulo
Θ	Fração de área
λ	Comprimento de onda de luz laser
μ	Potencial químico
ν	Viscosidade
Ξ	Viscosidade residual
Ψ	Parâmetro de interação binária
Γ	Coeficiente de atividade de grupo

Subscrita

0	Referência
1	Componente 1
11	Coeficiente virial binário entre duas moléculas do componente 1
f	Fusão
H^+	Íon hidrogênio
i	Componente i
ij	Coeficiente virial binário dos componentes i e j
ijk	Coeficiente virial ternário dos componentes i, j e k
j	Componente j
k	Componente k no modelo VERS
k	Grupo k
l	Grupo l no modelo VERS
m	Grupo m
$mist$	mistura
n	Grupo n
s	Soluto
w	Água

Sobrescrita

(0), (1), (2)	Índices dos parâmetros do modelo VERS
o	Componente puro
C	Termo combinatorial

E	Medida de excesso
FH	Termo de Flory-Huggins
id	ideal
R	Termo residual
$visc$	Viscosidade

Siglas

MD	Maltodextrina
MM	Massa molar
PEG	Polietileno glicol

1.6 Referêcias bibliográficas

Abrams, D.S.; Prausnitz, J.M. Statistical thermodynamics of liquid mixtures: a new expression for the excess Gibbs energy of partly or completely miscible systems. *AIChE J.* **1975**, 21, 116 – 128.

Achard, C.; Dussap, C. G. Prediction of pH in complex aqueous mixtures using a group contribution method. *AIChE J.* **1994**, 40, 1210 – 1222.

Alves, J. G. L. F.; Chumpitaz, L. D. A.; da Silva, L. H. M.; Franco, T. T.; Meirelles, A. J. A. Partitioning of whey proteins, bovine serum albumin, and porcine insulin in aqueous two-phase systems. *J. Chrom. B* **2000**, 743, 235 – 239.

Azuma, M., Ikeuchi, t., Kiritami, R., Kato, J., Ooshima, H. Increase in xylitol production by *Candida tropicalis* upon addition of salt. *Biomass & Bioenergy* **2000**, 19, 129 – 135.

Billaux, M.S.; Flourie,B.; Jacquemin C.; Messing, B. *Sugar alcohols*. Em *Handbook of sweeteners*. Edit. Marie, S.; Piggott, J.R., Glasgow:Blackie, N.Y. USA, 1991.

Bondi, A. *Physical Properties of Molecular Crystals, Liquids and Glasses*. Wiley, New York, 1968.

Cao, W.; Knudsen, K.; Fredenslund, A.; Rasmussen, P. Group-contribution viscosity predictions of liquid mixtures using UNIFAC-VLE parameters. *Ind. Eng. Chem. Res.* **1993**, 32, 2088 – 2092.

Catté, M.; Dussap, C-G; Achard, C.; Gros, J-B. Excess properties and solid-liquid equilibria for aqueous solutions of sugars using UNIQUAC model. *Fluid Phase Equilibria* **1994**, 96, 33 – 50.

Chirife, J.; Ferro-Fontan, C.F. A Study of the water activity lowering behavior of polyethylene glycols in the intermediate moisture range. *J. Food Sci.* **1980**, 45, 1717 – 1719.

Chumpitaz, L. D. A.; Coutinho, L. F.; Meirelles, A. J. A. Surface tension of fatty acids and triglycerides. *J. Am. Oil Chem. Society* **1999**, 76 (3), 379 – 382.

Coimbra, J. S. R.; Thommes, J.; Meirelles, A. J. A.; Kula, M.-R. Performance of a Graesser contactor in the continuous extraction of whey proteins: mixing, mass transfer and efficiency. *Bioseparation* **1995**, 5, 259 – 268.

Cruz, M. S.; Chumpitaz, L. D. A.; Alves, J. G. L. F.; Meirelles, A. J. A. Kinematic viscosities of poly(ethylene glycols). *J. Chem. Eng. Data* **2000**, 45, 61 – 63.

Cussler, E. L., Belter, P. A., Hu, W. S. Crystalization for bioseparations. *Chemtech.* **1989**, 19, 376 – 384.

Davidson, R. L. *Handbook of water-soluble gums and resins*. McGraw-Hill Book Company, New York, 1980.

Eyal, A.M.; Bressler, E. Mini review industrial separation of carboxylic and amino acids by liquid membranes: applicability, process considerations and potential advantages. *Biotech. Bioeng*. **1993**, 41, 287 – 291.

Feakins, D.; Lawrence, K. G. Relative viscosities of solutions of sodium and potassium chlorides and bromides in n-methylformamide at 25, 35 and 45 degrees. *J. Chem. Soc. A* **1966**, 2, 212 – 216.

Ferro Fontan, C.; Chirife, J. The evaluation of water activity in aqueous solutions from freezing point depression. *J. Food Technology* **1981**, 16, 21 – 30.

Flory, P. J. Thermodynamics of high polymer solutions. *J. Chem. Phys.* **1941**, 9, 660 – 661.

Fredenslund A.; Jones R.L.; Prausnitz, J.M. Group contribution estimation of activity coefficients in nonideal liquid mixtures. *AIChE J.* **1975**, 21, 1086 – 1099.

Glicksman, M. *Food Hydrocolloids* v III, CRC Press Inc., New York, 1986.

Gmehling, J.; Onken, U. *Vapor-Liquid Equilibirum Data Collection*. Frankfurt: Dechema, 1981.

Groβmann, C. Untersuchungen zur Verteilung von Aminosäuren und Peptiden auf wässrige Zwei-Phasen-Systeme. *Dissertação de Doutorado da Universidade de Kaiserslautern*, Alemanha, 1994.

Harned H. A.; Owen, B. B. *The Physical Chemistry of Electrolytic Solutions*. Reinhold Publications Co., 3rd. Ed., New York, 1965.

Kasapis, S., Morris, E. R., Norton, I. T., Clark, A. H. Phase equilibria and gelation in gelatin/maltodextrin systems – Part I: Gelation of individual components. *Carbohydrate Polymers* **1993**, 21, 243 – 248.

Kirk, R.E.; OThmer, D.F. *Encyclopedia of Chemical Technology*; John Wiley & Sons: New York, 1983.

Kumar A. A simple correlation for estimating viscosities of solutions of salts in aqueous, non-aqueous and mixed solvents applicable to high concentration, temperature and pressure. *Can. J. Chem. Eng.* **1993**, 71, 948 – 954.

Kurata, M. *Thermodynamics of Polymer Solutions*; Harwood Academic Publishers: New York, 1982.

Marchal, L. M.; Beeftink, H. H.; Tramper, J. Towards a rational design of commercial maltodextrins. *Trends in Food Science & Technology* **1999**, 10, 345 – 355.

Moreton, R. C., Armstrong, N. A. The effect of film composition on the diffusion of ethanol through soft gelatin films. *Int. J. Pharm* **1998**, 161, 123 – 131.

Mothé, C. G., Rao, M. A. Rheological behavior of aqueous dispersions of cashew gum and gum arabic: effect of concentration and blending. *Food Hydrocolloids* **1999**, 13, 501 – 506.

Pereira, G.; Moreira, R.; Vázquez, M. J.; Chenlo, F. Kinematic viscosity prediction for aqueous solutions with various solutes. *Chem. Eng. J.* **2001**, 81, 35 – 40.

Peres, A. M.; Macedo, E.A. A modified unifac model for the calculation of thermodynamic properties of aqueous and non-aqueous solutions containing sugars. *Fluid Phase Equilibria* **1997**, 139, 47 – 74.

Peres, A.M.; Macedo, E.A. Thermodynamic properties of sugars in aqueous solutions: correlation and prediction using a modified uniquac model. *Fluid Phase Equilibria* **1996**, 123, 71 – 95.

Pitzer, K. S. *Activity Coefficients in Electrolyte Solutions*. CRC Press, Boca Raton, 1991.

Porter, A. W. On the vapour pressures of mixtures. *Trans. Faraday Soc.* **1920**, 14, 335 – 345.

Prausnitz, J. M. *Molecular thermodynamics of fluid phase equilibria***.** Englewood Cliffs, N. J.: Prentice-Hall, 1969.

Prausnitz, J.M.; Lichtenthaler, R.N.; Azevedo, E.G. *Molecular thermodynamics of fluid phase equilibria*. Prentice Hall Inc., New Jersey, 1986.

Redlich, O.; Kister, C. E. Algebraic representation of thermodynamics properties and the classification of solutions. *Ind. Eng. Chem.* **1948**, 40, 345 – 348.

Sé, R. A. G.; Aznar, M. Liquid-liquid equilibrium of the aqueous two-phase system water + peg 4000 + potassium phosphate at four temperatures: experimental determination and thermodynamic modeling. *J. Chem. Eng. Data* **2002**, 47, 1401 – 1405.

Silva, L. H. M., Meirelles, A. J. A. Phase equilibrium and protein partitioning in aqueous mixtures of maltodextrin with polypropylene glycol. *Carbohydrate Polymers* **2001**, 46, 267 – 274.

Silva, L. H. M., Meirelles, A. J. A. Phase equilibrium in polyethylene glycol/maltodextrin aqueous two-phase systems. *Carbohydrate Polymers* **2000**, 42, 273 – 278.

Silva, S. S., Felipe, M. G. A. , Mancilha, I. M. Factors that affect the biosynthesis of xylitol by xylose-fermenting yeasts. *Appl. Biochem. Biotech.* **1998**, 70 – 72, 331 – 339.

Swift, G. Requirements for biodegradable water-soluble polymers. *Polymer Degradation and Stability*, **1998**, 59, 19 – 24.

Valeri, D.; Meirelles, A. J. A. Viscosities of fatty acids, triglycerides and their binary mixtures. *J. Am. Oil Chem. Society* **1997**, 74, 1221 – 1226.

Wilson, G. M.; Deal, C. H. Activity coefficients and molecular structure. *Ind. Eng. Chem. Fundam.* **1962**, 20 – 24.

Wilson, G.M. Vapor-liquid equilibrium XI. A new expression for the excess free energy of mixing. *J. Am. Chem. Soc.* 1964, 86, 127 – 134.

Capítulo 2

WATER ACTIVITY IN POLYOL SYSTEMS

L. Ninni, M.S. Camargo, Antonio J. A. Meirelles

Department of Food Engineering (DEA/FEA), State University of Campinas – UNICAMP,
Cidade Universitária "Zeferino Vaz", P.O. Box 6121 Zip Code 13083-970 Campinas – SP,
Brazil

Trabalho publicado na revista *Journal of Chemical Engineering and Data*, v. 45, p. 654 – 660, 2000.

2. Water activity in polyol systems

2.1 Abstract

Water activities of binary and ternary mixtures containing polyols were measured using an electronic hygrometer with temperature ranging from (10 to 35) °C. The concentrations of the mixtures varied according to the solubility limit for each polyol (D-sorbitol, D-mannitol, xylitol, *meso*-erythritol and glycerol). Results were compared with the group contribution-based models ASOG and UNIFAC. The predictions using parameters from the literature were poor, probably as a consequence of the strongly polar hydroxyl groups bounded to consecutive carbon atoms in the polyol molecule. Better agreement was obtained by readjusting some of the interaction parameters. The data bank used in this procedure included water activity data as well as polyol solubility data taken from the literature. The best results were achieved using the UNIFAC-Larsen model with an average relative deviation of 0.9% for water activity and solubility data.

2.2 Introduction

Polyols are polyhydroxy alcohols or sugar alcohols used in many diverse fields including foods, pharmaceuticals, and cosmetics. The knowledge of the phase equilibria in systems containing biological products, such as polyols, is an important support for modeling and designing industrial processes like concentration and purification in a separation unit. Thermodynamic models have been used for calculating some physicochemical properties – such as water activity- in food systems containing amino acids, sugars, organic salts and other solutes (Velezmoro and Meirelles, 1998; Ninni *et al.*, 1999a, 1999b; Velezmoro *et al.*, 2000). Water activity is an important physical chemical property in food engineering, since many chemical, enzymatic, and microbiological reactions that influence food stability are dependent on the availability of water.

Group contribution-based models such as UNIFAC (Fredenslund *et al.*, 1975) and ASOG (Kogima and Tochigi, 1979) are considered to provide good results for estimating activity coefficients in the liquid phase. Correa *et al.* (1994) studied the behavior of some aqueous polyol solutions: water activities (a_w) of binary (polyol + water) and ternary (urea + polyol + water and urea + sugar + water) solutions were measured and results compared with those of the ASOG group contribution model. New specific groups were defined: glucose and fructose rings, urea, polyalcohol, and cyclic polyalcohol. The results showed that readjustment of binary interaction parameters provided better agreement between the model and experimental a_w values when compared with the predictions using the original parameters from Kojima and Tochigi (1979). Recently, Peres and Macedo (1997) have shown that the UNIFAC-Larsen model can be successfully used for calculating thermodynamic properties of aqueous and nonaqueous solutions containing sugars.

In this work, water activity has been measured for the binary (polyol + water) and ternary (polyol + polyol + water) systems using an electronic hygrometer. Furthermore, new parameters for UNIFAC-Larsen and ASOG models were determined, allowing the calculation of water activity, solubility, and freezing point data of aqueous polyol solutions with low deviations between experimental and calculated values.

2.3 Experimental Section

Water activities of binary and ternary aqueous polyol systems were determined from (10 to 35) ºC. The following polyols used were: D-sorbitol, D-mannitol, xylitol, *meso*-erythritol and glycerol. They were analytical grade reagents from SIGMA with purity > 99%. The solutions were prepared by mass percent with distilled water using an analytical balance (Sartorius, Goettingen, Germany) with ±0.1 mg accuracy. The compositions were accurate to ±0.01% approximately in mass fraction. Before this solution were prepared, the water content in the solid polyols was determined by Karl Fischer titration (Metrohm, Herisau, Switzerland). The amount of water varied from 0.08 to 0.64 mass %, and it was considered for calculating the water concentration in solutions.

An electronic hygrometer AQUA-LAB CX-2 (DECAGON, Device Inc., Pullmann, USA) previously calibrated with saturated salt solutions was used for measuring the a_w. The temperature inside the hygrometer was regulated at the desired ±0.1 °C by circulation of thermostated water from water bath (Cole Parmer Instruments Co., Chicago, USA). Measurements were made in triplicate with a reproducibility of ±0.001 a_w units.

2.4 Results and Discussion

2.4.1 Water activity

The experimental water activity data obtained in this work for the binary and ternary mixtures are given in Tables 2.1 and 2.2, respectively. The concentrations are in mass fraction. For the same mass concentration, it was observed that the polyols with low molecular weight are better water activity depressors than those with high molecular weight. This difference is well visualized at high solute concentrations. The change of a_w with temperature is small. As can be seen in Figure 2.1, the experimental data for the system containing glycerol are in very good agreement with the available literature data (Scatchard *et al.*, 1938) which were measured using the isopiestic method. The mean relative deviation between these two data sets is 0.1%. Such result confirms the accuracy of experimental a_w data measured using the AQUA-LAB CX-2 (DECAGON Devices Inc., Pullman, USA). Similar results were also reported by Velezmoro *et al.* (2000) and Ninni *et al.* (1999a) for sugar solutions and poly(ethylene glycol) solutions, respectively. The work of Roa and Daza (1991) also emphasizes a good performance of a prior version of this electronic hygrometer (AQUA-LAB CX-1) for measuring water activity for various kinds of food systems.

Table 2.1. Water activity in binary polyol solutions as a function of mass fraction of polyol (w_2)

water (1) + sorbitol (2)						water (1) + mannitol (2)			
10.0°C		25.0°C		35.0°C		25.0°C		35.0°C	
w_2	a_w	w_2	a_w	w_2	a_w	w_2	a_w	w_2	a_w
0.0519	0.996	0.0497	0.997	0.0495	0.996	0.0510	0.996	0.0501	0.995
0.0992	0.992	0.0993	0.992	0.0995	0.991	0.1036	0.991	0.0751	0.992
0.1986	0.979	0.1491	0.986	0.1985	0.978	0.1263	0.987	0.1035	0.989
0.2965	0.960	0.1978	0.977	0.2982	0.961	0.1501	0.985	0.1246	0.987
0.3966	0.934	0.2485	0.970	0.3953	0.937	0.1750	0.982	0.1467	0.983
0.4918	0.899	0.2980	0.960	0.4944	0.901			0.1745	0.980
0.5952	0.844	0.3478	0.949	0.5706	0.862				
		0.3974	0.935	0.6946	0.755				
		0.4468	0.919						
		0.4966	0.897						
		0.5466	0.872						
		0.5955	0.843						
		0.6457	0.803						

Table 2.1 (cont.)

water (1) + xylitol (2)						water (1) + erythritol (2)			
10.0°C		25.0°C		35.0°C		25.0°C		30.0°C	
w_2	a_w	w_2	a_w	w_2	a_w	w_2	a_w	w_2	a_w
0.0502	0.996	0.0501	0.993	0.0502	0.994	0.0500	0.992	0.0486	0.993
0.1020	0.989	0.0997	0.988	0.1011	0.987	0.1095	0.982	0.0966	0.985
0.2005	0.974	0.1499	0.981	0.1510	0.980	0.1547	0.973	0.1501	0.975
0.3009	0.951	0.1997	0.972	0.2033	0.971	0.2002	0.963	0.2022	0.964
0.3906	0.925	0.2496	0.963	0.2504	0.962	0.2524	0.950	0.2334	0.956
0.5021	0.876	0.2983	0.951	0.2996	0.951	0.2996	0.936	0.2914	0.940
0.5423	0.854	0.3496	0.937	0.3479	0.938	0.3470	0.922	0.3345	0.926
		0.3995	0.921	0.3990	0.922	0.3690	0.912		
		0.4492	0.901	0.4489	0.903				
		0.4995	0.878	0.4969	0.880				
		0.5489	0.849	0.5533	0.850				
		0.5991	0.816	0.5670	0.840				
		0.6490	0.774	0.5993	0.818				

water (1) + glycerol (2)			
25.0°C		35.0°C	
w_2	a_w	w_2	a_w
0.0506	0.991	0.0498	0.990
0.0999	0.980	0.1001	0.979
0.1498	0.967	0.1499	0.967
0.1999	0.952	0.1996	0.953
0.2502	0.936	0.2496	0.937
0.3002	0.918	0.2995	0.919
0.3495	0.896	0.3494	0.897
0.3994	0.872	0.3995	0.874
0.4497	0.844	0.4491	0.847
0.4992	0.812	0.4986	0.816
0.5491	0.775	0.5489	0.780
0.5993	0.733	0.5970	0.740
0.6495	0.683	0.6487	0.689
0.6989	0.628	0.6987	0.632
0.7489	0.557		
0.7986	0.483		
0.8487	0.399		

Table 2.2. Water activity in ternary polyol solutions at 25.0ºC

water(1)+xylitol(2)+sorbitol(3)			water(1)+glycerol(2)+mannitol(3)			water(1)+glycerol(2)+sorbitol(3)		
w_2	w_3	a_w	w_2	w_3	a_w	w_2	w_3	a_w
0.0264	0.0249	0.993	0.0254	0.0250	0.991	0.0254	0.0254	0.993
0.0494	0.0491	0.988	0.0376	0.0383	0.988	0.0511	0.0501	0.984
0.0765	0.0756	0.981	0.0509	0.0511	0.982	0.1002	0.1152	0.961
0.1005	0.0994	0.973	0.0610	0.0605	0.979	0.1491	0.1490	0.938
0.1259	0.1245	0.965	0.0770	0.0761	0.974	0.2105	0.1958	0.897
0.1493	0.1485	0.954	0.0872	0.0866	0.970	0.2626	0.2389	0.848
0.1764	0.1779	0.940				0.3039	0.2960	0.780
0.1911	0.1904	0.932				0.3501	0.3480	0.684
0.2266	0.2229	0.908						
0.2494	0.2482	0.887						
0.3013	0.2974	0.827						
0.3262	0.3226	0.787						

water(1)+glycerol(2)+xylitol(3)			water(1)+xylitol(2)+mannitol(3)			water(1)+erythritol(2)+mannitol(3)		
w_2	w_3	a_w	w_2	w_3	a_w	w_2	w_3	a_w
0.0255	0.0251	0.992	0.0249	0.0250	0.993	0.0249	0.0250	0.994
0.0525	0.0505	0.982	0.0499	0.0500	0.987	0.0499	0.0498	0.987
0.1029	0.1023	0.960	0.0749	0.0750	0.980	0.0750	0.0749	0.979
0.1498	0.1503	0.895	0.0999	0.0999	0.972	0.0999	0.1004	0.971
0.2040	0.1977	0.871	0.1248	0.1249	0.964	0.1246	0.1245	0.959
0.2988	0.2998	0.772	0.1398	0.1399	0.957	0.1397	0.1398	0.953
0.3246	0.3249	0.726						

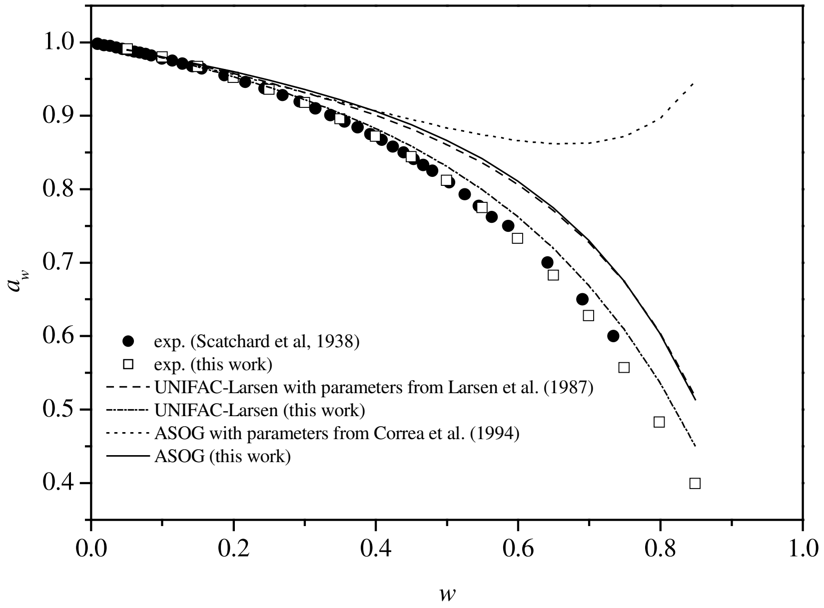

Figure 2.1. Prediction of water activities in the glycerol – water system.

The prediction of water activity using different versions of the UNIFAC model (Fredenslund *et al.*, 1975; Larsen *et al.*, 1987) and the ASOG model (Kojima and Tochigi, 1979) was carried out as a first estimate. The group assignments utilized for the polyols in the various attempts are summarized in Table 2.3. It was observed that the models were not sufficiently accurate to predict values of a_w at high solute concentrations. This poor estimation is attributed to the effect of strongly polar hydroxyl groups bounded to consecutive carbon atoms in the molecule. This suggests that there is an intramolecular proximity effect between these constituent groups, as proposed by Wu and Sandler (1991a, 1991b) and Abildskow *et al.* (1996). Another reason, also relative to chemical structure of the polyols, could be referred to the models being unable to distinguish between the molecular structure of isomers (mannitol and sorbitol).

Table 2.3. Group assignment for polyols

	UNIFAC^a	UNIFAC^b (v_k^i)	ASOG^c	
	v_k^i	v_k^i	v_k^i	v_i^{FH}
glycerol	1CHOH, 2CH_2OH	2CH_2, 1CH, 3OH	2.8CH_2, 3POH	6
meso-erythritol	2CHOH, 2CH_2OH	2CH_2, 2CH, 4OH	3.6CH_2, 4POH	8
xylitol	3CHOH, 2CH_2OH	2CH_2, 3CH, 5OH	4.4CH_2, 5POH	10
D-mannitol	4CHOH, 2CH_2OH	2CH_2, 4CH, 6OH	5.2CH_2, 6POH	12
D-sorbitol	4CHOH, 2CH_2OH	2CH_2, 4CH, 6OH	5.2CH_2, 6POH	12

^{a} CH_2OH, CHOH are groups proposed by Wu and Sandler (1991a, b). ^{b} CH_2, CH, OH are groups proposed by Skjold-Jorgensen *et al.* (1979). ^{c} POH is a group proposed by Correa *et al.* (1994). v_k^i is the number of groups *k* in molecule *i*. v_i^{FH} is the number of atoms (other than hydrogen atoms) in molecule *i*.

For the ASOG model with parameters from Correa *et al.* (1994), the predictions were similarly poor. This could be a consequence of using a restricted range of solute concentrations for the adjustment of the parameters. This was well observed in the system containing glycerol, which presented a mean deviation of 0.8% in a restricted range of water activity (0.998 to 0.875) but a high deviation (15,6%) for the whole concentration range studied in this work (see Figure 2.1).

An average relative deviation, including all experimental a_w values from this work and from the literature (Scatchard *et al.*, 1938; Robinson and Stockes, 1961; Bower and Robinson, 1963), was found as 2.1 % for the ASOG model (with parameters from Correa *et al.* (1994)); 1.2% for the original UNIFAC model (Skjold-Jorgensen *et al.*, 1979) and 1.8% when the UNIFAC-Larsen model (Larsen *et al.*, 1987) was used in the predictions.

On the basis of these results and considering the proximity effect of the hydroxyl groups, some of the UNIFAC and ASOG interaction parameters were readjusted.

2.4.2 Readjustment of group interaction parameters

To readjust some of the interaction parameters of the UNIFAC and ASOG models, different strategies were used. In the UNIFAC model, we have used the original equation and the UNIFAC-Larsen version. For each version we have assumed two alternatives for the division of groups: the first one proposed by Wu and Sandler (1991a,b) and the second one suggested by Skjold-Jorgensen *et al.* (1979), (see Table 2.3). For the ASOG model we have used the group assignment proposed by Correa *et al.* (1994). The binary interaction parameters readjusted in this work are given in Tables 2.4 and 2.5 for the UNIFAC-Larsen and ASOG models, respectively.

Table 2.4. UNIFAC-Larsen interaction parameters

	CH_2	CH	OH	H_2O
CH_2		0.0	972.8[b]	1857.0[b]
CH	0.0		972.8[b]	1857.0[b]
OH	637.5[b]	637.5[b]		278.7[a]
H_2O	410.7[b]	410.7[b]	-175.9[a]	

[a] Parameters readjusted in this work. [b] Parameters obtained from Larsen *et al.* (1987).

Table 2.5. ASOG interaction parameters

	CH_2	POH	H_2O	
CH_2		2434.7[a]	-277.3[b]	*n*
		-9.0831[a]	-0.2727[b]	*m*
POH	-2.3184[a]		-42.76[a]	*n*
	-3.2184[a]		-0.2868[a]	*m*
H_2O	-2382.7[b]	257.5[a]		*n*
	0.5045[b]	-0.6705[a]		*m*

[a] Parameters readjusted in this work. [b] Parameters obtained from Kogima and Tochigi (1979).

The other group interaction parameters were set equal to the values available in the literature (Kogima and Tochigi, 1979; Skjold-Jorgensen, 1979; Larsen *et al.*, 1987), and they are also given in Tables 2.4 and 2.5 for the UNIFAC-Larsen and ASOG models. To readjust some of the parameters, the Marquardt method (Marquardt, 1963) was used for minimizing the following objective function (OF)

$$OF = \sum_{n} \frac{\left| a_{w_{calc}} - a_{w_{exp}} \right|}{a_{w_{exp}}} + \sum_{k} \frac{\left| sol_{cal} - sol_{exp} \right|}{sol_{exp}} \tag{2.1}$$

where *n* and *k* are the number of experimental water activity and solubility data, respectively; sol is the solubility; and the subscripts calc and exp mean calculated and experimental values. The systems used for readjusting the interaction parameters are given in Table 2.6.

Table 2.6. Systems used for readjusting the group interaction parameters

aqueous system	temp range/^{o}C	reference data
	Water Activity	
D-sorbitol	10-35	this work
D-sorbitol	25	Bower and Robinson, 1963
D-mannitol	25-35	this work
D-mannitol	25	Robinson and Stokes, 1961
xylitol	10-35	this work
meso-erythritol	25-30	this work
	Solubility	
D-sorbitol	0-50	Mullin, 1993; Billaux *et al.*, 1991
D-mannitol	0-100	Mullin, 1993; Billaux *et al.*, 1991
xylitol	20-50	Billaux *et al.*, 1991
erythritol	20-25	Röper *et al.*, 1993

The best results were obtained using the UNIFAC-Larsen model with the group assignment proposed by Skjold-Jorgensen *et al.* (1979). The results calculated by both the UNIFAC-Larsen and ASOG models are shown in Figures 2.2 – 2.4 for the binary systems of xylitol, D-sorbitol, and D- mannitol. The UNIFAC-Larsen model was capable of providing good results even at high solute concentrations. Moreover, in comparison with the obtained results from Correa *et al.* (1994), the readjustment of the ASOG parameters between the POH group and the other mixture constituent groups improved the calculated a_w values for these systems. In these cases, the use of a wide range of solute concentrations and different types of polyols makes it possible to attain significant interaction parameters for use in calculation of the thermodynamical properties studied.

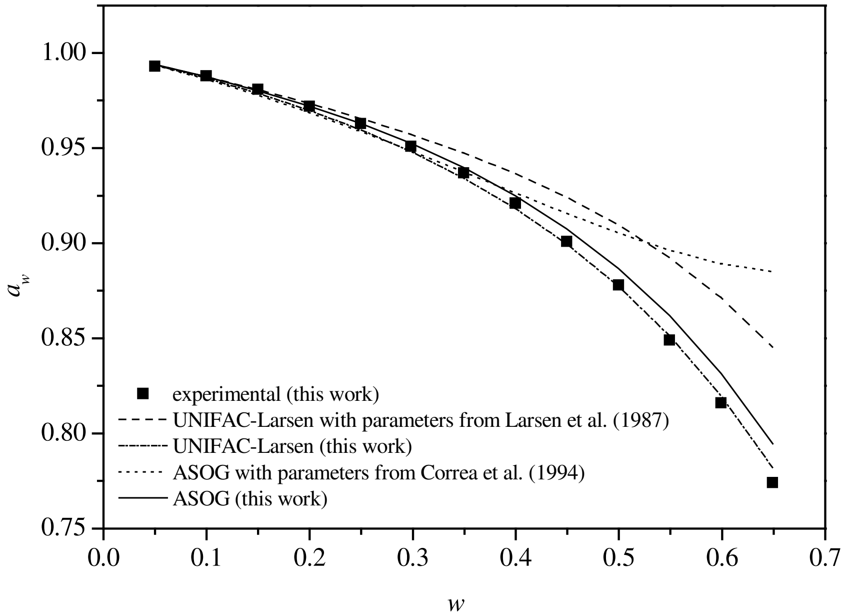

Figure 2.2. Experimental and calculated water activities for xylitol solutions at 25 °C.

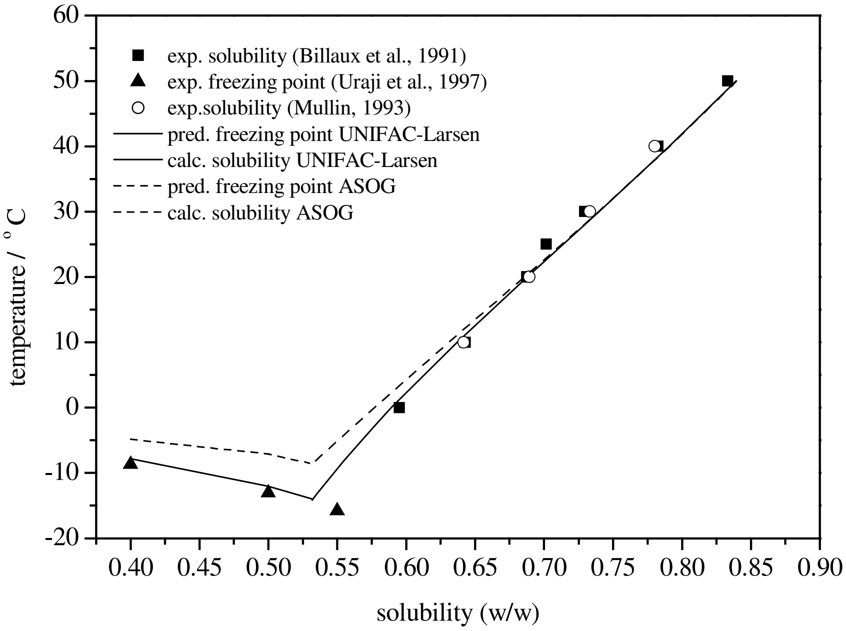

Figure 2.3. Solid-liquid equilibria for sorbitol aqueous solutions (solubility and freezing point depression).

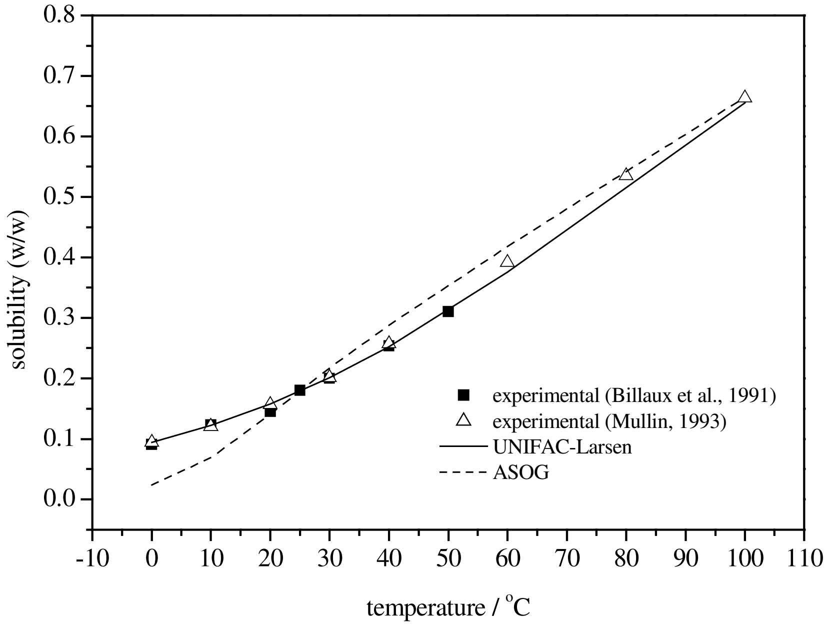

Figure 2.4. Experimental and calculated solubilities for D-mannitol at different temperatures.

Tables 2.7 shows a comparison between the average relative deviations obtained in this work and those from the literature for water activities. The deviations between experimental and calculated solubilities using the sets of parameters adjusted in this work are given in Table 2.8.

Table 2.7. Mean relative deviations between experimental and calculated a_w data points

aqueous system	% deviation				reference
	UNIFAC-Larsen		ASOG		
	Larsen et al. (1987)	this work	Correa et al. (1994)	this work	
D-sorbitol	2.51	0.51	3.04	0.64	this work
D-sorbitol	0.68	0.23	0.35	0.12	Bower and Robinson, 1963
D-mannitol	0.08	0.17	0.30	0.16	this work
D-mannitol	0.11	0.06	0.19	0.02	Robinson and Stockes, 1961
xylitol	2.01	0.26	2.11	0.76	this work
meso-erythritol	0.69	0.19	0.42	0.60	this work
avg deviation	1.01	0.24	1.07	0.38	

Table 2.8. Mean relative deviations between experimental and calculated solubility data

aqueous system	temperature range/°C	% deviation UNIFAC-Larsen	 ASOG	reference
D-sorbitol	0 - 50	0.91	1.32	Mullin,1993; Billaux et al., 1991
D-mannitol	0 - 100	1.86	20.80	Mullin, 1993; Billaux et al., 1991
xylitol	20 - 50	0.51	0.80	Billaux et al., 1991
erythritol	20 - 25	3.23	4.22	Röper et al., 1993
avg		1.63	6.79	

For the calculation of polyol solubility in water the same equation adopted by Peres and Macedo (1996, 1997) was used. The thermodynamic properties needed for the determination of solubilities are reported in Table 2.9 as well as the data used for water in the calculations of the freezing point depression of sorbitol and xylitol solutions. The values in bold type were used in this work. Table 2.9 also indicates published values for ΔC_p from the literature, and excluding the data for mannitol and erythritol, values were measured at only one temperature. There is only one literature source in which experimental C_p values were measured for a wide range of temperatures. These are for the solid and liquid phases of erythritol and mannitol (Spaght et al., 1932). The other cited literature (Barone *et al.* 1990) used a group contribution approach to estimate the C_p values for the liquid polyol. Moreover, in some cases, the experimental values taken from distinct literature sources are expressively different. For these reasons we opted for estimating ΔC_p as a linear function of temperature. This assumption was already used in previews works from Catté *et al.* (1994) and Peres and Macedo (1996, 1997) for systems containing sugars. The expression for representing the difference between the heat capacities of the pure liquid and those of the pure solid polyols (ΔC_p) is given below:

$$\Delta C_p = \Delta A + \Delta B \left(T - T_{ref}\right) \tag{2.2}$$

where T_{ref} is a reference temperature which was set equal to 25°C and where ΔA and ΔB are two adjustable parameters. The parameters ΔA and ΔB were adjusted for each polyol using the experimental solubilities at various temperatures taken from the literature (Billaux et al., 1991; Mullin, 1993; Röper, 1993). The values for ΔA and ΔB are presented in Table 2.10. It should be observed that the ΔA values estimated in this work are relatively close to the experimental ΔC_p

values at 25 °C. For instance, in the case of the UNIFAC-Larsen model (with the groups CH_2, CH, OH, and H_2O), a mean relative deviation of about 16% was found between the calculated values and the ΔC_p experimental data at 25 °C. In general, these deviations were higher for the other models used in this work. For example, in the case of the original UNIFAC model, the deviation between the ΔA and ΔC_p values amounts to approximately 35%. Furthermore, the minimum values for the deviation concerning solubility data were obtained for the UNIFAC-Larsen model (with the groups CH_2, CH, OH, and H_2O), as can be seen in Table 2.8.

Table 2.9. Thermodynamic data of polyols and water

polyol	melting temp, T_m/K	enthalpy of fusion, $\Delta_{fus}H$/kJ·mol^{-1}	ΔC_p (25°C)/ J·K^{-1}·mol^{-1}
sorbitol	**366.5**[a]	**30.2**	191[a]
mannitol	**439.1**[a]	**56.1**[a]	191[a]
	433.2[b]	53.58[b], 52.8[c]	290.36[b]
xylitol	**365.7**[a]	**37.4**[a]	157[a]
	367.0[d]	38.0[c]	
erythritol	**390.9**[a]	**39.4**[a]	122[a]
	391.6[b]	42.36[b]	155.42[b]
		40.3[c]	
water	**273.15**[e]	**6.002**[e]	**38.03**[e]

[a] Barone *et al.* (1990). [b] Spaght *et al.* (1932), (the values for ΔC_p are results from regression of the experimental data). [c] Raemy and Schweizer (1983). [d] Fassman (1975). [e] Daubert and Danner (1985), (the ΔC_p for water was considered constant with temperature).

Table 2.10. Values of ΔA and ΔB for the calculations of ΔC_p with linear temperature dependency

polyol	UNIFAC-Larsen		ASOG	
	ΔA	ΔB	ΔA	ΔB
	J·K^{-1}·mol^{-1}	J·K^{-2}·mol^{-1}	J·K^{-1}·mol^{-1}	J·K^{-2}·mol^{-1}
D-sorbitol	214.9	-2.9712	215.7	-4.1643
D-mannitol	215.0	0.0618	225.8	-0.2073
xylitol	128.0	3.3261	124.5	2.7738
meso-erythritol	117.2	1.0924	115.8	1.9598

It must be stressed that, for the UNIFAC-Larsen model, we readjusted only two temperature-independent interaction parameters between the groups OH/H_2O and H_2O/OH. Otherwise, for the ASOG model, better results were achieved only after the readjustment of four pairs of temperature-dependent interaction parameters.

2.4.3 Predictions with the new set of parameters

The experimental freezing point data available in the literature as well as the a_w values of the ternary systems and of the binary system containing glycerol were used only for comparison with predicted values. For freezing point calculations, an expression proposed by Ferro Fontan and Chirife (1981) was used. Table 2.11 indicates the average mean deviations obtained for the water activities of the ternary mixtures and the binary systems containing glycerol. It can be noted that the deviations for glycerol were higher than those for the ternary systems but significantly lower in comparison to the predictions with parameters from the literature (see Figure 2.1). Correa et al. (1994) have already commented about the difficulties in obtaining good results for the systems with glycerol. Figure 2.5 shows calculated and experimental a_w values for the ternary mixture xylitol-sorbitol-water at 25°C. However, the predictions of freezing point depression did not present the same accuracy, with mean deviations of 10% for the UNIFAC-Larsen model and 47% for the ASOG model. The experimental data are from Uraji *et al.* (1997), and the results achieved for sorbitol are also represented in Figure 2.3. The prediction of the eutectic points for xylitol and sorbitol aqueous solutions was also performed. These results are given in Table 2.12 for the ASOG and UNIFAC-Larsen models. Note that a good prediction for the eutectic point concentration was obtained for both systems.

Table 2.11. Water activity prediction in polyol mixtures

polyol mixture	a_w range	% deviation			
		UNIFAC-Larsen		ASOG	
		Larsen *et al.* (1987)	this work	Correa *et al.* (1994)	this work
xylitol+sorbitol	0.993 - 0.787	2.10	0.23	2.16	0.27
glycerol+mannitol	0.991 - 0.970	0.16	0.08	0.08	0.18
glycerol+sorbitol	0.993 - 0.684	3.99	0.95	2.63	2.63
glycerol+xylitol	0.992 - 0.726	4.48	1.87	3.65	3.65
xylitol+mannitol	0.993 - 0.957	0.35	0.09	0.17	0.14
erythritol+mannitol	0.994 - 0.953	0.37	0.13	0.16	0.12
glycerol	0.990 – 0.399	6.30	2.55	15.60	6.40
glycerol[a]	0.998 – 0.762	2.20	0.88	2.94	2.54
avg		2.49	0.85	4.21	1.99

[a] Scatchard *et al.* (1938).

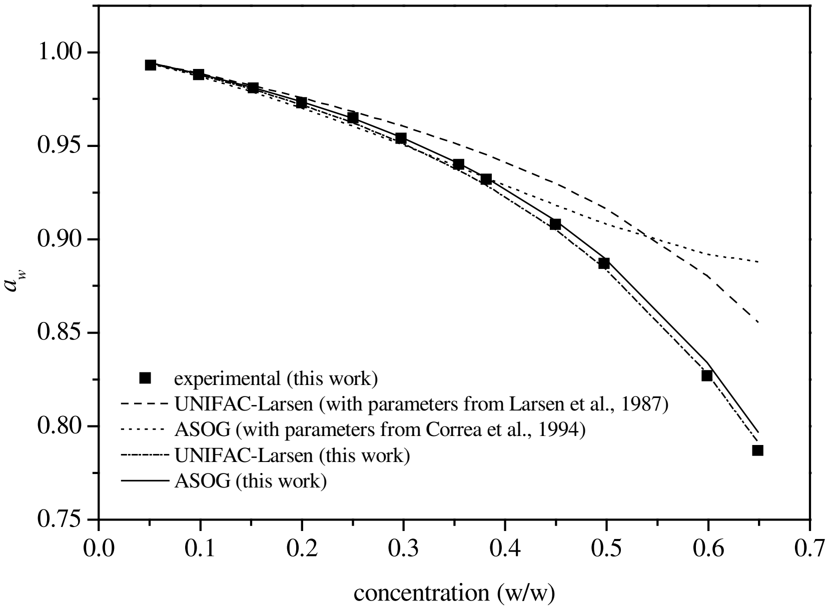

Figure 2.5. Predictions of water activities for the ternary system water – xylitol – sorbitol at 25.0 °C.

Table 2.12. Experimental and calculated eutetic points of xylitol and sorbitol aqueous solutions

	experimental		ASOG		UNIFAC-Larsen	
	T/°C	conc/(*w*/*w*)	*T*/°C	conc/(*w*/*w*)	*T*/°C	conc/(*w*/*w*)
xylitol	-12.2	0.43	-5.3	0.43	-10.8	0.44
sorbitol	-15.5	0.54	-8.5	0.53	-13.9	0.53

2.5 Literature Cited

Abildskov, J.; Constantinou, L.; Gani, R. Towards the development of a second-order approximation in activity coefficient models based on group contributions. *Fluid Phase Equilib.* **1996**, 118, 1 – 12.

Barone, G.; Della Gatta, G.; Ferro, D.; Piacente, V. Enthalpies and entropies of sublimation, vaporization and fusion of nine polyhydric alcohols. *J. Chem. Soc. Faraday Trans.* **1990**, 86, 75 – 79.

Billaux, M.S.; Flourie, B., Jacquimin, C. Sugar alcohols. *In: Handbook of sweeteners*; Marie, S., Piggott, J.R., Eds.; Glasgow: Blackie: New York, 1991.

Bower, V.E.; Robinson, R.A. Isopiestic vapour pressure measurements of the ternary system: sorbitol-sodium chloride-water at 25°C. *J. Phys. Chem.* **1963**, 67, 1540 – 1541.

Catté, M.; Dussap, C-G; Achard, C.; Gros, J-B. Excess properties and solid-liquid equilibria for aqueous solutions of sugars using UNIQUAC model. *Fluid Phase Equilib.* **1994**, 96, 33 – 50.

Correa, A.; Comesaña, J.F.; Sereno, A.M. Measurement of water activity in water-urea-sugar and water-urea-polyol systems, and its prediction by the ASOG group contribution method. *Fluid Phase Equilib.* **1994**, 98, 189 – 199.

Daubert, T.E.; Danner, R.P. *Data Compilation Tables of Properties of Pure Compounds*; AIChE/DIPPR: New York, 1985.

Fassman, G.D. *Handbook of biochemistry and molecular biology*, CRC Press: Cleveland, OH, 1975.

Ferro Fontan, C.; Chirife, J. The evaluation of water activity in aqueous solutions from freezing point depression. *J. Food Technol.* **1981**, 16, 21 – 30.

Fredenslund A.; Jones R.L.; Prausnitz, J.M. Group contribution estimation of activity coefficients in nonideal liquid mixtures. *AIChE J.* **1975**, 21, 1086 – 1099.

Kojima, K.; Tochigi, K. *Prediction of Vapour-Liquid Equilibria by the ASOG Method*, Elsevier: Tokyo, 1979.

Larsen, B.L.; Rasmussen, P.; Fredenslund, A. A modified UNIFAC group contribution model for prediction of phase equilibria and heats of mixing. *Ind. Eng. Chem. Res.* **1987**, 26, 2274 – 2286.

Marquardt, D.W. An algorithm for least-squares estimation of nonlinear parameters. *J. Soc. Indust. Appl. Math.* **1963**, 11, 431 – 441.

Mullin J.W. *Crystallization*, Butherworth – Heinemann: New York, 1993.

Ninni, L.; Camargo, M.S.; Meirelles, A.J.A. Water activity in poly(ethylene glycol) aqueous solutions. *Thermochim. Acta* **1999a**, 328, 169 – 176.

Ninni, L.; Camargo, M.S.; Meirelles, A.J.A. Modeling and prediction of pH and water activity in aqueous amino acid solutions. *Computers and Chemical Engineering* **1999b**, 23 (supplement) S383 – S386.

Peres, A.M.; Macedo, E.A. Thermodynamic properties of sugars in aqueous solutions: correlation and prediction using a modified UNIQUAC model. *Fluid Phase Equilib.* **1996**, 123, 71 – 95.

Peres, A.M.; Macedo, E.A. A modified UNIFAC model for the calculation of thermodynamic properties of aqueous and non-aqueous solutions containing sugars. *Fluid Phase Equilib.* **1997**, 139, 47 – 74.

Raemy, A.; Schweizer, T.F. Thermal behaviour of carbohydrates studied by heat flow calorimeter. *J. Therm. Anal.* **1983**, 28, 95 – 108.

Roa, V.; Daza, M.S.T. Evaluation of water activity measurements with a dew point electronic humidity meter. *Lebensm.-Wiss. Technol.* **1991**, 24, 208 –213.

Robinson, R.A.; Stockes, R.H. Activity coefficients in aqueous solutions of sucrose, mannitol and their mixtures at 25°C. *J. Phys. Chem.* **1961**, 65, 1954 – 1958.

Röper, H.; Goossens, J. Erythritol, a new material for food and non-food applications. *Starch* **1993**, 11, 400 – 405.

Scatchard, G.; Hamer, W.J.; Wood, S.E. Isotonic solutions. 1. The chemical potencial of water in aqueous solutions of sodium chloride, potassium chloride, sulphuric acid, sucrose, urea and glycerol at 25°C. *J. Am. Chem. Soc.* **1938**,60, 3061 – 3070.

Skjold-Jorgensen, S.; Kolbe, B; Gmehling, J.; Rasmussen, P. Vapor-liquid equilibria by UNIFAC group contribution. Revision and extension. *Ind. Eng. Chem. Process Des. Dev.* **1979**, 18, 714 – 722.

Spaght, M.E.; Thomas, S.B.; Parks, G.S. Some heat capacity data on organic compounds obtained with a radiation calorimeter. *J. Phys. Chem.* **1932**, 36, 882 – 888.

Uraji, T.; Kohno, H.; Nakashima, K.; Shimoyamada, M.; Watanabe, K. Thermal Analyses of polyol-aqueous solutions below 0°C by differential scanning calorimetry. *J. Japanese Soc. Food Sci. Tech.* **1997**, 44, 380 – 385.

Velezmoro, C.; Meirelles, A.J.A. Water activity in solutions containing organic acids. *Drying Technol.* **1998**, 16, 1789 –1805.

Velezmoro, C.; Meirelles, A.J.A.; Vitali, A. Engineering and Food at ICEF 7, Proceedings of the Seventh International Congress on Engineering and Food, Part 1, Brighnton, UK, **1997**, p. A145.

Wu, H.S.; Sandler, S.I. Use of ab initio quantum mechanics calculations in group contribution methods. 1. Theory and the basis for group identifications. *Ind. Eng. Chem. Res.* **1991a**, 30, 881 – 889.

Wu, H.S.; Sandler, S.I. Use of ab initio quantum mechanics calculations in group contribution methods. 2. Test of new groups in UNIFAC. *Ind. Eng. Chem. Res.* **1991b**, 30, 881 – 897.

2.6 Acknowledgment

This work was supported financially by research grants from Fundação de Amparo à Pesquisa do Estado de São Paulo (FAPESP - Proc. 95/02617-5) and Conselho Nacional de Desenvolvimento Científico e Tecnológico (CNPq - Proc. 521011/95-7).

Capítulo 3

WATER ACTIVITY, PH AND DENSITY OF AQUEOUS AMINO ACIDS SOLUTIONS

Luciana Ninni, Antonio J. A. Meirelles

Department of Food Engineering (DEA/FEA), Faculty of Food Engineering, State University of Campinas (UNICAMP), Cidade Universitária "Zeferino Vaz", PO Box 6121, Zip Code 13083-970, Campinas, SP, Brasil

Trabalho publicado na revista *Biotechnology Progress*, v. 17 (4), p. 703 – 711, 2001.

3. Water Activity, pH and Density of Aqueous Amino Acids Solutions

3.1 Abstract

The water activity, pH and density of some aqueous amino acid solutions were determined at 25 °C in three different types of solvents. Previous published experimental data on water activity and solubility of amino acids in aqueous solutions were used together with data from this work to test the applicability of a group contribution model. The activity coefficients were estimated by the UNIFAC-Larsen model combined with the Debye-Hückel equation, taking also into account the partial dissociation phenomena of species in solution. Interaction energies between the charged species Na^+ and Cl^- and the specific groups of amino acids (COOH and NH_2) were adjusted using experimental solubility data.

3.2 Introduction

The crescent advances in the biotechnological industry have raised interest for the development of efficient separation, concentration and purification processes of biomolecules. In the design of equipments and processes it is necessary the knowledge of some physical-chemical properties such as solubility, water activity (a_w) and the influence of different pH values on these properties in mixtures containing biomolecules. Among the biochemicals, amino acids are of much research interest because of their simplicity and importance for understanding the behavior of molecules such as peptides and proteins in more complex solutions. In general the amino acids are produced by microorganisms in aqueous media containing solutes like salts, organic acids, etc. Thus, it is relevant to study the physical-chemical properties of systems containing such compounds at various concentrations and pH values.

In this work we present experimental data on water activity, pH and density of aqueous solutions containing the amino acids glycine, dl-alanine, l-arginine and l-proline in three different types of solvents: water, acid and basic buffers. The iterative procedure proposed by Achard *et al.* (1994a) was utilized for modeling the properties (a_w, pH, and solubility), considering the partial dissociation of the amino acids and the other solutes that form the aqueous systems. The UNIFAC-Larsen model and the Debye-Hückel equation were associated with this procedure to allow for the non-ideality of the systems studied. Such approach has been successfully applied to other aqueous solutions of weak electrolytes like citric, tartaric and malic acids for the prediction of water activity and pH of those solutions (Maffia and Meirelles, 2000; Velezmoro and Meirelles, 1998).

Moreover, the procedure mentioned above is further tested by using a comprehensive data bank on other physical-chemical properties of amino acid solutions available in the literature. Data on solubility of amino acids in water, buffers and salt solutions were included in this data bank. The objective of the work reported here is to test and extend the procedure proposed by Achard *et al.* (1994a,b) to the estimation of physical-chemical properties of amino acid solutions. In contrast to prior works the present study takes into account a more comprehensive data bank on different physical-chemical properties of amino acid solutions and model these properties considering the partial dissociation of weak electrolytes.

3.3 Materials and Methods

3.3.1 Materials

Samples of the amino acids glycine, dl-alanine, l-arginine and l-proline were supplied by Merck with purity greater than 99 mass %. No further purification was employed. Other chemicals of >99 mass % purity (NaOH, citric acid and sodium citrate) were also purchased from Merck and used to prepare the buffer systems. Solutions were prepared gravimetrically with deionised water (Millipore, USA) using an analytical balance (Sartorius, Germany) with precision of 1×10^{-4} g. The compositions were accurate to ± 0.0001 approximately in mass fraction.

3.3.2 Experimental Procedure

Water activity was measured at 25.0±0.1 °C and pH at room temperature (24.7±0.3 °C) at various solute concentrations. The influence of pH on water activity was also verified by the use of acidic and basic buffer solutions. The buffers were prepared with citric acid/sodium citrate and glycine/NaOH, resulting in 3.09 and 9.22 pH values, and 0.0113 (ratio: 0.0084 citric acid/0.0029 sodium citrate) and 0.0043 (ratio: 0.0038 glycine/0.0005 NaOH) total solid mass fractions, respectively.

The pH was measured with a Chem Cadet 5986-50 pH meter (Cole-Parmer Instrument Co., USA) calibrated with buffer solutions (pH=4 and 7) supplied by Merck, and the results used later in the modeling of this property. The mean standard deviation obtained for the whole set of experimental data was 0.02 pH units. An electric hygrometer AQUA-LAB CX-2 (Decagon, USA) previously calibrated with saturated salt solutions (analytical grade reagents from Merck, >99 mass % purity: potassium sulfate, potassium chloride, sodium chloride and potassium carbonate) was used for measuring a_w. The temperature inside the hygrometer was regulated at 25.0 ± 0.1 °C by circulation of thermostated water from a water bath (Cole Parmer Instrument Co., USA). Measurements were made in triplicate with a reproducibility of ± 0.001 a_w units. Density measurements were carried out in triplicate using a digital densimeter (DMA 58, Anton Paar, Austria) (for the systems amino acid + buffer) and a picnometer (for the systems amino acid + water) at 25.0±0.1 °C. The digital densimeter was calibrated with air and water as standards while the picnometer was calibrated with water at the corresponding working temperature. The accuracy of the density measurements was estimated as 3×10^{-5} and 3×10^{-4} g cm^{-3} for the digital densimeter and picnometer, respectively. Experimental density measurements were performed in the systems cited above for the conversion of solute mass fractions into molar concentrations.

3.3.3 Experimental Results

Experimental water activity, pH and density data for the amino acid solutions are summarized respectively in Tables 3.1 to 3.3. Kuramochi *et al.* (1997b) measured the partial pressure of water for glycine and alanine aqueous solutions. The corresponding experimental water activity data for glycine were compared to the data determined in the present work (see Figure 3.1). The mean relative deviations between both data sets were 0.151% for glycine and 0.051% for alanine, resulting in an average value of 0.101% for both amino acid solutions.

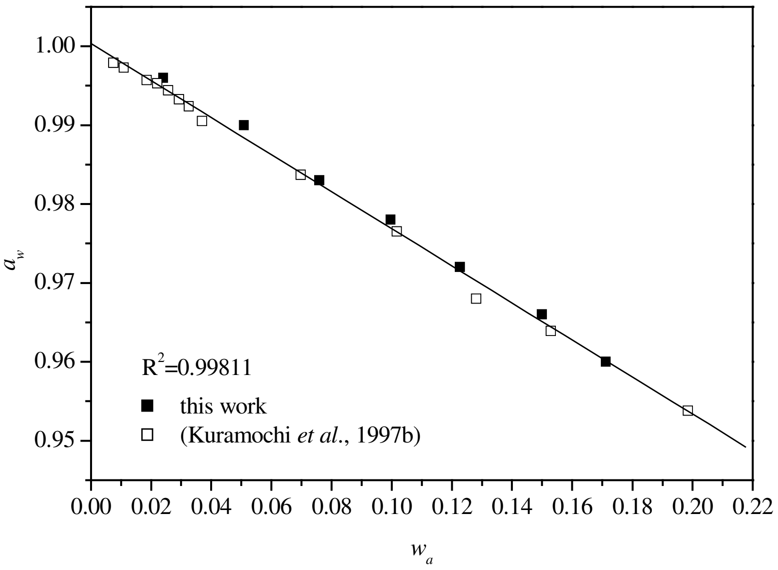

Figure 3.1. Water activities determined in the present work and data taken from ref 5 for the amino acid glycine.

Table 3.1. Experimental water activities of glycine, dl-alanine, l-arginine and proline as a function of amino acid mass fraction (w_a), at 25.0 ±0.1 °C

w_a	a_w	w_a	a_w	w_a	a_w
glycine + water		glycine + acid buffer		glycine + basic buffer	
0.0241	0.996	0.0252	0.993	0.0309	0.992
0.0505	0.990	0.0496	0.988	0.0573	0.985
0.0759	0.983	0.0714	0.982	0.0772	0.981
0.0997	0.978	0.0996	0.975	0.0997	0.975
0.1227	0.972	0.1210	0.970	0.1233	0.970
0.1500	0.966	0.1481	0.963	0.1484	0.964
0.1712	0.960	0.1713	0.957	0.1770	0.956
dl-alanine + water		dl-alanine + acid buffer		dl-alanine + basic buffer	
0.0251	0.995	0.0247	0.994	0.0243	0.993
0.0503	0.990	0.0498	0.990	0.0530	0.988
0.0677	0.987	0.0615	0.987	0.0640	0.985
0.0766	0.985	0.0752	0.984	0.0721	0.982
0.1000	0.979	0.0889	0.981	0.0865	0.980
0.1237	0.974	0.0981	0.979	0.0945	0.978
0.1353	0.971	0.1195	0.973	0.1242	0.971
		0.1315	0.971		
l-proline + water		l-proline + acid buffer		l-proline + basic buffer	
0.0504	0.992	0.0495	0.991	0.0498	0.993
0.0961	0.983	0.0918	0.983	0.0943	0.983
0.1503	0.972	0.2021	0.957	0.2003	0.958
0.2002	0.959	0.2951	0.923	0.2936	0.924
0.2501	0.944	0.4025	0.866	0.3355	0.905
0.2942	0.927	0.4900	0.799		
0.3497	0.901				
0.3799	0.886				
l-arginine + water		l-arginine + acid buffer		l-arginine + basic buffer	
0.0253	0.998	0.0247	0.998	0.0258	0.997
0.0376	0.997	0.0498	0.996	0.0494	0.994
0.0500	0.996	0.0616	0.995	0.0545	0.993
0.0597	0.995	0.0748	0.994	0.0744	0.991
0.0755	0.994	0.0863	0.992	0.0873	0.990
0.0876	0.992	0.0997	0.990	0.0996	0.989
0.1006	0.992	0.1110	0.991	0.1123	0.988
0.1127	0.990	0.1244	0.988	0.1233	0.986
0.1239	0.989				

Table 3.2. Experimental pH of glycine, dl-alanine, l-arginine and l-proline in water and in basic and acid buffers (w_a=amino acid mass fraction) 24.7 ±0.3 °C

w_a	pI	w_a	acid buffer	w_a	basic buffer
		glycine			
0.0241	5.79	0.0252	3.75	0.0309	8.31
0.0505	5.81	0.0496	3.95	0.0573	7.99
0.0759	5.86	0.0714	4.06	0.0772	7.89
0.0997	5.92	0.0996	4.19	0.0997	7.78
0.1227	5.96	0.1210	4.27	0.1233	7.69
0.1500	5.97	0.1481	4.36	0.1484	7.65
0.1712	5.99	0.1713	4.46	0.1770	7.58
		dl-alanine			
0.0251	5.71	0.0247	3.67	0.0243	8.58
0.0503	5.75	0.0498	3.90	0.0530	8.25
0.0677	5.78	0.0615	3.92	0.0640	8.17
0.0766	5.80	0.0752	3.99	0.0721	8.11
0.1000	5.88	0.0889	4.04	0.0865	8.04
0.1237	5.91	0.0981	4.10	0.0945	8.01
0.1353	5.95	0.1195	4.20	0.1242	7.84
		0.1315	4.21		
		l-proline			
0.0504	6.15	0.0495	3.62	0.0498	8.81
0.0961	6.21	0.0918	3.82	0.0943	8.61
0.1503	6.32	0.2021	4.22	0.2003	8.32
0.2002	6.39	0.2951	4.52	0.2936	8.21
0.2501	6.46	0.4025	4.88	0.3355	8.14
0.2942	6.52	0.4900	5.25		
0.3497	6.65				
0.3799	6.76				
		l-arginine			
0.0253	11.01	0.0498	9.49	0.0258	9.96
0.0376	11.03	0.0616	9.64	0.0494	10.08
0.0500	11.09	0.0748	9.77	0.0545	10.12
0.0597	11.13	0.0863	9.84	0.0744	10.25
0.0755	11.17	0.0997	9.93	0.0873	10.38
0.0876	11.20	0.1110	10.00	0.0996	10.42
0.1006	11.23	0.1244	10.09	0.1123	10.44
0.1127	11.25			0.1233	10.52
0.1239	11.27				

Table 3.3. Densities of aqueous solutions of glycine, dl-alanine, l-arginine and l-proline as a function of total solute mass fraction (w_t), 25.0 ±0.1 °C[a]

w_t	ρ (g cm^{-3})	w_t	ρ (g cm^{-3})	w_t	ρ (g cm^{-3})
glycine + water		glycine + acid buffer		glycine + basic buffer	
0.0241	1.0069	0.0365	1.01249	0.0352	1.01283
0.0505	1.0195	0.0609	1.02283	0.0616	1.02453
0.0759	1.0283	0.0827	1.03221	0.0815	1.03282
0.0997	1.0402	0.1109	1.04395	0.1040	1.04262
0.1227	1.0505	0.1323	1.05320	0.1276	1.05341
0.1500	1.0590	0.1594	1.06450	0.1527	1.06379
0.1712	1.0718	0.1826	1.07421	0.1813	1.07590
dl-alanine + water		dl-alanine + acid buffer		dl-alanine + basic buffer	
0.0255	1.0053	0.0360	1.00991	0.0286	1.00578
0.0514	1.0137	0.0611	1.01783	0.0573	1.01458
0.1000	1.029	0.0728	1.02144	0.0683	1.01846
0.1157	1.0345	0.0865	1.02597	0.0764	1.02043
0.1237	1.0371	0.1002	1.03055	0.0908	1.02450
0.1352	1.0409	0.1094	1.03332	0.0988	1.02750
		0.1308	1.04010	0.1285	1.03661
		0.1428	1.04393		
l-proline + water		l-proline + acid buffer		l-proline + basic buffer	
0.0280	1.0048	0.0608	1.01572	0.0541	1.01281
0.0961	1.0250	0.1031	1.02796	0.0986	1.02576
0.1503	1.0398	0.2134	1.06098	0.2046	1.05680
0.2002	1.0551	0.3064	1.08851	0.2979	1.08500
0.2756	1.0766	0.4138	1.12111	0.3398	1.09632
0.2942	1.0841	0.5013	1.14700		
0.3497	1.1022				
0.3799	1.1097				
l-arginine + water		l-arginine + acid buffer		l-arginine + basic buffer	
0.0187	1.0022	0.0360	1.00848	0.0301	1.00626
0.0376	1.0077	0.0611	1.01641	0.0588	1.01379
0.0533	1.0118	0.0729	1.02052	0.0787	1.01896
0.0597	1.0133	0.0861	1.02416	0.1039	1.02512
0.0755	1.0178	0.0976	1.02777	0.1276	1.03288
0.0876	1.0219	0.111	1.03185		
0.1008	1.0250	0.1223	1.03467		
0.1127	1.0283	0.1357	1.03870		
0.1239	1.0315				

[a] w_t corresponds to total solute mass fraction considering the concentration of the amino acid (w_a) and the solutes of the buffers (w_b), i.e., $w_t = w_a + w_b$.

A very slight influence of pH on a_w values was noted for arginine, glycine, proline and alanine. The addition of buffer solutions containing a strong electrolyte (NaOH) or an acid/salt (citric acid/sodium citrate) solution gives rise to interactions between the amino acid groups and the ionic species from the acid, base or salt. The buffer solutions were used in very low concentrations (total buffer solutes weight fractions: 0.0113 and 0.0043 for acid and basic buffers, respectively) yielding a_w values equal to 0.999 measured by the electric hygrometer, at 25.0 °C. Therefore, there was no significant interference of the buffer solutions upon the a_w data measured in the present work through short-range type interactions. The presence of buffers containing ionizable species contributes to changes in the net charges of the amino acids according to pH value. As a consequence, it was observed that higher concentrations of the cationic and anionic species in solution lead to a slightly decrease in the a_w values.

Figure 3.2 shows a comparison between density data for aqueous solutions of dl-alanine and glycine at 25.0 °C reported in literature (Soto *et al.*, 1998; Dalton and Schmidt, 1933) and determined in this work. As can be seen, the agreement is very satisfactory (mean relative deviations equal to 0.07% and 0.004% for aqueous solutions of glycine and dl-alanine, respectively).

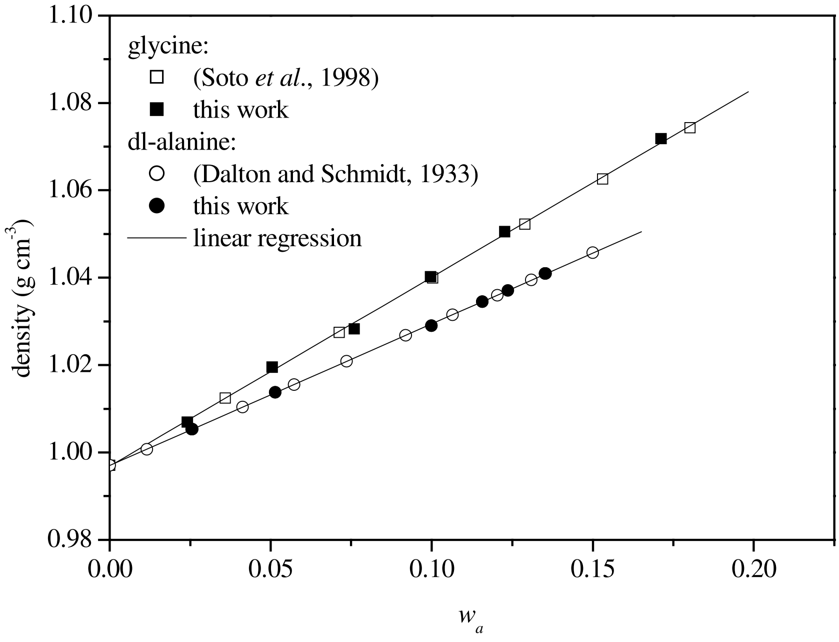

Figure 3.2. Comparison between experimental densities from literature and those determined in the present work.

3.4 Thermodynamic Modeling

3.4.1 Modified UNIFAC Model for Electrolytes

Recently, attention has been given to the modeling of phase behavior in aqueous systems containing biochemicals like amino acids (Khoshkbarchi and Vera, 1996, 1997; Kuramochi *et al.*, 1996, 1997a; Pradhan and Vera, 1998; Pinho *et al.*, 1994). In several publications, the non-ideality of such systems was represented either by local composition models (Nass, 1988; Chen *et al.*, 1989) or by group contribution models (Pinho *et al.*, 1994; Gupta and Heidemann, 1990; Ninni *et al.*, 1999). To account for the electrostatic forces in the amino acid solutions, the Debye-Hückel term (Pitzer, 1980) has been added to the activity coefficient models in some reported works in the literature (Pinho *et al.*, 1994; Peres and Macedo, 1994). In this work we used the model presented by Kuramochi *et al.* (1996, 1997a), based on the UNIFAC-Larsen model, combined with the Debye-Hückel term. Amino acids molecules were divided into several main groups including new group assignments proposed by the cited authors: α-CH_2 (alkane bounded to the α carbon atom in the amino acid molecule), sc-CH_2 (side chain alkane), NH_2 and COOH. In Table 4, the constituent groups of the amino acids considered in this work are given.

Table 3.4. Division of groups for the amino acids used in this work

amino acid	groups[a]
glycine[b]	α-CH_2, NH_2, COOH
l-arginine	α-CH, 2×scCH_2, COOH, NH_2, $C(NH_2)NH$, CH_2NH
dl-alanine	NH_2, α-CH, COOH, scCH_3
dl-valine	NH_2, COOH, α-CH, scCH, 2×scCH_3
serine	NH_2, COOH, α-CH, scCH_2, OH
l-proline	CH_2NH, COOH, α-CH, 2×scCH_2

[a] sc=side chain, α=group bounded to the α carbon in the molecule. [b] For the zwitterion glycine the groups are α-CH_2, NH_3^+, COO^-; for the anionic: α-CH_2, NH_2, COO^-; and for the cationic form: α-CH_2, NH_3^+, COOH.

The amino acids appear in various ionic forms - cationic, anionic and zwitterion - when dissolved in water according to the pH of the solution. For example, the distribution of the different ionic forms of the amino acid glycine as a function of pH was obtained by Max *et al.* (1998) using a numerical treatment of the infrared spectra data. The following species were observed for glycine in water: cationic (pH 0 to 5); zwitterion (pH 0 to 12.5) and anionic (pH 7 to 14).

For modeling the amino acid systems it is assumed that the constituent groups of the anionic and cationic species are the same as those of the zwitterion form (see Table 3.4). Structural parameters R_k and Q_k for the ionic groups of the amino acids were considered equal to the neutral ones. To estimate the concentrations of the different ionic forms present in solution, the iterative procedure proposed by Achard *et al.* (1994a) was utilized in the present work. The method takes into account the partial dissociation phenomena of the amino acids and combines equilibrium relations, mass and electroneutrality balances for calculating the true concentrations of the species and their activity coefficients. This set of equations requires initial solute and water concentrations, as well as equilibrium constants describing the chemical equilibrium. In aqueous solution, the following series of reactions takes place simultaneously when an amino acid is dissolved in an acidic buffer containing citric acid ($\mathrm{H_3citric}$)/sodium citrate ($\mathrm{Na_3citric}$):

$$\mathrm{NH_2RCOOH} \Leftrightarrow \mathrm{NH_3^+RCOO^-} \qquad K_D \tag{3.1}$$

$$\mathrm{NH_3^+RCOOH} \Leftrightarrow \mathrm{NH_3^+RCOO^-} + \mathrm{H^+} \qquad K_1 \tag{3.2}$$

$$\mathrm{NH_3^+RCOO^-} \Leftrightarrow \mathrm{NH_2RCOO^-} + \mathrm{H^+} \qquad K_2 \tag{3.3}$$

$$\mathrm{H_3citric} \Leftrightarrow \mathrm{H^+} + \mathrm{H_2citric^-} \qquad K_{A1} \tag{3.4}$$

$$\mathrm{H_2citric^-} \Leftrightarrow \mathrm{H^+} + \mathrm{Hcitric^{--}} \qquad K_{A2} \tag{3.5}$$

$$\mathrm{Hcitric^{--}} \Leftrightarrow \mathrm{H^+} + \mathrm{citric^{---}} \qquad K_{A3} \tag{3.6}$$

$$\mathrm{Na_3citric} \Rightarrow 3\,\mathrm{Na^+} + \mathrm{citric^{---}} \tag{3.7}$$

$$\mathrm{H_2O} \Leftrightarrow \mathrm{H^+} + \mathrm{OH^-} \qquad K_w \tag{3.8}$$

Reaction 3.1 corresponds to the formation of the zwitterion ($\mathrm{NH_3^+RCOO^-}$) with dual electric charges, which can originate the amino acid cationic and anionic species (reactions 3.2 and 3.3, respectively). The equilibrium constant K_D is generally very large (10^5 - 10^6). This means that the uncharged amino acid is almost completely converted to the zwitterion form. The equilibrium constants (K_i and K_{Ai}, i=1, 2...) can be obtained as: 10^{-pK}. Values for pK_i and pK_w used in this work were found in (Greenstein and Winitz, 1961; King, 1951; Smith *et al.*, 1937; Izatt and

Christensen, 1970). For the amino acids and water, the effect of the temperature on the equilibrium constants were taken into account by adjusting eq 3.9 to the available experimental data.

$$\mathrm{p}K_\mathrm{i} = \mathrm{A} + \frac{\mathrm{B}}{(T+\mathrm{C})} \tag{3.9}$$

where A, B and C are adjustable parameters and T the temperature in Kelvin. Values of A, B and C are given in Table 3.5. Dissociation constants ($\mathrm{p}K_\mathrm{Ai}$) for citric acid at 25 °C were found in (Izatt and Christensen, 1970) and their values are following: $\mathrm{p}K_\mathrm{A1}$=3.131; $\mathrm{p}K_\mathrm{A2}$=4.762; $\mathrm{p}K_\mathrm{A3}$=6.397.

Table 3.5. Coefficients for correlating pK values with temperature[a]

substance		A	B	C	deviation[b]
glycine	$\mathrm{p}K_1$	2.2641	3.6254	-256.2	0.071
	$\mathrm{p}K_2$	3.2125	1663.1	-44.88	0.004
dl-alanine	$\mathrm{p}K_1$	2.2839	3.1010	-252.4	0.008
	$\mathrm{p}K_2$	3.3074	1594.9	-55.04	0.010
l-proline	$\mathrm{p}K_1$	1.9489	0.1900	-271.1	0.155
	$\mathrm{p}K_2$	3.1602	2232.3	0.2012	0.011
dl-valine	$\mathrm{p}K_1$	2.2984	-0.0430	-276.14	0.272
	$\mathrm{p}K_2$	3.1443	1650.4	-47.11	0.009
dl-serine	$\mathrm{p}K_1$	1.9823	13.944	-229.7	0.015
	$\mathrm{p}K_2$	2.5850	1724.7	-37.73	0.003
water	$\mathrm{p}K_\mathrm{w}$	8.0618	1077.3	-116.5	0.011

[a] According to eq 3.9 in the text, temperature in K. [b] Mean relative deviation (%) between estimated and experimental values calculated by: $\left[\left(\sum_n \frac{\left|\mathrm{p}K_n^{\exp} - \mathrm{p}K_n^{cal}\right|}{\mathrm{p}K_n^{\exp}}\right)\right] \times \frac{100}{n}$,where n=number of experimental data points.

Reactions 3.4 to 3.7 correspond to citric acid and sodium citrate dissociations in the aqueous system. Eleven species are present in the mixture mentioned above. The system of equations (equilibrium relations, mass and electroneutrality balances) that allows to calculate simultaneously the activity coefficients and the concentration of species is given below:

equilibrium relations

$$K_1 = \frac{c_{\mathrm{NH_3^+RCOO^-}}\, c_{\mathrm{H^+}}}{c_{\mathrm{NH_3^+RCOOH}}} \frac{\gamma^*_{\mathrm{(NH_3^+RCOO^-)}}\, \gamma^*_{\mathrm{H^+}}}{\gamma^*_{\mathrm{(NH_3^+RCOOH)}}} \frac{v_m^L}{v_w^{oL}} \tag{3.10}$$

$$K_2 = \frac{c_{\mathrm{NH_2RCOO^-}}\, c_{\mathrm{H^+}}}{c_{\mathrm{NH_3^+RCOO^-}}} \frac{\gamma^*_{\mathrm{(NH_2RCOO^-)}}\, \gamma^*_{\mathrm{H^+}}}{\gamma^*_{\mathrm{(NH_3^+RCOO^-)}}} \frac{v_m^L}{v_w^{oL}} \tag{3.11}$$

$$K_{\mathrm{A1}} = \frac{c_{\mathrm{H^+}}\, c_{\mathrm{H_2citric^-}}}{c_{\mathrm{H_3citric}}} \frac{\gamma^*_{\mathrm{H^+}}\, \gamma^*_{\mathrm{H_2citric^-}}}{\gamma^*_{\mathrm{H_3citric}}} \frac{v_m^L}{v_w^{oL}} \tag{3.12}$$

$$K_{\mathrm{A2}} = \frac{c_{\mathrm{H^+}}\, c_{\mathrm{Hcitric^{--}}}}{c_{\mathrm{H_2citric^-}}} \frac{\gamma^*_{\mathrm{H^+}}\, \gamma^*_{\mathrm{Hcitric^{--}}}}{\gamma^*_{\mathrm{H_2citric}}} \frac{v_m^L}{v_w^{oL}} \tag{3.13}$$

$$K_{\mathrm{A3}} = \frac{c_{\mathrm{H^+}}\, c_{\mathrm{citric^{---}}}}{c_{\mathrm{Hcitric^{--}}}} \frac{\gamma^*_{\mathrm{H^+}}\, \gamma^*_{\mathrm{citric^{--}}}}{\gamma^*_{\mathrm{Hcitric}}} \frac{v_m^L}{v_w^{oL}} \tag{3.14}$$

$$K_w = c_{\mathrm{H^+}}\, c_{\mathrm{OH^-}} \frac{\gamma^*_{\mathrm{H^+}}\, \gamma^*_{\mathrm{OH^-}}}{a_w} \left(\frac{v_m^L}{v_w^{oL}}\right)^2 \tag{3.15}$$

electroneutrality balance

$$c_{\mathrm{H^+}} + c_{\mathrm{NH_3^+RCOOH}} + c_{\mathrm{Na^+}} = c_{\mathrm{OH^-}} + c_{\mathrm{NH_2RCOO^-}} + \mathrm{c}_{\mathrm{H_2citric^-}} + 2\,c_{\mathrm{Hcitric^{--}}} + 3\,c_{\mathrm{citric^{---}}} \tag{3.16}$$

mass balances

$$c_{\mathrm{H_3citric,0}} + c_{\mathrm{Na_3citric,0}} = c_{\mathrm{H_3citric}} + c_{\mathrm{H_2citric^-}} + c_{\mathrm{Hcitric^{--}}} + c_{\mathrm{citric^{---}}} \tag{3.17}$$

$$c_{\mathrm{Na_3citric,0}} = c_{\mathrm{Na^+}} \tag{3.18}$$

$$c_{\mathrm{NH_2RCOOH}} = c_{\mathrm{NH_3^+RCOO^-,0}} = c_{\mathrm{NH_3^+RCOO^-}} + c_{\mathrm{NH_3^+RCOOH}} + c_{\mathrm{NH_2RCOO^-}} \tag{3.19}$$

$$c_{\mathrm{H_2O,0}} = c_{\mathrm{H_2O}} + c_{\mathrm{OH^-}} \tag{3.20}$$

where c in the equations above are the molar concentrations (mol $\mathrm{L^{-1}}$) of the species; v_m^L and v_w^{oL} are the molar volumes of the mixture and water (L $\mathrm{mol^{-1}}$), respectively and γ_i^* refers to the activity coefficient of specie i in the asymmetric convention (infinite dilution basis). The subscript 0 refers to the initial concentration of solute.

In this work, the activity coefficient (in the asymmetric convention) of a specie *i* is expressed by long-range (electrostatic interactions) and short-range (physical interactions) contributions:

$$\ln \gamma_i^* = \ln \gamma_i^{*S-R} + \ln \gamma_i^{*L-R} \tag{3.21}$$

where, the superscript *S-R* and *L-R* refer respectively to short- and long-range interactions.

For the solvent (water), the activity coefficient is calculated in the symmetric convention as follows:

$$\ln \gamma_w = \ln \gamma_w^{S-R} + \ln \gamma_w^{L-R} \tag{3.22}$$

In addition, the short-range contribution combines the UNIFAC-Larsen model with solvation equations for chemical interactions between water and ionic species. As a result, structural parameters of solvated species, concentrations, and activity coefficients are estimated considering the occurrence of solvation. The equations corresponding to this phenomenon are presented below:

structural parameters of species k

$$R_k^H = R_k + Nh_k R_w \tag{3.23}$$

$$Q_k^H = Q_k + Nh_k Q_w \tag{3.24}$$

where superscript *H* refers to the hydrated state, *Nh*$_k$ is the hydration number of specie *k*, and R_w and Q_w stands for volume and area parameters of water, respectively.

mole fractions of hydrated species

$$x_w^H = \frac{x_w - \sum_{j,j\neq w} Nh_j x_j}{1 - \sum_{j,j\neq w} Nh_j x_j} \tag{3.25}$$

$$x_i^H = \frac{x_i}{1 - \sum_{j,j\neq w} Nh_j x_j} \tag{3.26}$$

where x_w^H and x_i^H are the mole fractions of water and ionic species *i*, respectively. The summations in eq 3.25 and 3.26 should be performed upon all species *j* in solution except for water.

conversion between hydrated and non-hydrated activity coefficients

$$\gamma_w^{S-R} = \gamma_w^{S-R,H} \frac{x_w^H}{x_w} \tag{3.27}$$

$$\gamma_i^{S-R} = \gamma_i^{S-R,H} \frac{x_i^H}{x_i} \left[\gamma_w^{S-R,H} x_w^H\right]^{-Nh_i} \tag{3.28}$$

$\gamma_w^{S-R,H}$ and $\gamma_i^{S-R,H}$ are calculated by the UNIFAC-Larsen equation using mole fractions and structural parameters of the hydrated species.

The selected UNIFAC model proposed by Larsen *et al.* (1987) gives symmetric activity coefficients in the mole fraction scale (γ_i) that have to be normalized to the standard state for the ionic species (asymmetric convention):

$$\ln \gamma_i^* = \ln \gamma_i - \ln \gamma_i^\bullet \tag{3.29}$$

where $\gamma_i^\bullet$ is the activity coefficient at infinite dilution of all solutes in the mixture:

$$\gamma_i^\bullet = \lim_{x_w \to 1} \gamma_i \tag{3.30}$$

where x_w is the water mole fraction.

The long-range contribution to the activity coefficients was calculated using the Debye-Hückel equation, with the closest approach parameter equal to 17.1, as suggested by Achard *et al.* (1994a).

The solution non-ideality is considered in the eqs 3.10 to 3.15 in which true concentration ratios can be estimated using the framework developed by Achard *et al.* (1994a). It follows that the pH and a_w values can be estimated using the true concentrations of the ionic species ($a_\mathrm{w} = \gamma_w x_w$ and $pH = -\log[\gamma^*_{c_{\mathrm{H}^+}} c_{\mathrm{H}^+}]$). In the particular case of pH, activity of H$^+$ ions in molar concentration scale can be obtained from the calculated activity in molar fraction scale by the equation below:

$$pH = -\log\left[\gamma^*_{c_{\mathrm{H}^+}} c_{\mathrm{H}^+}\right] = -\log\left[\frac{\gamma^*_{\mathrm{H}^+} x_{\mathrm{H}^+}}{v_w^{oL}}\right] \tag{3.31}$$

where c_{H^+} and x_{H^+} stand for molar concentration and molar fraction of ions H$^+$, respectively; and v_w^{oL} is the molar volume of water.

3.4.2 Solubility of Amino Acids in Aqueous Solutions

The solid-liquid equilibrium of an aqueous amino acid solution and the pure solid amino acid, can be written in terms of the zwitterion form:

$$x_{\mathrm{A}\pm}\,\gamma^{*}_{\mathrm{A}\pm}\,f_o^L = f_{\mathrm{A}}^S \tag{3.32}$$

f_o^L is the reference fugacity in the asymmetric convention, and f_{A}^S is the fugacity of the pure solid amino acid.

The ratio f_{A}^S/f_o^L can be related to the temperature of the system through the following relation:

$$\frac{f_{\mathrm{A}}^S}{f_o^L} = \exp\left(\frac{\Delta s}{R} - \frac{\Delta h}{RT}\right) \tag{3.33}$$

where Δs and Δh are the change in molar enthalpy and entropy of the amino acid from the reference state to the solid state (Prausnitz *et al.*, 1996). These values are generally obtained from solubility studies. The activity coefficient $\gamma^{*}_{\mathrm{A}\pm}$ can be estimated by the UNIFAC-Larsen model combined with the Debye-Hückel equation, once the mole fraction of the amino acid is known. Therefore, it is necessary to perform an iterative method to obtain the solubility of that molecule using eqs 3.32 and 3.33. Δs and Δh in eq 3.33 were adjusted by regression from the solubility data of the amino acids dl-alanine, l-proline and dl-serine. The values of Δs and Δh for the other amino acids studied in this work (glycine and dl-valine) were maintained equal to the literature values (see Table 3.6).

Table 3.6. Δs e Δh values used in this work (in bold script) and obtained from literature

amino acid	Δs/R	$\Delta h/R$ (K)
glycine	**2.4184**[b]; 2.61[b], 2.042[d]	**1654.55**[b]; 1711.1[c], 885.689[d]
dl-alanine	**1.3628**[a]; 0.2127[b], 2.060[d]	**1390.96**[a]; 1115.07[b];1110.97[d], 1107.2[c]
dl-valine	**-0.1305**[b], 2.305[d]	**1264.96**[b]; 754.9[c], 1217.946[d]
dl-serine	2.7173[b]; **4.003**[a]	2265.35[b]; 2717.7[c]; **2641.65**[a]
l-proline	**5.1835**[a]; 2.6235[b]; 1.96[c]	**1476.6**[a]; 959.77[b]; 654.2[c]

[a] Adjusted in this work. [b] Khoshkbarchi and Vera, 1996, [c] Fasman, 1976, [d] Gupta and Heidemann, 1990.

The total solubility (x_A) can be written as:

$$x_A = x_{A^\pm} + x_{A^+} + x_{A^-} \qquad (3.34)$$

where, $x_{A^\pm}$, x_{A^+}, x_{A^-} are the mole fractions of the zwitterion, cationic and anionic species.

There are several literature data reporting the influence of acids, bases and salts on the aqueous solubility of amino acids within a certain pH range. Pradhan and Vera (1998) reported the effect of the addition of strong acids and bases on the solubility of amino acids at various pH values. It was observed that there was no significant influence of different ions (K^+, Na^+, Cl^-, and NO_3^-) on the solubility of dl-alanine at 25 °C within the pH range of 2 to 10. It is also reported in literature (Carta and Tola, 1996) experimental solubility data of some amino acids at various pH and NaCl concentrations. The pH was varied from 0 to 13 using HCl or NaOH. The experimental data shows the dependence of the solubility of amino acids on the addition of salts, bases and acids. Experimental data reported by Needham *et al.* (1971) shows the influence of acid or base on the solubility of amino acids in two different solvents: water and ethanol. In the present work, the solubility of amino acids in aqueous electrolyte solutions has been estimated using the UNIFAC-Larsen model combined with the Debye-Hückel equation.

3.5 Results and Discussion

3.5.1 Density data

In the calculations of activity coefficients and true concentration of species, it is necessary to estimate the densities of the amino acid solutions. Linear equations were fitted to experimental density data at 25 °C for the amino acid systems considered in the present work. The equations are given in Table 3.7. To estimate solubilities of the amino acids in water, density data at temperatures other than 25 °C were also required. We used the following approach to estimate such densities: the densities of the amino acid (i) solutions at 25 °C relative to water (subscript w) at the same reference temperature were multiplied by the density of water at the desired temperature, as can be seen by eq 3.35:

$$\rho_i(t) = \frac{\rho_i(25^\circ C)}{\rho_w(25^\circ C)} \rho_w(t) \qquad (3.35)$$

Table 3.7. Linear fitting for the densities of amino acids, salts, acid and base in aqueous solutions[a]

system	equation: $\rho=\rho(w_t)$ g cm^{-3}	reference	R^2
glycine + water	$0.4327w_t+0.9967$	Soto *et al.* (1998); this work	$\underline{3}$,36
glycine + acid buffer	$0.4229w_t+0.9971$	this work	$\underline{4}$,80
glycine + basic buffer	$0.4349w_t+0.9974$	this work	$\underline{3}$,88
dl-alanine + water	$0.3241w_t+0.9970$	Dalton and Schmidt (1933); this work	$\underline{4}$,60
dl-alanine + acid buffer	$0.3258w_t+0.9977$	this work	$\underline{3}$,52
dl-alanine + basic buffer	$0.3072w_t+0.9970$	this work	$\underline{3}$,62
l-proline + water	$0.2982w_t+0.9962$	this work	$\underline{3}$,32
l-proline + acid buffer	$0.2988w_t+0.9972$	this work	$\underline{4}$,80
l-proline + basic buffer	$0.2935w_t+0.9970$	this work	$\underline{4}$,20
l-arginine + water	$0.2782w_t+0.9970$	this work	$\underline{3}$,64
l-arginine + acid buffer	$0.3073w_t+0.9975$	this work	$\underline{3}$,16
l-arginine + basic buffer	$0.2781w_t+0.9974$	this work	$\underline{3}$,48
l-serine + water	$0.4450w_t+0.9998$	Yan *et al.* (1999)	$\underline{4}$,60
dl-valine + water	$0.2276w_t+0.9970$	Dalton and Schmidt (1933)	$\underline{4}$,60
NaOH + water	$1.0599w_t+1.0013$	Lobo and Quaresma (1989)	$\underline{4}$,80
HCl + water	$0.5037w_t+0.9994$	Lobo and Quaresma (1989)	$\underline{4}$,53
NaCl + water	$0.7585w_t+0.9980$	Lobo and Quaresma (1989)	$\underline{3}$,42

[a] Correlation coefficients such as 0.999980 given as $\underline{4}$,80.

The prediction capacity of eq 3.35 was tested using experimental densities of binary aqueous solutions containing a non-electrolyte solute (sucrose) (Norrish, 1967) or an electrolyte solute (KCl) (Lobo and Quaresma, 1989) at various temperatures (20 - 90 °C for sucrose and 25 - 100 °C for KCl) and solute concentrations (1 - 85 mass % for sucrose and 0.7 - 20 mass % for KCl).

In the case of sucrose solutions the reference temperature was 20 °C and for KCl solutions it was 25 °C. Mean relative deviations between experimental density data and those calculated by eq 3.35 were equal to 0.09% and 0.1% for sucrose and KCl solutions, respectively. Such result clearly shows the good performance of the selected approach to estimate densities at various temperatures. Eq 3.35 is based on the assumption that $d\rho_i/dw_i$ (the derivative of solution density in relation to solute concentration) does not dependent on temperature, so that the solution density at some specified solute concentration changes with temperature only as a consequence of the change in the solvent density.

For the ternary (amino acid + base/acid + water, or amino acid + salt + water) and the quaternary (amino acid + base/acid + salt + water) systems it was utilized a semi-empirical equation for calculating the corresponding densities. It requires densities of the binary solutions (solute + solvent) as is shown below (Zafarani-Moattar *et al.*, 1995):

$$\rho_{mix} - \rho_w = \sum_{i, i \neq w} (\rho_i - \rho_w) \tag{3.36}$$

ρ_{mix}, ρ_w, and ρ_i represent the densities of the multicomponent mixture, density of pure water and density of the binary aqueous mixtures containing component i, respectively. Component i could be a salt, an acid or a base. The summation in eq 3.36 should be performed upon all the components i in solution, except for water.

To test the accuracy of the eq 3.36, calculated densities for aqueous solutions of glycine and salts were compared with experimental ones from literature (Lobo and Quaresma, 1989; Soto *et al.*, 1999). The relative mean deviation was found to be 0.3% for the ternary systems: glycine + NaCl + water and glycine + KCl + water. This result confirms the applicability of the equation for calculating the densities of the multicomponent systems involved in this work.

3.5.2 Equilibrium data

The UNIFAC-Larsen model was then used to calculate the short-range contribution to the activity coefficients of the different species in solution considering the hydration of ions H^+ and Na^+, with hydration numbers (*Nh*) equal to 2.959 and 2.606, respectively (Achard *et al.*, 1994a). The interaction parameters used were found in Achard *et al.* (1994a) (for interaction parameters involving charged species), Kuramochi *et al.* (1996, 1997a) (for interaction parameters involving new groups such as sc-CH, α-CH) and Larsen *et al.* (1987). Interaction energies (u_{ij}) between the charged species Na^+ and Cl^- and the specific groups of the amino acids (COOH and NH_2) were adjusted using the available solubility data. The option for adjusting the interaction energies u_{ij}, instead of the interaction parameters a_{ij}, allows to reduce the number of parameters to be fitted. Interaction parameters a_{ij} are related to the interaction energies u_{ij} and u_{jj} according to eq 3.37, given below:

$$a_{ij} = u_{ij} - u_{jj} \tag{3.37}$$

Adjusted group interaction energies (u_{ij}) between the amino acid groups (COOH and NH_2) and the ions Na^+ and Cl^- are given in Table 3.8. The u_{jj} values ($u_{COOH,COOH}$ and $u_{NH2,NH2}$) required for a_{ij} calculations had been estimated by the following expression (Achard *et al.*, 1994b) and are reported in Table 3.9:

$$u_{jj} = a_{jw} - a_{wj} + u_{ww} \tag{3.38}$$

where the subscripts *w* and *j* stand for water and specie *j*, respectively.

Values for $a_{\mathrm{COOH},w}$, $a_{w,\mathrm{COOH}}$, $a_{\mathrm{NH_2},w}$, $a_{w,\mathrm{NH_2}}$ were taken from Larsen's tables (Larsen *et al.*, 1987), and the values for $u_{w,w}$, $u_{\mathrm{Na^+,Na^+}}$ and $u_{\mathrm{Cl^-,Cl^-}}$ were obtained in ref (Achard *et al.*, 1994b).

Table 3.8. Group interaction energies u_{ij} (K) between ions and amino acid characteristic groups

	Na^+	Cl^-
COOH	442.785	-1459.36
NH_2	357.724	-1521.50

Table 3.9. Group interaction energies u_{jj} between like groups

	u_{jj} (K)
COOH-COOH	-622.18
NH_2-NH_2	-878.10

In Figure 3.3 it is shown a comparison between experimental and predicted a_w values for the amino acid l-proline in water and in very diluted buffer solutions. Figure 3.4 depicts the estimated pH values for mixtures containing glycine in three different solvents (water, acid buffer and basic buffer). As can be observed, the UNIFAC-Larsen model combined with the Debye-Hückel term yields a good fit to these data. Mean relative average deviations for the systems with glycine, l-proline, l-arginine and dl-alanine are given in Table 3.10.

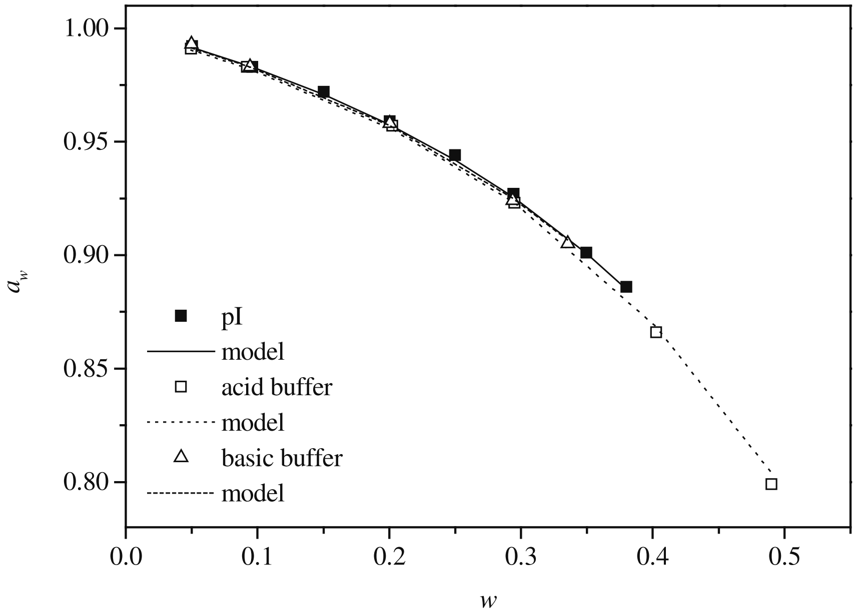

Figure 3.3. Experimental and calculated a_w of aqueous solutions containing l-proline.

The deviations for the solubility data are also given in Table 3.10, and some of the results are shown in Figure 3.5. The model reproduces well the observed experimental data.

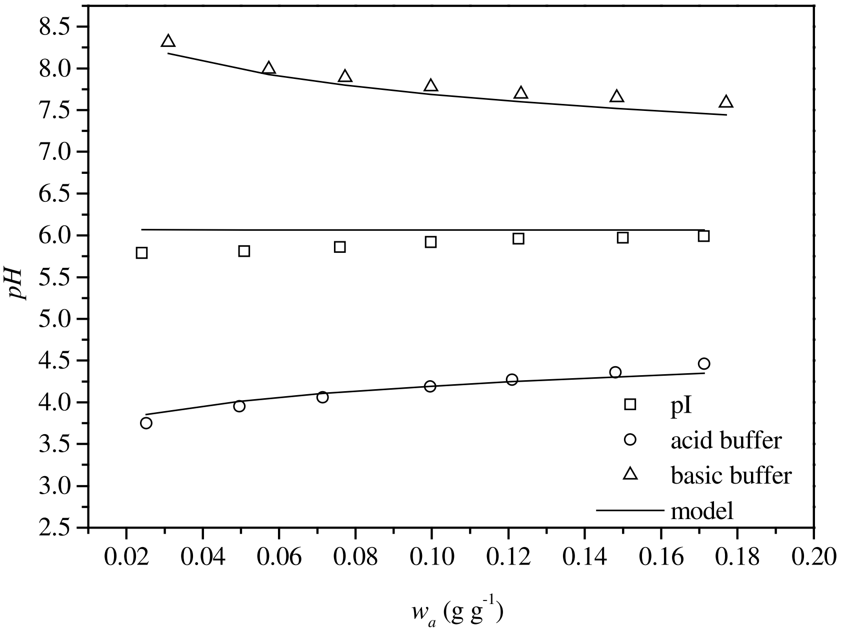

Figure 3.4. Experimental and estimated *pH* of glycine solutions.

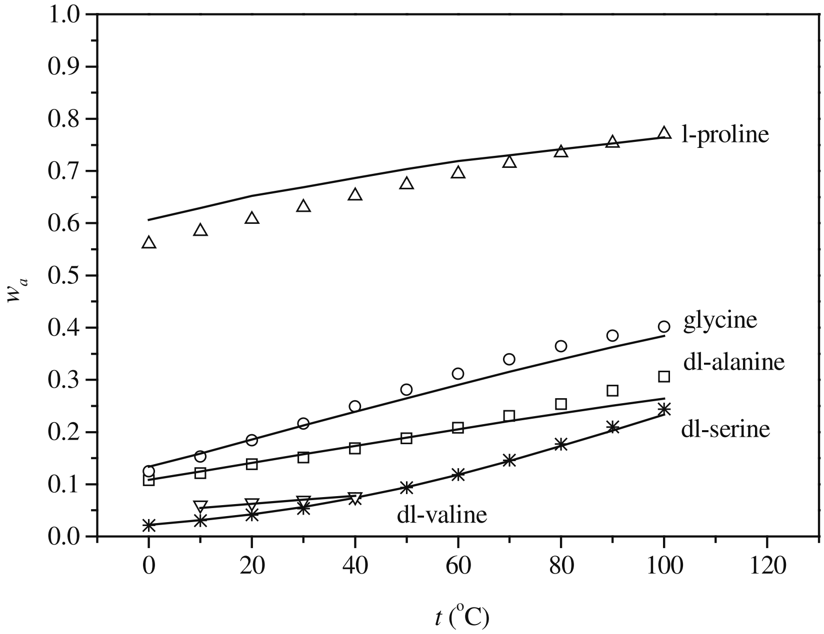

Figure 3.5. Experimental and calculated solubility of some amino acids.

Results concerning solubility of glycine in salt solutions (glycine + NaCl + water + HCl/NaOH) at different pH values are presented in Figure 3.6. Most experimental data are from the work of Carta and Tola (1996). It must be stressed that studies about pH influence on solubility of amino acids do not report the concentrations of acid and base utilized. Some works (Pradhan and Vera, 1998) report the final pH of a mixture containing the amino acid, the acid or the base, while others (Carta and Tola, 1996) provide the pH of the initial solutions – before the addition of the amino acid. In both cases, the amount of acid or base in the present work was selected – through analysis of the estimated pH by the model – to obtain the desirable pH or when $pH_{calc}=pH_{exp}$. For example, when experimental solubility data as a function of final pH is given for a mixture containing the amino acid + acid or base, the concentrations of acid or base were selected when the pH estimated by the model reached the experimental pH. In the other case, when the pH values of the initial solutions were reported, the total acid or base concentrations were selected from the analysis of the experimental and estimated pH for aqueous solutions containing the acid or the base only. Finally, the concentrations of acid or base were utilized to estimate solubility of some amino acids in a wide range of pH values. Figure 3.6 shows the results of the calculated solubilities of the amino acid glycine at various pH values and NaCl concentrations. From Figure 3.6, it can be seen that good agreement is observed between experimental and calculated solubilities at high NaCl concentrations (5 and 15%), while the calculated results for the amino acid at the isoelectric point agree well with experimental data from (Needham *et al.*, 1971, Dalton and Schmidt, 1933).

Table 3.10 also shows the mean relative deviations for a_w, pH and solubility of the amino acids in aqueous solutions considering the ideal case, that is activity coefficients for all species equal to 1 ($\gamma_{i,\forall i}=1$). It was observed that, the a_w values calculated for the ideal case had an expressive difference from experimental results for the systems containing the amino acid proline (mean relative deviations of about 1.4%). For the other systems containing the amino acids glycine, alanine and arginine this difference was less pronounced but greater than that obtained considering the non-ideality of the systems. Such deviations are outside the range of the experimental error for a_w measurements provided by the manufacturer (0.3%) and also much higher than the standard deviation observed in the experimental measurements (0.1%).

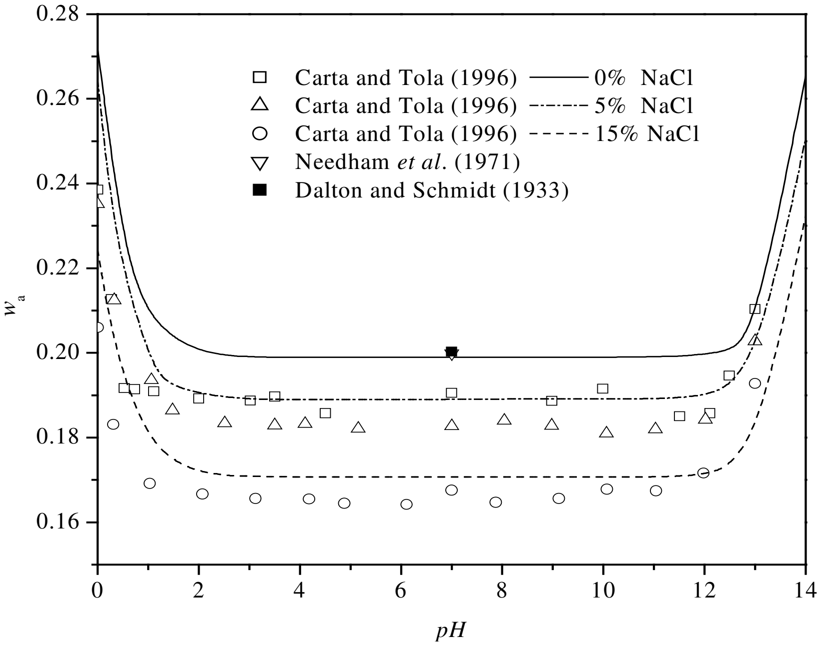

Figure 3.6. Experimental and estimated solubilities of glycine at various *pH* values and NaCl concentrations.

Table 3.10. Average relative deviations between calculated and experimental data

property	% deviation		reference
	real	ideal	
	a_w		
pI			
this work	0.11	0.51	this work
literature	0.08	0.12	Kuramochi *et al.*, 1997b
acid buffer	0.18	0.96	this work
basic buffer	0.15	0.40	this work
	pH		
pI	3.63	3.61	this work
acid buffer	2.93	3.12	this work
basic buffer	0.94	0.91	this work
	solubility		
proline + water	4.26	59.60	Fasman, 1976
alanine + water	4.51	11.26	Fasman, 1976
glycine + water	4.99	14.99	Fasman, 1976
valine + water	3.77	7.18	Fasman, 1976
serine + water	2.43	6.90	Fasman, 1976
glycine + NaCl + HCl or NaOH	5.41	14.32	Carta and Tola, 1996
alanine + NaCl	0.13	8.64	Khoshkbarchi and Vera, 1997
valine + NaCl	0.55	12.06	Khoshkbarchi and Vera, 1997
serine + NaCl	6.73	17.76	Khoshkbarchi and Vera, 1997
alanine + HCl or NaOH	6.47	12.44	Pradhan and Vera, 1998
glycine + HCl or NaOH	7.66	28.76	Needham *et al.*, 1971
total deviation	3.05	17.63	

Concerning the deviations between real and ideal pH values, it was verified slight differences between them. This case can be further visualized in Figure 3.7 in which the distribution of the three ionic species of glycine as a function of pH is shown. Unfortunately, numerical data for the distribution of the species is not available in the literature, but it can be noted in Figure 3.7 that the ranges in which such species appear in the various forms agree well with those reported by (Max et al., 1998) (cationic pH 0 to 5; zwitterionic pH 0 to 12.5 and anionic pH 7 to 14). Although it is not possible to verify which of the curves (real or ideal pH) represent well the ionic distribution of glycine, those curves yield different concentrations of the species within the pH range of 1-3.5 and 8-11.

Large discrepancies can also be noted between calculated (ideal case) and experimental data for solubility (see Table 3.10). In the case of glycine and valine the values of Δ*s* and Δ*h* were taken from literature and then were not adjusted in the present work even though the results of the calculated solubility considering the ideal case presented very high deviations from experimental data.

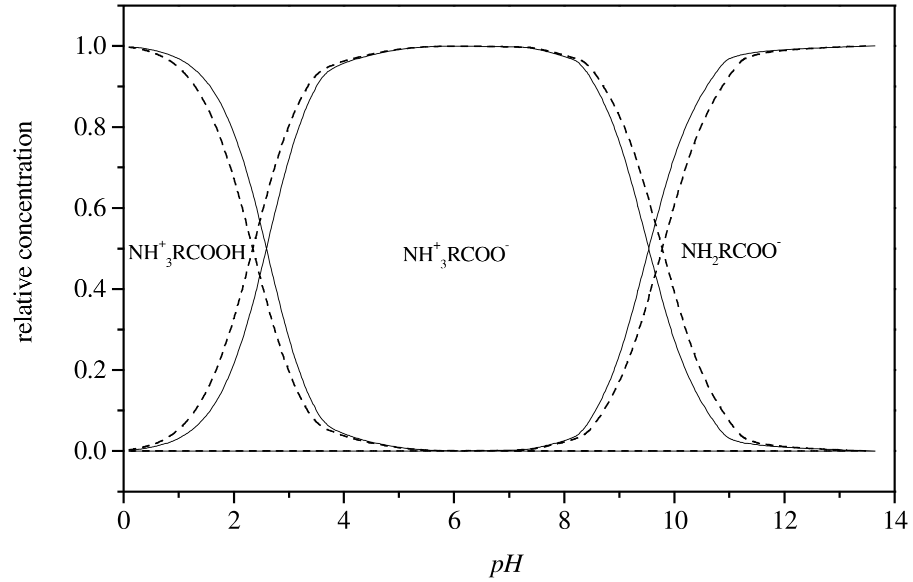

Figure 3.7. Comparison between the distribution of the ionic species of glycine as a function of real (—) and ideal (----) *pH*.

3.6 Conclusions

This work has presented experimental data on water activity, pH and density of mixtures containing amino acids. The use of the UNIFAC group contribution model with solvation equations as proposed by Achard et al. (1994a) combined with the Debye-Hückel term, was extended to estimate physical-chemical properties such as water activity, pH and solubility of amino acids. The model provided good results for such properties. The interaction parameters between Na^+ and Cl^- and the amino acid specific groups were adjusted, yielding reasonable results concerning pH influence on the solubility of the amino acids in more complex mixtures.

3.7 References

Achard, C.; Dussap, C.-G.; Gros, J. B. Representation of Vapour-Liquid Equilibria in Water-Alcohol-Electrolyte Mixtures with a Modified UNIFAC Group-Contribution Method. *Fluid Phase Equilibria* **1994b**, 98, 71- 89.

Achard, C.; Dussap, C.-G.; Gros, J.-B. Prediction of pH in Complex Aqueous Mixtures Using a Group Contribution Method. *AIChE J.* **1994a**, 40, 1210-1222.

Carta, R.; Tola, G. Solubilities of l-Cystine, l-Tyrosine, l-Leucine, and Glycine in Aqueous Solutions at Various pHs and NaCl Concentrations. *J. Chem. Eng. Data* **1996**, 41, 414-417.

Chen, C. C.; Zhu, Y.; Evans, L. B. Phase Partitioning of Biomolecules: Solubilities of Aminoacids. *Biotechnol. Prog*. **1989**, 5, 111-118.

Dalton, J. B.; Schmidt, C. L. A. The Solubilities of Certain Amino Acids in Water, the Densities of their Solutions at Twenty-Five Degrees, and the Calculated Heats of Solution and Partial Molal Volumes. *J. Biol. Chem.* **1933**, 103, 549-578.

Fasman, G. D. *Handbook of Biochemistry and Molecular Biology*, 3rd ed., Physical and Chemical Data; CRC Press: Cleveland, 1976; pp 115.

Greenstein, J. P.; Winitz, M. *Chemistry of the Amino Acids Vol. 1*; John Wiley & Sons: New York, 1961; pp 486-491.

Gupta, R. B.; Heidemann, R. A. Solubility Models for Amino Acids and Antibiotics. *AIChE J.* **1990**, 36, 333-341.

Izatt, R. M.; Christensen, J. J. Heats of Proton Ionization, pK and Related Thermodynamic Quantities. In *Handbook of Biochemistry: Selected Data for Molecular Biology,* 2nd ed.; H. A. Sober, Ed., The Chem. Rubber Co.: Cleveland, 1970; pp J 79.

Khoshkbarchi, M. K.; Vera, J. H. A Simplified Pertubed Hard-Sphere Model for the Activity Coefficients of Amino Acids and Peptides in Aqueous Solutions. *Ind. Eng. Chem. Res.* **1996**, 35, 4319-4327.

Khoshkbarchi, M. K.; Vera, J. H. Effect of NaCl and KCl on the Solubility of Amino Acids in Aqueous Solutions at 298.2 K: Measurement and Modeling. *Ind. Eng. Chem. Res.* **1997**, 36, 2445-2451.

King, E. The Ionization Constants of Glycine and the Effect of Sodium Chloride upon its Second Ionization. *J. Am. Chem. Soc.* **1951**, 73, 155-159.

Kuramochi, H., Noritomi, D. H., Hoshino, D., Nagahama, K. Measurements of Vapor Pressures of Aqueous Amino Acids Solutions and Determination of Activity Coefficients of Amino Acids. *J. Chem. Eng. Data* **1997b**, 42, 470-474.

Kuramochi, H., Noritomi, D. H., Nagahama, K. Representation of Activity Coefficients of Fundamental Biochemicals in Water by the UNIFAC Model. *Fluid Phase Equilibria* **1997a**, 130, 117-132.

Kuramochi, H.; Noritomi, H.; Hoshino, D.; Nagahama, K. Measurement of Solubilities of Two Amino Acids in Water and Prediction by the UNIFAC Model. *Biotechnol. Prog.* **1996**, 12, 371-379.

Larsen, B. L.; Rasmussen, P.; Fredenslund, A. A Modified UNIFAC Group-Contribution Model for Prediction of Phase Equilibria and Heats of Mixing. *Ind. Eng, Chem. Res.* **1987**, 26, 2274-2286.

Lobo, V. M. M.; Quaresma, J. L. *Handbook of Electrolyte Solutions;* Elsevier Sci. Publishers: New York, 1989; parts A and B, pp 1643, 1818-1819.

Maffia, M. C.; Meirelles, A. J. A. Water Activity and pH in Aqueous Polycarboxylic Acid Systems. *J. Chem. Eng. Data* **2000**,46, 582-587.

Max, J-J; Trudel M.; Chapados, C. Infrared Titration of Aqueous Glycine. *Applied Spectroscopy* **1998**, 52, 226-233.

Nass, K. K. Representation of the Solubility Behavior of Amino Acids in Water. *AIChE J.* **1988**, 34, 1257-1266.

Needham, T. E.; Paruta, A. N.; Gerraughty, R. J. Solubility of Amino Acids in Pure Solvent Systems. *Journal of Pharmaceutical Sciences* **1971**, 60, 565-567.

Ninni, L.; Camargo, M. S.; Meirelles, A. J. A. Modeling and Prediction of pH and Water Activity in Aqueous Amino Acid Solutions. *Comp. Chem. Eng.* **1999**, 23 (Supplement), 383-386.

Norrish, R. S. Selected Tables of Physical Properties of Sugar Solutions. *Scientific and Technical Surveys*; The British Food Manufacturing Industries Research Association: Leatherhead, 1967; pp 26.

Peres, A. M., Macedo, E. A. Representation of Solubilities of Amino Acids Using the UNIQUAC Model for Electrolytes. *Chem. Eng. Sci.* **1994**, 49, 3803-3812.

Pinho, S. P., Silva, C. M., Macedo, E. A. Solubility of Amino Acids: a Group Contribution Model Involving Phase and Chemical Equilibria. *Ind. Eng. Chem. Res.* **1994**, 33, 1341-1347.

Pitzer, K. S. Electrolytes: From Dilute Solutions to Fused Salts. *J. Am. Chem. Soc.* **1980**, 102, 2902-2906.

Pradhan, A. A.; Vera, J. H. Effect of Acids and Bases on the Solubility of Amino Acids. *Fluid Phase Equilibria* **1998**, 152, 121-132.

Prausnitz, J. M.; Lichtenthaler, R. N.; Azevedo, E. G. *Molecular Thermodynamics of Fluid Phase Equilibria*; Englewood Cliffs: New York, 1996; pp 418-420.

Smith, P. K.; Taylor, A. C.; Smith, E. R. B. Thermodynamic Properties of Solutions of Amino Acids and Related Substances. *J. Biol. Chem.* **1937**, 109-123.

Soto, A.; Alberto, A.; Khoshkbarchi, M. K. Effect of Cation and Anion of an Electrolyte on Apparent Molar Volume, Isoentropic Compressibility and Refractive Index of Glycine in Aqueous Solutions. *Biophysical Chemistry* **1999**, 76, 73-82.

Soto, A.; Alberto, A.; Khoshkbarchi, M. K. Experimental Data and Modelling of Apparent Molar Volumes, Isoentropic Compressibilities and Refractive Indices in Aqueous Solutions of Glycine + NaCl. *Biophysical Chemistry* **1998**, 74, 165-173.

Velezmoro, C. E.; Meirelles, A. J. A. Water Activity in Solutions Containing Organic Acids. *Drying Technol.* **1998**, 16, 1789-1805.

Yan, Z. N.; Wang, J. J.; Liu, W. B.; Lu, J. S. Apparent Molar Volumes and Viscosity B-Coefficients of Some Alpha-Amino Acids in Aqueous Solutions from 278.15 to 308.15 K. *Thermochimica Acta* **1999**, 334, 17-27.

Zafarani-Moattar, M. T.; Salabat, A.; Kabiri-Badr, M. Volumetric Properties of PEG + Salt + Water. *Journal of Chemical Engineering Data* **1995**, 40, 559-562.

3.8 Acknowledgment

This work was supported financially by research grants from Fundação de Amparo à Pesquisa do Estado de São Paulo (FAPESP - Proc. 98/12302-3) and Conselho Nacional de Desenvolvimento Científico e Tecnológico (CNPq - Proc. 145941/99, 466680/00-7 and 521011/95-7).

Capítulo 4

KINEMATIC VISCOSITIES OF POLY(ETHYLENE GLYCOL) BLENDS

Luciana Ninni, Wong H. Fung, Antonio J. A. Meirelles

LASEFI - Faculty of Food Engineering - State University of Campinas (UNICAMP)

P.O. Box 6121 Zip Code 13083-970 Campinas – SP, Brazil

Trabalho publicado na revista *Journal of Chemical & Engineering Data*, v. 47, p. 835 – 838, 2002.

4. Kinematic Viscosities of Poly(ethylene glycol) Blends

4.1 Abstract

Kinematic viscosities of binary and multicomponent mixtures containing poly(ethylene glycols) were measured as a function of temperature. Viscosities of the binary mixtures were used to calculate the excess molar Gibbs energy of activation for viscous flow G^{*E}. The G^{*E} values are positive over the entire composition range and they increase as the difference in the molecular masses of the two polymers increases. The group-contribution viscosity model GC-UNIMOD was employed to correlate the viscosity of the binary systems and then to predict the viscosities of the multicomponent mixtures. Average absolute deviation around 3.5% was obtained for the viscosity calculations using the GC-UNIMOD model.

4.2 Introduction

Poly(ethylene glycol) (PEG) belongs to a class of synthetic polymers that finds several industrial applications due to their availability in a wide range of molecular masses besides having unusual combination of properties such as water solubility, lubricity, low toxicity, etc. Blends of different molecular masses are desired to obtain combinations of properties. For instance, blends of PEG 300 and 1450 are available from most suppliers for use in pharmaceutical and cosmetic products. PEGs are also used as processing aids in making other products. An example is the use of molten PEGs in heat transfer baths (Powell, 1980). Hence, because of the industrial interest, experimental viscosity data and models for estimating viscosities of PEG mixtures are important. In a previous paper (Cruz *et al.*, 2000), a generalized correlation based on the number of carbon atoms was developed for calculating kinematic viscosities of pure PEGs in a molecular mass range between 200 and 3350 as a function of temperature. In the case of mixtures, there are many empirical or semi-empirical equations in the literature (Domínguez *et al.*, 2000; Nhaesi and Asfour, 2000) for estimating viscosity data. Among them there is the group-contribution viscosity model GC-UNIMOD (Cao *et al.*, 1993), which requires binary interaction parameters between constituent groups of molecules in the mixture and viscosities of pure components. The GC-UNIMOD has been used to predict the viscosity of systems containing mixtures of organic solvents (Domínguez *et al.*, 2000; Nhaesi and Asfour, 2000) and working fluid pairs such as methanol and some poly(ethylene glycol) dimethyl ether (PEGDME) mixtures (Herraiz *et al.*, 1999). In the case of the last mentioned system, the authors reported an average absolute deviation around 20 % for viscosity predictions and observed that these predictions were getting worse with the increase of the molecular size of PEGDME. The aim of this paper is to extend our prior studies (Cruz *et al.*, 2000) to binary and multicomponent blends of PEGs using the GC-UNIMOD model. Therefore, the kinematic viscosities of blends of PEGs covering a wide range of mixture molecular masses were measured at various temperatures, and the GC-UNIMOD model was used to correlate and predict these experimental data.

4.3 Experimental

4.3.1 Materials

The samples of poly(ethylene glycol) of different average molecular masses, ranging from (200 to 3350) g mol^{-1}, were supplied by Sigma, except PEG 1500, which was purchased from Fluka. They were analytical grade reagents used without further purification. Their polydispersity index was determined by gel permeation chromatography (GPC) using a Ultrahydrogel column Waters device. The following experimental conditions were employed for the GPC runs: water as the mobile phase at a rate of 0.8 mL min^{-1}, injection temperature of 313.15 K, volume of the sample injected equal to 100 μL, and a refractive index detector.

The water content of the PEG samples was previously determined by Karl Fischer titration using a Metrohm device (Switzerland). In Table 4.1 the characteristics of the polymers used in this work are given together with the nominal and true carbon numbers for each PEG. The denomination nominal carbon number refers to carbon numbers calculated from the molecular mass given by PEG manufacturers such as PEG 200, PEG 3350, while the true carbon number was evaluated from the results of the GPC molecular mass distribution.

Table 4.1. Poly(ethylene glycol) Characterization

PEG	avg molecular mass (M_n)	polydispersity index	water content (mass %)	NCN [a]	TCN [b]
200	202	1.095	0.20 ± 0.02	8	8
400	400	1.086	0.23 ± 0.02	18	18
600	616	1.069	0.27 ± 0.02	26	28
1000	987	1.067	1.54 ± 0.02	44	44
1500	1468	1.069	1.09 ± 0.01	68	66
3350	2806	1.073	0.75 ± 0.01	152	126

[a] Nominal carbon number based on the molecular mass according to the PEG denomination. [b] True carbon number based on the average molecular mass determined by GPC.

4.3.2 Apparatus and procedures

The solutions were prepared by mass on an analytical balance (Sartorius Analytic - GmbH) with ± 0.1 mg accuracy. The estimated error in mass fraction was 1 in 10 000. Calibrated Cannon-Fenske type viscometers were used to measure the kinematic viscosities at different temperatures (Cannon Instrument Co.). The viscometer sizes were 150, 200, 300 and 350, appropriate for the range of viscosity values measured in the present work. The viscometers were placed in a constant temperature water bath controlled to ± 0.1 °C. An electronic timer with 0.01 s accuracy was used for measuring the efflux time. The experiments were replicated at least five times for each PEG mixture and the results reported are the average values.

4.4 Results and Discussion

The viscosity data are presented in Tables 4.2 to 4.5 as a function of mass fraction (w) and temperature T. The kinematic viscosities ν were calculated from the efflux time and the instrument constant provided by the manufacturer. The maximal standard deviation of the measured viscosities was 1.3×10^{-7} m^2 s^{-1} and the minimal, 1.9×10^{-9} m^2 s^{-1}, resulting in an average deviation of 2.6×10^{-8} m^2 s^{-1}. The average uncertainty of the viscosity values was estimated to be equal to 0.3 %.

Table 4.2. Viscosity of Binary Blends of Poly(ethylene glycol)s at Various Temperatures

T/K	w_1	$\nu/10^{-6}$ m^2 s^{-1}	w_1	$\nu/10^{-6}$ m^2 s^{-1}	w_1	$\nu/10^{-6}$ m^2 s^{-1}
	200(1)+400(2)		200(1)+600(2)		400(1)+600(2)	
293.15	0.4999	77.53	0.5031	93.89	0.5043	127.44
298.15	0.4999	59.73	0.5031	72.95	0.4999	99.61
303.15	0.4999	46.49	0.5031	58.41	0.5007	77.66
308.15	0.4999	37.18	0.5031	46.52	0.5007	60.86
313.15	0.4999	30.13	0.5031	37.90	0.5007	49.25
318.15	0.4999	24.73	0.5031	30.94	0.5007	40.49
323.15	0.4999	20.62	0.5031	25.80	0.5007	33.58
	600(1)+1000(2)		400(1)+1500(2)		600(1)+3350(2)	
333.15	0.5001	36.19	0.4918	40.99	0.4999	97.32
343.15	0.5001	26.44	0.4918	29.81	0.4999	70.85
353.15	0.5001	21.27	0.4836	23.11	0.4999	54.27
363.15	0.5001	15.87	0.4836	18.20	0.4999	41.97

Table 4.2. (continued)

T/K	w_1	$\nu/10^{-6}$ m^2 s^{-1}	w_1	$\nu/10^{-6}$ m^2 s^{-1}
	1000(1)+3350(2)		400(1)+3350(2)	
333.15	0.5001	114.79	0.5000	88.09
343.15	0.5001	84.10	0.5000	63.76
353.15	0.5001	62.07	0.5000	48.92
363.15	0.5001	49.94	0.5000	38.66

Table 4.3. Viscosity of Binary Blends Containing Poly(ethylene glycol) 400 at Various Concentrations

T/K	w_1	$\nu/10^{-6}$ m^2 s^{-1}	w_1	$\nu/10^{-6}$ m^2 s^{-1}	w_1	$\nu/10^{-6}$ m^2 s^{-1}
	400(1)+600(2)		400(1)+1500(2)		400(1)+3350(2)	
293.15	0.1010	154.96				
293.15	0.2000	146.25				
293.15	0.2999	139.42				
293.15	0.3992	133.61				
293.15	0.7000	121.82				
293.15	0.8998	110.98				
293.15	0.9482	105.77				
333.15	0.0996	28.04	0.0511	70.91	0.0273	224.82
333.15	0.2001	26.87	0.0997	68.69	0.0513	219.00
333.15	0.2999	25.63	0.1513	63.49	0.1029	196.70
333.15	0.3992	24.84	0.2500	56.83	0.2000	162.98
333.15	0.5000	23.76	0.3496	50.02	0.2500	147.14
333.15	0.7000	21.80	0.7006	31.17	0.6998	52.48
333.15	0.8998	20.04	0.9003	23.27	0.8002	39.62
333.15	0.9482	19.78				

In this work, the GC-UNIMOD model was selected for viscosity calculations. Moreover, the viscosity data for the systems containing PEG 400 have been used to calculate the excess molar Gibbs energy of activation for viscous flow.

Table 4.4. Viscosities of Ternary Mixtures of Poly(ethylene glycol)s at Various Temperatures

T/K	w_1	w_2	$\nu/10^{-6}$ m^2 s^{-1}	w_1	w_2	$\nu/10^{-6}$ m^2 s^{-1}
	400(1)+600(2)+1000(3)			600(1)+1000(2)+1500(3)		
333.15	0.3339	0.3334	30.26	0.3332	0.3335	47.10
343.15	0.3339	0.3334	22.01	0.3332	0.3335	34.20
353.15	0.3339	0.3334	16.77	0.3332	0.3335	26.67
363.15	0.3339	0.3334	13.21	0.3332	0.3335	21.00
	400(1)+1000(2)+3350(3)			1000(1)+1500(2)+3350(3)		
333.15	0.3334	0.3331	71.25	0.3330	0.3334	109.27
343.15	0.3334	0.3331	52.29	0.3330	0.3334	79.28
353.15	0.3334	0.3331	38.85	0.3330	0.3334	60.59
363.15	0.3334	0.3331	31.23	0.3330	0.3334	47.59

Table 4.5. Viscosities of a Multicomponent Mixture of Poly(ethylene glycol)s at Various Temperatures

T/K	w_1	w_2	w_3	w_4	$\nu/10^{-6}$ m^2 s^{-1}
		400(1)+600(2)+1000(3)+1500(4)+3350(5)			
333.15	0.2000	0.1997	0.1999	0.2002	61.40
343.15	0.2000	0.1997	0.1999	0.2002	44.84
353.15	0.2000	0.1997	0.1999	0.2002	34.13
363.15	0.2000	0.1997	0.1999	0.2002	26.77

4.4.1 Excess molar Gibbs energy of activation for viscous flow

Viscosities of binary mixtures (PEGs 400+600, 400+1500 and 400+3350) have been used to calculate the excess molar Gibbs energy of activation for viscous flow, $G^{*\mathrm{E}}$, through the following equation:

$$G^{*\mathrm{E}} = RT\left(\ln(\nu M) - \sum_{i=1}^{n} x_i \ln(\nu_i M_i) \right) \tag{4.1}$$

where M is the mixture molar mass, R is the gas constant, T is the absolute temperature, ν and ν_i are the kinematic viscosities of the mixture and of the pure components, respectively, x_i is component i mole fraction, and n is the number of components in the mixture. The pure component viscosities were calculated using the equation proposed by Cruz *et al.* (2000) and the true carbon numbers given in Table 4.1.

The G^{*E} (in J mol^{-1}) for the binary mixtures was fitted to a Redlich-Kister's equation:

$$G^{*E} = x_i x_j \sum_{p=0}^{3} A_p (x_i - x_j)^p \tag{4.2}$$

where x_i and x_j denotes the mole fractions of components i and j, respectively, and A_p are adjustable parameters. The G^{*E} experimental values and the Redlich-Kister's fitted polynomials are plotted in Figure 4.1. The coefficients A_p and the average absolute deviations (AAD) between experimental and calculated G^{*E} values are given in Table 4.6. The G^{*E} values are positive over the entire composition range and they increase as the difference in the molecular masses of the two polymers increases. The increase of the temperature has a similar effect (Fig. 4.1).

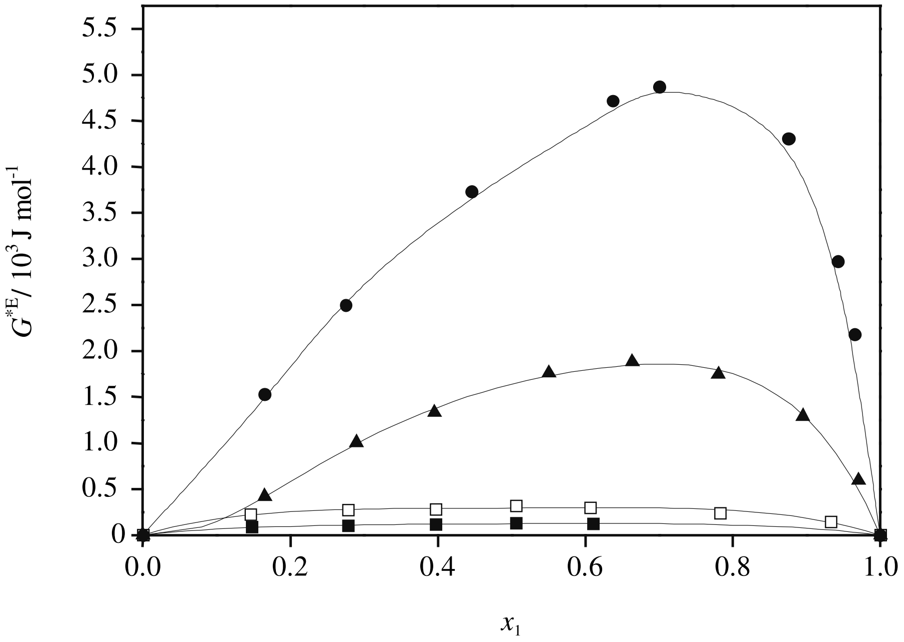

Figure 4.1. Excess molar Gibbs energy of activation for viscous flow of PEG binary mixtures (■ 400+600 at 293.15 K; □ 400+600 at 333.15 K; ▲ 400+1500; ● 400+3350; — Redlich-Kister).

4.4.2 GC-UNIMOD model

The GC-UNIMOD viscosity equation, like the UNIFAC (Fredenslund *et al.*, 1975) model, is expressed as the sum of combinatorial and residual terms. The combinatorial term of both the viscosity equation and the UNIFAC model is dependent on the molecular size and shape, while the residual term takes into account the interaction energy between different groups present in the mixture. In order to estimate the kinematic viscosities of the PEG mixtures, the viscosities of the pure components must be known. The equation for pure PEGs (Cruz *et al.*, 2000) was used for calculating the polymer viscosities required in the GC-UNIMOD model.

Table 4.6. Coefficients of the Redlich-Kister Equation (A_p) and Average Absolute Deviations (AAD) between Experimental and Calculated G^{*E} values

T/K	A_0	A_1	A_2	A_3	AAD
400 (1)+600 (2)					
293.15	495.3292	70.6134	409.3651		5.30
333.15	1172.855	73.1809	1249.925		5.20
400 (1)+1500 (2)					
333.15	6549.193	3957.076	2049.027	5960.119	4.01
400 (1)+3350(2)					
333.15	15771.32	8805.127	16811.02	22896.8	4.63

As a first attempt, the GC-UNIMOD model, with energy interaction parameters obtained from UNIFAC-VLE tables (Skjold-Jorgensen, 1979), was tested for estimating the viscosities of the binary mixtures measured in this work. For these predictions the PEG molecule was divided in three functional groups: CH_2, OH and CH_2O. An average absolute deviation of 15.9 % was obtained. It was also verified that specially for the binary mixtures containing polymers with very different molecular masses (for example, the mixture of PEGs 600 and 3350) the model predictions were poor. A readjustment of the energy interaction parameters becomes necessary to improve the predictive capability of the model. The experimental data of the binary mixtures (Tables 4.2 and 4.3) were used for this readjustment.

As suggested by Herraiz *et al.* (1999), different possibilities of dividing the polymer molecules in functional groups were considered. PEG molecules can be divided in the following groups: OH, CH_2O, CH_2 (option 1) (Skjold-Jorgensen, 1979); OH, CH_2CH_2O, CH_2 (option 2) (Ninni *et al.*, 1999; Rasmussen and Rasmussen, 1989); or CH_2OH, CH_2O, CH_2 (option 3) (Herskowitz and Gottlieb, 1984). As can be seen, three pairs of interaction parameters have to be adjusted in each one of the above options. The new parameters were obtained using a nonlinear estimation method (Marquardt, 1963). The average absolute deviations (AAD) between experimental and estimated values were calculated according to the following equation:

$$\mathrm{AAD} = \left[\sum_{i=1}^{m} \left(\frac{\left| \nu_{\mathrm{exp},i} - \nu_{\mathrm{calc},i} \right|}{\nu_{\mathrm{exp},i}} \right) \right] \times \frac{100}{m} \tag{4.3}$$

where $\nu_{\mathrm{exp},i}$ and $\nu_{\mathrm{calc},i}$ are the experimental and calculated kinematic viscosities, respectively, and m is the number of experimental points.

Better agreement between experimental and calculated data for the binary mixtures was obtained using options 1 and 2, with AAD global values of 3.62 % and 3.76 %, respectively (see Table 4.7). The GC-UNIMOD model was also capable of predicting rather well the viscosities of the multicomponent mixtures, but in this case options 2 and 3 result in slightly better AAD global values, around 2.9 % (Table 4.7). The energy interaction parameters for option 2 are given in Table 4.8. Figure 4.2 shows the viscosity values calculated by the GC-UNIMOD model compared with the experimental binary data given in Table 4.2. The comparison for the ternary and quinary mixtures is shown in Figure 4.3.

Table 4.7. Average Absolute Deviations (AAD) for the Viscosity Estimation

	AAD				AAD		
Binary Mixtures	Option 1	Option 2	Option 3	Multicomponent Mixtures	Option 1	Option 2	Option 3
200+400	4.16	4.20	4.74	400+600+1000	5.53	5.50	5.77
200+600	7.45	7.53	8.54	600+1000+1500	1.09	1.12	1.00
400+600	3.20	3.43	3.27	400+1000+3350	1.46	1.04	0.94
600+1000	2.20	2.18	2.28	1000+1500+3350	4.86	4.59	4.74
400+1500	2.89	2.75	3.07	400+600+1000+ 1500+3350	2.52	2.03	2.03
600+3350	1.90	1.10	1.09				
1000+3350	0.97	0.82	0.91				
400+3350	4.54	5.36	6.75				
global	3.62	3.76	4.14		3.09	2.86	2.90

Table 4.8. Energy Interaction Parameters (in Kelvin) for the GC-UNIMOD Model

	CH_2CH_2O	CH_2	OH
CH_2CH_2O	-	-93.8155	-250.3
CH_2	52.7182	-	-101.3
OH	41.4333	85.4514	-

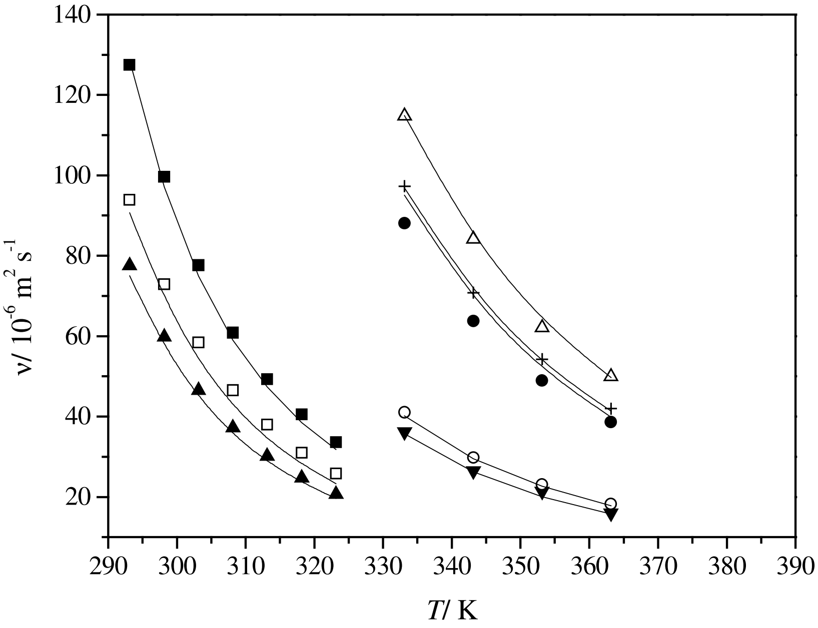

Figure 4.2. Experimental and correlated viscosities of binary PEG mixtures (experimental data of Table 4.2: ▲ 200+400; □ 200+600; ■ 400+600; ○ 400+1500; ● 400+3350; ▼ 600+1000; + 600+3350; △1000+3350; — GC-UNIMOD/ option 2).

As can be observed in Table 4.7 the highest AAD values were obtained for those binary mixtures containing PEGs 200 and/or 400. In the case of the multicomponent systems no experimental values were measured for mixtures containing PEG 200. Probably this is the reason why the AAD values for the predictions (multicomponent mixtures) were slightly lower than those obtained for the correlation of the binary mixtures (Table 4.7).

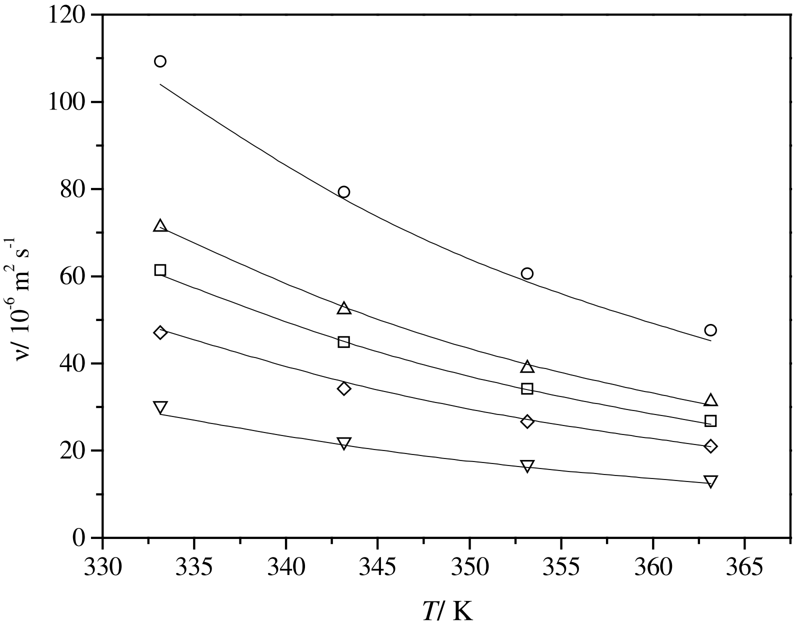

Figure 4.3. Experimental and predicted viscosities of multicomponent PEG mixtures (∇ 400+600+1000; △ 400+1000+3350; □ 400+600+1000+1500+3350; ◇ 600+1000+1500; ○ 1000+1500+3350; — GC-UNIMOD/ option 2).

The GC-UNIMOD model, with new set of interaction parameters, works well for estimating the viscosity data measured in the present work. For comparison purposes, some correlation and prediction results reported in the literature should be mentioned. The authors of the GC-UNIMOD reported deviations in the range of 2.7 to 5.3 % for predictions of mixture viscosities using energy interaction parameters from UNIFAC-VLE tables. It is also depicted in the literature (Herraiz *et al.*, 1999) predictions of the GC-UNIMOD model for mixtures of some polyethylene glycol dimethyl ethers and methanol over a wide range of temperatures. The results showed that the predictions were getting worse with the increase of the polymer molecular mass. The reported average absolute deviations were around 20 %. Rabelo *et al.* (2000) employed the GC-UNIMOD model for predicting the viscosity of fatty systems. In this case the AAD values varied in the range of 0.8 to 14.0 %. The comparison can also include some empirical equations used for correlating experimental viscosities of aqueous systems containing PEGs. Some of these works (Gündüz, 1996; Mei *et al.*, 1995; González-Tello *et al.*, 1994; Gündüz, 2000) reported results for concentrated and/or diluted solutions with AAD values varying in the range of 1.2 to 6.8 %.

The unique experimental data available in the literature (Powell, 1980) for PEG mixtures is the viscosity of a blend of PEGs 300 and 1500 at equal mass proportion of both compounds. This data was compared to the value predicted by the GC-UNIMOD model (option 2), yielding an AAD value of 10.6 %. Although such deviation is comparatively greater than those obtained for the correlation and prediction of our experimental data, it should be noted that for this prediction we had to use the nominal carbon number, not the true carbon number, to estimate the pure PEG viscosities.

4.5 Conclusions

In this work the kinematic viscosities of blends of poly(ethylene glycol)s with nominal molecular masses ranging from (200 to 3350) g mol^{-1} were determined at various temperatures. The GC-UNIMOD model was tested for correlating and predicting viscosity data. In most cases a good agreement between experimental and calculated values was obtained.

4.6 Literature Cited

Cao, W.; Knudsen, K.; Fredenslund, A.; Rasmussen, P. Group-Contribution Viscosity Predictions of Liquid Mixtures Using UNIFAC-VLE Parameters. *Ind. Eng. Chem. Res.* **1993**, 32, 2088-2092.

Cruz, M. S.; Chumpitaz, L. D. A.; Alves, J. G. L. F.; Meirelles, A. J. A. Kinematic Viscosities of Poly(Ethylene Glycols). *J. Chem. Eng. Data* **2000**, 45, 61-63.

Domínguez, M.; Pardo, J. I.; Gascón, I.; Royo, F. M.; Urieta, J. S. Viscosities of the Ternary Mixture (2-butanol + n-hexane + 1-butylamine) at 298.15 and 313.15 K. *Fluid Phase Equilib.* **2000**, 169, 277-292.

Fredenslund, A.; Jones, R. L.; Prausnitz, J. M. Group Contribution Estimation of Activity Coefficients in Nonideal Liquid Mixtures. *AIChE* J. **1975**, 21, 1086-1099.

González-Tello, P.; Camacho, F.; Blázquez, G. Density and Viscosity of Concentrated Aqueous Solutions of Polyethylene Glycol. *J. Chem. Eng. Data* **1994**, 39, 611-614.

Gündüz, U. Evaluation of Viscosities of Polymer-Water Solutions used in Aqueous Two-Phase Systems. *J. Chromatogr. B* **1996**, 680, 263-266.

Gündüz, U. Viscosity Prediction of Polyethylene Glycol - Dextran - Water Solutions used in Aqueous Two-Phase Systems. *J. Chromatogr. B* **2000**, 743, 181-185.

Herraiz, J.; Shen, S.; Fernández, J.; Coronas, A. Thermophysical Properties of Methanol + Some Polyethylene Glycol Dimethyl Ether by UNIFAC and DISQUAC Group-Contribution Models for Absorption Heat Pumps. *Fluid Phase Equilib.* **1999**, 155, 327-337.

Herskowitz, M.; Gottlieb, M. Vapor-Liquid Equilibrium in Aqueous Solutions of Various Glycols and Poly(ethylene glycols). 2. Tetraethylene Glycol and Estimation of UNIFAC Parameters. *J. Chem. Eng. Data* **1984**, 29, 450-452.

Marquardt, D. W. An Algorithm for Least-Square Estimation of Nonlinear Parameters. *J. Soc. Indust. Appl. Math.* **1963**, 11, 431-441.

Mei, L.-H.; Lin, D.-Q.; Zhu, Z.-Q.; Han, Z.-X. Densities and Viscosities of Polyethylene Glycol + Salt + Water Systems at 20°C. *J. Chem. Eng. Data* **1995**, 40, 1168-1171.

Nhaesi, A. H.; Asfour, A-F A. Prediction of the Viscosity of Multi-Component Liquid Mixtures: a Generalized McAllister Three-Body Interaction Model. *Chem. Eng. Sci.* **2000**, 55, 2861-2873.

Ninni, L.; Camargo, M. S.; Meirelles, A. J. A. Water Activity in Poly(Ethylene Glycol) Aqueous Solutions. *Thermochim. Acta* **1999**, 328, 169-176.

Powell, G. M. Polyethylene Glycol. In *Handbook of Water Soluble Gums and Resins*; Davidson, R. L., Ed.; McGraw-Hill Book Company: New York, 1980; Chapter 18.

Rabelo, J.; Batista, E.; Cavaleri, F. W.; Meirelles, A. J. A. Viscosity Prediction for Fatty Systems. *J. Am. Oil Chem. Soc.* **2000**, 77, 1255-1261.

Rasmussen, D.; Rasmussen, P. Phase Equilibria in Aqueous Polymer Solutions. Chem. Eng. Progress **1989**, 85, 50-56.

Skjold-Jorgensen, S.; Kolbe, B.; Gmehling, J.; Rasmussen, P. Vapor-Liquid Equilibria by UNIFAC Group-Contribution. Revision and extension. *Ind. Eng. Chem. Process Des. Dev.* **1979**, 18, 714-722.

4.7 Acknowledgments

The authors gratefully acknowledge the financial support of FAPESP (Fundação de Amparo à Pesquisa do Estado de São Paulo – 01/10137-6) and CNPq (Conselho Nacional de Desenvolvimento Científico e Tecnológico - 521011/95-7, 466680/00-7, 145941/99).

Capítulo 5

KINEMATIC VISCOSITIES OF POLY(ETHYLENE GLYCOL) AQUEOUS SOLUTIONS

Luciana Ninni, Helcio Burd, Wong H. Fung, Antonio J. A. Meirelles

Department of Food Engineering (DEA/FEA), State University of Campinas – UNICAMP, Cidade Universitária "Zeferino Vaz", PO Box 6121, Zip Code 13083-970, Campinas, SP, Brazil

Trabalho publicado na revista *Journal of Chemical & Engineering Data*, v. 48, p. 324 – 329, 2003.

5. Kinematic Viscosities of Poly(ethylene glycol) Aqueous Solutions

5.1 Abstract

Kinematic viscosities of aqueous mixtures containing poly(ethylene glycol)s (PEG) with nominal molecular masses ranging from (200 to 10,000) g·mol^{-1} have been determined at various concentrations and temperatures. The binary experimental data were used for adjusting the parameters of a Kumar-like equation. Relative errors around 5.5% were observed between calculated and experimental results. The adjusted parameters also allowed the viscosity prediction for multicomponent mixtures, with an overall deviation of 9.9%.

5.2 Introduction

Poly(ethylene glycol) (PEG) is a linear, neutral polyether, available in a variety of molecular masses, soluble in water and most organic solvents (Powell, 1980). PEG has a variety of properties that make it suitable for applications in the biomedical and biotechnological areas. Among them one can cite the formation of two-phase systems with aqueous solutions of other polymers or salts, its non-toxicity, and the formation of complex with metal cations, etc. (Harris, 1992) Aqueous two-phase systems are increasingly used for separation of biomolecules, cells and cell particles (Bradoo *et al.*, 1999; Gündüz, 2000). Such systems are composed of two incompatible polymers, e.g. dextran and poly(ethylene glycol) (PEG), or of one polymer (PEG) and a salt (usually a phosphate or sulfate salt). The use of PEGs in aqueous two-phase systems (ATPS) has been reported by several authors (Zaslavsky, 1995; Silva *et al.*, 2001; Grossmann *et al.*, 1998), since such systems allow the separation and purification of biomolecules in a gentle environment. Extraction using ATPS can be performed continuously in available commercial separators (Coimbra *et al.*, 1995; Porto *et al.*, 2000; Gongxi *et al.*, 1999). The advantages of using aqueous two-phase extraction lie in volume reduction, high capacity and fast separation; moreover, it is relatively straightforward to scale up a separation process (Persson *et al.*, 1999). In addition to the knowledge of phase equilibrium, data on the properties of the phases are necessary for the design of ATPS extraction processes in large-scale applications. The knowledge of physical properties, such as the viscosity of aqueous mixtures containing PEGs, is important because these solutions are used in many industrial and biotechnological applications (Albertson, 1971). However, it is not viable to measure viscosities at all conditions of interest, and consequently, methods for the estimation of viscosities at various temperatures, concentrations and solute types are of great practical interest. Numerous empirical and semi-empirical methods have been proposed to calculate liquid viscosity of mixtures (Mehrotra *et al.*, 1996; Gündüz, 1996; Pereira *et al.*, 2001; Cao *et al.*, 1993; Gündüz, 2000). Nevertheless, some equations are inappropriate for concentrated and/or multicomponent mixtures.

In the present work, the reformulated Kumar's equation (Pereira *et al.*, 2001) has been employed to correlate and predict kinematic viscosities of aqueous solutions containing PEGs in a wide range of polymer concentrations and at different temperatures. The difference between the data treatment from this work and other related works (Gündüz, 1996; Pereira *et al.*, 2001; Cao *et al.*, 1993; Gündüz, 2000; Mei *et al.*, 1995; Gonzaléz-Tello *et al.*, 1994) is that viscosity of concentrated PEG solutions were employed together with literature viscosity data at various temperatures, concentrations and PEG molecular masses. Moreover, for each polymer employed, hydration numbers were estimated and compared with available values in the literature (Antonsen and Hoffman, 1992; Kirinčič and Klofutar, 1999; Moulik and Gupta, 1989, Bieze *et al.*, 1994; Bisal *et al.*, 1990). A generalized correlation for estimating kinematic viscosities of PEG aqueous solutions as a function of polymer molecular mass, concentration and temperature was also developed.

5.3 Experimental Section

5.3.1 Materials

Analytical grade PEGs with nominal molecular masses ranging from (200 to 10,000) g·mol^{-1} were purchased from SIGMA and used without further purification. Water was distilled, deionized with a Mili-Q water system (Millipore, USA) and used for preparing the PEG solutions. The solutions were prepared on a mass basis using an analytical balance (Sartorius Analytic, GmbH) accurate to ±0.0001 g. PEG concentrations in the solutions varied up to 50 mass % for systems containing PEGs 200, 400, 600, 1000 and 1500, up to 30 mass% for PEG 3350, and up to 25 mass % for PEGs 8000 and 10 000. The estimated error in the mass fractions was 2 in 10 000. PEGs were characterized according to their molecular masses and water content using the procedures described in a previous article (Cruz *et al.*, 2000). The characteristics of the polymers used in the present work are given in Table 5.1. The water content in the polymer samples was taken into account for calculating the solution concentrations.

Table 5.1. Average relative molar masses (M_n), polydispersity index and water content of PEGs used in this work

PEG	avg rel molar mass (M_n)	polydispersity index	water content (mass %)
200	202	1.095	0.20 ± 0.02
400	400	1.086	0.23 ± 0.02
600	616	1.069	0.27 ± 0.02
1000	987	1.067	1.54 ± 0.02
1500	1529	1.069	1.09 ± 0.01
3350	2806	1.073	0.75 ± 0.01
8000	7975	1.099	0.36 ± 0.08
10 000	10 475	1.106	0.66 ± 0.05

5.3.2 Apparatus and Procedures

Calibrated Cannon-Fenske glass capillary viscometers (sizes 50, 75, 100, 150 and 200) were used to measure the kinematic viscosities (Cannon Instrument Co., USA). The viscometers were placed in a water bath (Anton Paar, Austria) for holding the temperature constant within ±0.1 °C. The measurements were performed at temperatures varying between (293.15 and 323.15) K. An electronic timer with 0.01 s accuracy was used for measuring the efflux time. The experiments were replicated at least three times for each PEG mixture and the results given below are the average values. The standard deviations of the viscosity determinations varied within the range 1.9×10^{-7} $m^2\cdot s^{-1}$ to 1.1×10^{-9} $m^2\cdot s^{-1}$, being the lowest figures obtained for the lowest viscosity values. The variation coefficient varies within the range 0.1% to 0.7%, so that the uncertainty of the experimental measurements can be estimated as not higher than 0.7%.

5.4 Results and Discussion

The kinematic viscosities for the binary and multicomponent PEG solutions determined in this work are given in Tables 5.2 – 5.4.

Table 5.2. Kinematic viscosities, ν, in aqueous solutions of PEGs at 293.15 K and various mass fractions, *w*

w	ν / 10^{-6} m^2 s^{-1}	*w*	ν / 10^{-6} m^2 s^{-1}	*w*	ν / 10^{-6} m^2 s^{-1}
PEG 400		PEG 600		PEG 1000	
0.0248	1.121	0.0249	1.143	0.0243	1.169
0.0497	1.239	0.0501	1.311	0.0492	1.356
0.0748	1.379	0.0749	1.470	0.0737	1.588
0.1002	1.543	0.0996	1.656	0.0985	1.854
0.1529	1.941	0.1491	2.143	0.1477	2.510
0.1998	2.415	0.1994	2.793	0.1960	3.406
0.2998	3.956	0.2993	4.900	0.2953	6.304
PEG 1500		PEG 3350			
0.0246	1.216	0.0248	1.345		
0.0498	1.456	0.0492	1.747		
0.0741	1.751	0.0744	2.267		
0.0992	2.094	0.0995	2.936		
0.1482	2.994	0.1489	4.669		
0.1980	4.252	0.1983	7.215		
0.2967	8.443	0.2987	16.693		

Table 5.3. Kinematic viscosities, ν, in aqueous solutions of PEGs at various temperatures and mass fractions, *w*

T/K	*w*	ν / 10^{-6} m^2 s^{-1}	*w*	ν / 10^{-6} m^2 s^{-1}
	PEG 200		PEG 400	
293.15			0.2487	3.167
303.15	0.2399	1.829	0.2487	2.365
313.15	0.2399	1.416	0.2487	1.828
323.15	0.2399	1.148		
293.15	0.4902	7.231	0.4958	10.917
303.15	0.4902	4.971	0.4958	7.425
313.15	0.4902	3.649		
323.15	0.4902	2.835	0.4958	4.180
	PEG 600		PEG 1000	
293.15	0.2490	3.684	0.2275	4.425
303.15	0.2490	2.745	0.2275	3.237
313.15	0.2490	2.089	0.2275	2.539
323.15	0.2490	1.696	0.2275	2.028
293.15	0.4899	15.534	0.4777	21.823
303.15	0.4899	10.389	0.4777	14.524
313.15	0.4899	7.361	0.4777	10.256
323.15	0.4899	5.501	0.4777	7.502

Table 5.3. (cont.)

	PEG 1500		PEG 3350	
293.15	0.1223	2.387	0.0969	2.965
303.15	0.1223	1.833	0.0969	2.329
313.15	0.1223	1.457	0.0969	1.838
323.15	0.1223	1.191	0.0969	1.496
293.15	0.2349	6.046	0.2492	12.125
303.15	0.2349	4.473	0.2492	8.863
313.15	0.2349	3.444	0.2492	6.757
323.15	0.2349	2.716	0.2492	5.312
293.15	0.4534	28.784	0.3389	22.824
303.15	0.4534	19.228	0.3389	16.250
313.15			0.3389	12.086
323.15	0.4534	9.967	0.3389	9.281
	PEG 8000		PEG 10 000	
293.15	0.0530	2.748	0.0499	3.119
303.15	0.0530	2.128	0.0499	2.376
313.15	0.0530	1.679	0.0499	1.922
323.15	0.0530	1.364	0.0499	1.519
293.15	0.1000	5.623		
303.15	0.1000	4.396	0.0977	5.196
313.15	0.1000	3.338	0.0977	4.037
323.15	0.1000	2.664	0.0977	2.980
293.15	0.2554	33.655		
303.15	0.2554	24.476	0.2441	31.977
313.15	0.2554	18.904	0.2441	24.496
323.15	0.2554	14.715	0.2441	19.314

Table 5.4. Kinematic viscosities, ν, of multicomponent poly(ethylene glycol) aqueous solutions at various temperatures

T/K	w_1	w_2	w_3	w_4	ν / 10^{-6} m^2 s^{-1}
PEG 400 (1) + PEG 600(2) + PEG 1000(3) + PEG 1500(4)					
293.15	0.1005	0.1006	0.0999	0.1032	11.430
303.15	0.1005	0.1006	0.0999	0.1032	8.166
313.15	0.1005	0.1006	0.0999	0.1032	5.936
323.15	0.1005	0.1006	0.0999	0.1032	4.657
PEG 3350 (1) + PEG 8000(2) + PEG 10 000(3)					
293.15	0.0997	0.1012	0.0495		23.468
303.15	0.0997	0.1012	0.0495		17.170
313.15	0.0997	0.1012	0.0495		13.051
323.15	0.0997	0.1012	0.0495		10.248
PEG 400 (1) + PEG 8000(2)					
293.15	0.1003	0.1000			8.221
303.15	0.1003	0.1000			6.078
313.15	0.1003	0.1000			4.675
323.15	0.1003	0.1000			3.702

5.4.1 Kumar's equation for viscosity correlation in PEG mixtures

The Kumar expression (Kumar, 1993) is one of the equations presented in the literature for calculating dynamic viscosities of solutions as a function of solute concentration. Initially, Kumar's expression was formulated to estimate viscosities in aqueous and non-aqueous salt solutions. Such correlation involves two parameters, the hydration number and the ion-solvent interaction coefficient, as given below:

$$\frac{\eta}{\eta_0} = 1 + \frac{bx}{1 - hx} \tag{5.1}$$

where η is the solution dynamic viscosity, η_0 is the solvent dynamic viscosity, x is the solute mole fraction, b and h are the solute-solvent interaction coefficient and the hydration number (number of molecules of bound solvent per molecule of solute), respectively.

The Kumar expression was later reformulated (Pereira *et al.*, 2001) to allow the calculation of kinematic viscosities of aqueous solutions containing salts or organic solutes. The resulting equation is a function of relative density between solution and solvent, mass fraction of solute and temperature. Pereira *et al.* (2001) investigated the predictive capacity of the equation for ternary, quaternary and quinary solutions.

The reformulated Kumar equation was used in this work to correlate and predict the kinematic viscosities of the aqueous PEG mixtures. The equations for binary and multicomponent systems are given as follows:

$$\nu_{\mathrm{rel}} = \frac{1}{\rho_{\mathrm{rel}}}\left[1 + \frac{Bw}{1 - Hw}\right] \tag{5.2}$$

$$\nu_{\mathrm{rel}} = \frac{1}{\rho_{\mathrm{rel}}}\left[1 + \frac{\sum_i Bw_i}{1 - \sum_i Hw_i}\right] \tag{5.3}$$

where the parameters *B* and *H* are interpreted, respectively, as a coefficient of solute-solvent interaction and as the number of solvent molecules solvating the solute, both functions of temperature; *w* is the mass fraction of solute; ν_{rel} and ρ_{rel} are the ratios between the kinematic viscosities and densities of the solution and the corresponding values for the pure solvent, respectively and *i* represents the solutes in the multicomponent mixture. Dependence of the parameters *B* and *H* on temperature is given by polynomials in (T - T_{ref}), as follows:

$$B = B_{\mathrm{ref}} + \sum_{\mathrm{n}} B_{\mathrm{n}}(T - T_{\mathrm{ref}})^{\mathrm{n}} \tag{5.4}$$

$$H = H_{\mathrm{ref}} + \sum_{\mathrm{n}} H_{\mathrm{n}}(T - T_{\mathrm{ref}})^{\mathrm{n}} \tag{5.5}$$

where T_{ref} is the reference temperature equal to 298.15 K.

As can be seen, eqs 5.2 and 5.3 require the information of densities of pure water and of aqueous PEG solutions. For this reason, linear equations were fitted to experimental density data of PEGs in water (González-Tello *et al.*, 1994; Kirinčič and Klofutar, 1998) at 298.15 K. The coefficients of the linear equations are given in Table 5.5.

Table 5.5. Linear fittings for the densities of poly(ethylene glycol)s in aqueous solutions

equation: $\rho/(10^3 \text{ kg m}^{-3}) = a + b\,w$

PEG	a	b	R^2	PEG	a	b	R^2
300	0.996 04	0.166 97	3,66[a]	4000	0.996 01	0.17836	3,71
400	0.996 11	0.169 85	3,74	6000	0.995 75	0.18059	3,72
600	0.996 23	0.172 33	3,68	8000[b]	0.996 67	0.17701	3,49
900	0.995 68	0.176 62	3,76	10 000	0.995 42	0.18295	3,75
1000	0.995 70	0.176 30	3,76	12 000	0.995 86	0.18234	3,68
1500	0.995 63	0.175 87	3,72	15 000	0.995 86	0.18140	3,76
2000	0.995 77	0.178 62	3,75	20 000	0.996 04	0.18068	3,63
3000	0.995 74	0.179 43	3,71	35 000	0.996 17	0.18117	3,80
3350[b]	0.996 48	0.175 64	3,67				

[a] Correlation coefficients such as 0.999 80 given as 3,80.

[b] Experimental density data from González-Tello *et al.* (1994). All other sets of density data were taken from Kirinčič and Klofutar, 1998.

In addition, to estimate the densities of the PEGs in water at temperatures other than 298.15 K the following approach was used, since these data are not available in the literature: the densities of the PEG solutions at 298.15 K relative to water (subscript *w*) at the same reference temperature were multiplied by the density of water at the desired temperature:

$$\rho_i(T) = \frac{\rho_i(298.15K)}{\rho_w(298.15K)}\rho_w(T) \tag{5.6}$$

In dealing with multicomponent systems, a semi-empirical equation was used for calculating the corresponding densities. It requires densities of the binary solutions (solute + solvent), and is given by:

$$\rho_{mix} - \rho_w = \sum_{i,i\neq w}(\rho_i - \rho_w) \tag{5.7}$$

where ρ_{mix}, ρ_w, and ρ_i represent the densities of the multicomponent mixture, of pure water and of the binary aqueous mixtures containing component *i*, respectively. The summation in eq 5.7 should be performed upon all the components *i* in solution, except for water. Equations 5.6 and 5.7 were used in a prior work (Ninni and Meirelles, 2001) for estimating the densities of aqueous solutions containing different solutes with very good agreement between experimental and calculated values.

By nonlinear regression (Marquardt, 1963) of eq 5.2, the values of B_{ref}, B_1, B_2 and H_{ref}, H_1, H_2 were obtained for each PEG + water system. A data bank comprising experimental viscosities of binary systems reported in this work and those from literature (Mei *et al.*, 1995; Kirinčič and Klofutar, 1999), in a wide range of PEG molecular masses, concentrations and temperatures was employed in the correlations. The data bank comprises a total of 259 experimental points. The adjusted parameters as well as the average absolute deviations (AAD) between experimental and calculated viscosities are presented in Table 5.6.

Table 5.6. Adjusted coefficients of eqs 5.2, 5.4 and 5.5 for calculating kinematic viscosities of aqueous PEG solutions[a]

PEG	w	T/K	B_{ref}	$B_1/10^{-3}$	$B_2/10^{-3}$	H_{ref}	$H_1/10^{-3}$	$H_2/10^{-3}$	AAD[b]
200	≤0.49	303 – 323	3.4444	55.3	-2.38	1.3862	-5.44	0.106	5.9
300	≤0.29	298	4.5680	0.0	0.0	1.4256	0.0	0.0	2.4
400	≤0.50	293 – 323	5.4186	37.8	-2.38	1.4487	-12.7	0.29	3.4
600	≤0.49	293 – 323	6.7086	-1.05	-0.002	1.5693	-9.62	0.068	4.9
900	≤0.21	298	7.3506	0.0	0.0	1.5891	0.0	0.0	3.7
1000	≤0.50	293 – 323	7.6304	2.0	1.03	1.6762	0.385	-0.36	5.7
1500	≤0.45	293 – 323	10.3957	-1.89	1.10	1.7942	-7.76	0.0	7.9
2000	≤0.40	298	11.3580	0.0	0.0	1.9760	0.0	0.0	4.7
3000	≤0.12	298	13.1893	0.0	0.0	2.2100	0.0	0.0	2.7
3350	≤0.34	293 – 323	16.2610	-0.02	1.27	2.2050	1.94	0.039	10.8
4000	≤0.10	298	16.6385	0.0	0.0	2.3424	0.0	0.0	2.6
6000	≤0.25	298	24.3935	0.0	0.0	2.7669	0.0	0.0	7.8
8000	≤0.26	293 – 323	29.8474	-4.56	-4.60	2.9778	-8.34	0.253	4.3
10 000	≤0.24	293 – 323	34.1380	5.36	-10.3	3.2098	3.66	0.0	7.0
12 000	≤0.04	298	41.0170	0.0	0.0	3.2500	0.0	0.0	2.5
15 000	≤0.04	298	45.3602	0.0	0.0	3.4566	0.0	0.0	3.4
20 000	≤0.03	298	48.9736	0.0	0.0	3.6566	0.0	0.0	2.3
35 000	≤0.03	298	70.2625	0.0	0.0	4.0611	0.0	0.0	3.8
global									5.4

[a] Experimental viscosity data from the present work and from the literature (Mei *et al.*, 1995; Kirinčič and Klofutar, 1999).

[b] $$\mathrm{AAD} = \left[\sum_{i=1}^{n}\left(\frac{\left|\nu_{\exp,i} - \nu_{\mathrm{calc},i}\right|}{\nu_{\exp,i}}\right)\right] \times \frac{100}{n}$$

It was observed that H_{ref} and B_{ref} exhibit a dependence on the polymer molecular mass as depicted in Figures 5.1 and 5.2. For this reason, it is interesting to compare H_{ref} values obtained in the present work with the hydration numbers reported in the literature, since there are reports about the variation of hydration numbers with molecular mass of different PEG molecules.

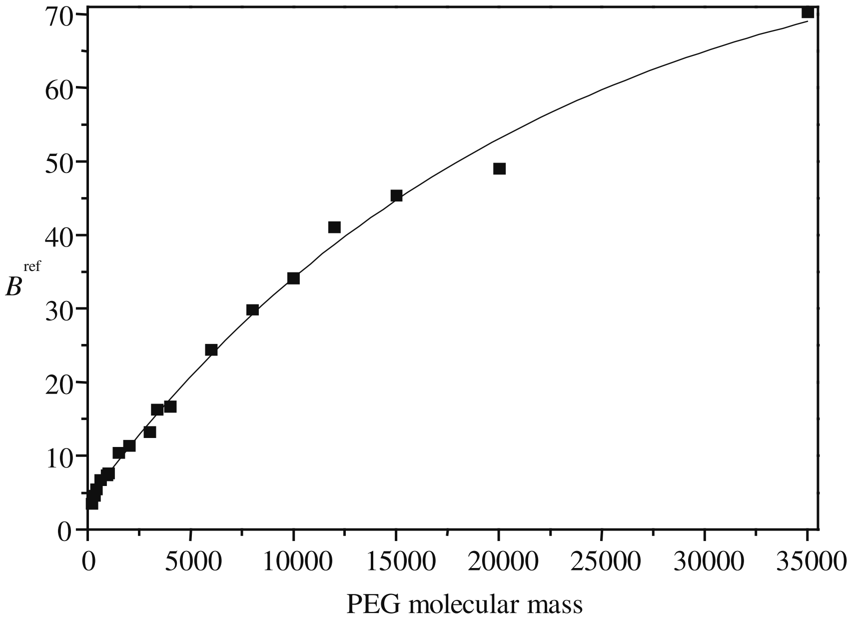

Figure 5.1. B_{ref} values as a function of PEG molecular mass.

The number of water molecules, which are thought to be bounded in the PEG molecules, varies widely according to the experimental measurement techniques, which include conductometry (Bisal *et al.*, 1990), differential scanning calorimetry (DSC) (Antonsen and Hoffman, 1992), I. R. spectrophotometry (Moulik and Gupta, 1989), and viscometry (Kirinčič and Klofutar, 1999). Values between 0.9 and 6 water molecules per monomer have been quoted (Bieze *et al.*, 1994). It is also reported that PEGs of higher molecular masses show increased hydration (Antonsen and Hoffman, 1992).

According to Moulik and Gupta (1989), 4 to 6 water molecules per oxygen for a PEG of molecular mass 20 000 have been obtained, and a minor temperature dependence of hydration has been observed. The same authors obtained hydration numbers (molecules of bound water per monomer unit) of 1.53 for PEG 400 and 1.93 for PEG 600. Bahri and Guveli (1988) have reported that 0.16 to 3.20 water molecules may bind a single oxygen center for PEGs with molecular masses in the range of (200 and 1000) g·mol^{-1}. Hydration numbers obtained from viscometry were presented by Bisal *et al.* (1990) for PEGs 200, 300, 400, 600 and 1000 with values equal to 0.79, 0.95, 1.07, 1.21 and 2.45, respectively. Hydration numbers determined by viscometry are also reported by Kirinčič and Klofutar (1999). The values varied from 2.06 to 28.44 for PEGs with molecular masses between (300 and 35 000) g·mol^{-1}. The explanation given for such high values was that, as the molecular mass increases, the polymer chain begins to fold in on itself, forming segment-segment interactions as it traps additional, more loosely bound water between the segments. A different result was obtained by DSC determinations of bound water (Antonsen and Hoffman, 1992). In the work of Antonsen and Hoffman (1992), the amount of water bound per polymer repeated unit varied from 2.3 to 3.8 for PEG molecular masses between 200 and 2.3 × 10^5 g·mol^{-1}. They also observed that the amount bound at higher molecular masses is greater than at low molecular masses.

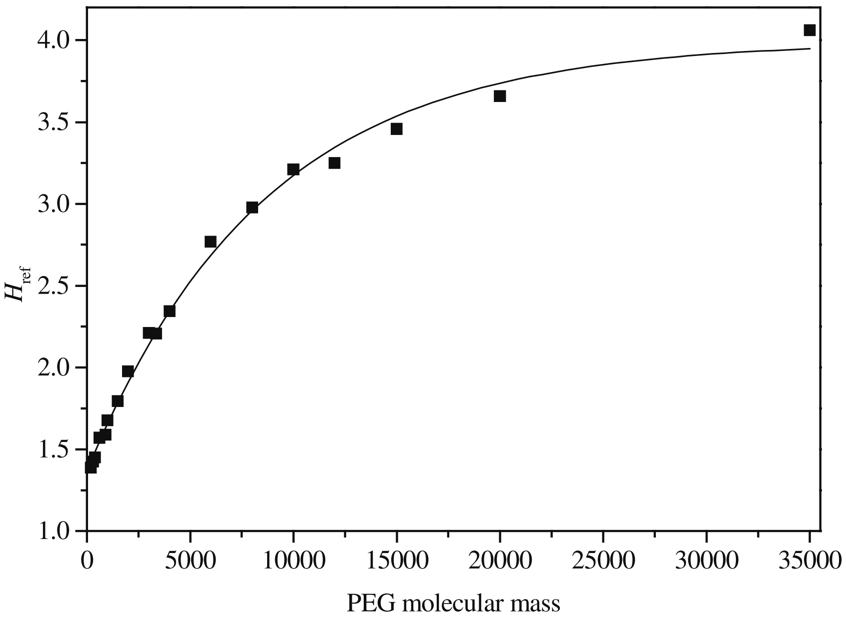

Figure 5.2. H_{ref} values as a function of PEG molecular mass.

Hence, comparing the H_{ref} values from Table 5.6 and the hydration numbers reported in the literature, it seems that in the present work the H_{ref} values might be interpreted as the number of molecules of bound water per oxyethylene unit. In general, based on the figures presented previously, it can be observed that the hydration numbers at 298.15 K (H_{ref}) obtained in this work are in agreement with part of the data reported in the literature. Therefore, the physical meaning of eq 5.2 for calculating viscosities of aqueous PEG solutions becomes more consistent despite some discrepancies, as described above. In any case, the data presented here are closely related to the general conclusion that between one and four water molecules are bound per repeated oxyethylene unit of the polymer, and that hydration numbers rise with the PEG molecular mass.

Considering that the values of B_{ref} and H_{ref} are functions of the polymer molecular masses (as shown in Figures 5.1 and 5.2), such values were regressed to an exponential type equation as given below:

$$Y_{\text{ref}} = C_1 + C_2 \exp(-M_{\text{w}} / C_3) \tag{5.8}$$

where Y_{ref} is B_{ref} or H_{ref}, M_{w} is the molecular mass of the PEG molecule and C_{i}'s are adjusted constants. Correlation coefficients of 0.9974 and 0.9977 were obtained in the regression for estimating B_{ref} and H_{ref} values, respectively. The molecular masses used in this correlation were the values given by the PEG denomination, such as PEG 1000 or PEG 3350. Although Table 5.1 gives the average molecular masses for the PEGs used in the present work, such information is not available for the viscosity data taken from the literature.

Taking B_{ref} and H_{ref} as functions of PEG molecular mass, a generalized correlation could be obtained using eq 5.2 for calculating the viscosities of the systems studied. Substituting eq 5.8 in eqs 5.4 and 5.5, a generalized expression was obtained for the H and B parameters of eq 5.2. The parameters of this generalized equation were estimated employing the entire set of experimental data. Results of the regression are given in Tables 5.7 and 5.8 and Figures 5.3 and 5.4.

Table 5.7. Constants for the generalized equation

H^{a}	B^{a}
$C_1 = 3.99096$	$C_1 = 83.9795$
$C_2 = -2.59861$	$C_2 = -80.2152$
$C_3 = 7891.5$	$C_3 = 22077.1$
$H_1 = 1.08 \times 10^{-3}$	$B_1 = -0.1424$
$H_2 = -0.32 \times 10^{-3}$	$B_2 = 6.32 \times 10^{-3}$

[a] H_{ref} and B_{ref} are calculated by eq 5.8 using the parameters C_{i} given above.

Table 5.8. Results of the generalized correlation for viscosity calculations

PEG	AAD%	PEG	AAD%
200	16.7	3350	7.6
300	4.4	4000	2.9
400	5.6	6000	6.8
600	5.2	8000	5.0
900	2.8	10 000	7.0
1000	6.4	12 000	2.8
1500	6.6	15 000	3.1
2000	3.6	20 000	3.5
3000	3.1	35 000	3.5
global			5.5

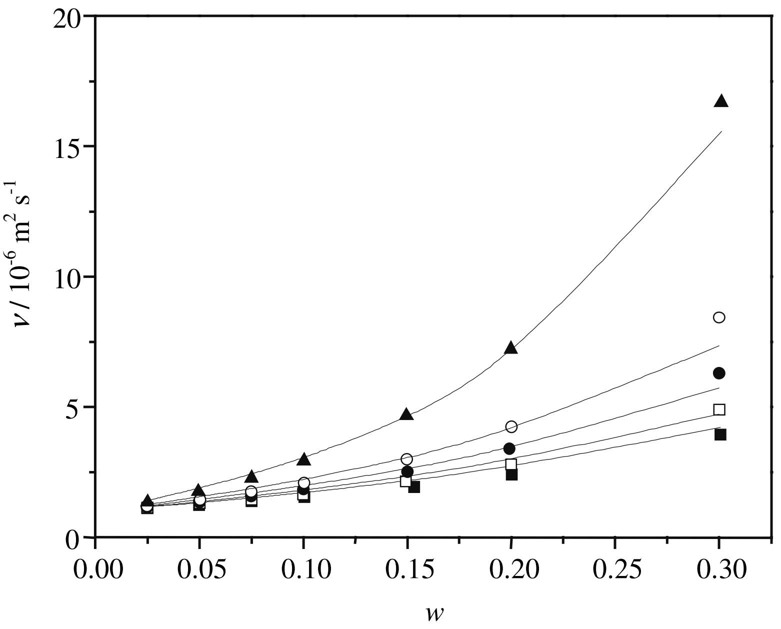

Figure 5.3. Experimental and calculated viscosities at 293.15 K and various concentrations: ■, PEG 400; □, PEG 600; ●, PEG 1000; ○, PEG 1500; ▲, PEG 3350; —, calculated values.

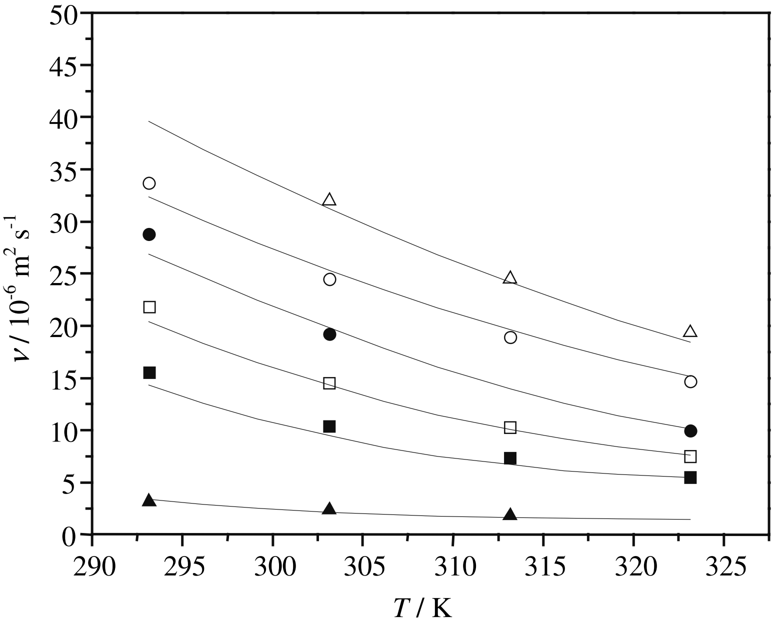

Figure 5.4. Experimental and calculated viscosities at various temperatures and concentrations: ▲, PEG 400, w=0.2487; ■, PEG 600, w=0.4899; □, PEG 1000, w=0.4777; ●, PEG 1500, w=0.4534; ○, PEG 8000, w=0.2554; △, PEG 10 000, w=0.2441.

The AAD-value for the whole set of experimental data was 5.5% (Table 5.8). The systems containing PEG 200 or 3350 are those with the higher deviations between experimental and calculated viscosities. In case of PEG 3350 the main reason for such deviation is probably the expressive difference between the nominal and the average molecular masses (Table 5.1), a difference not so large for the other PEG denominations. In case of PEG 200 the relatively low experimental viscosity values might have contributed for the large deviation observed, but it also seems that such values do not fit so well in the suggested dependence of parameters B_{ref} and H_{ref} on the polymer molecular mass. Some authors suggested that for poly(ethylene glycol)s of low molecular mass, such as PEG 200, only tightly bound water is associated to the polymer chain. For polymers of larger molecular mass the chain begins to fold in itself, trapping additional water between the segments of the polymer chain (Antonsen and Hoffman, 1992; Kirinčič and Klofutar, 1999). This difference observed in the polymer behavior according to its molecular mass can eventually explain the larger deviation obtained for aqueous solutions of PEG 200.

It is also important to contrast the results of the correlation obtained in the present work with those reported in the literature for the viscosity of aqueous PEG systems. González-Tello *et al.*

(1994) reported an AAD-value of 3.5% for dynamic viscosities (η) greater than 10 mPa·s, and 17.5% for viscosities lower than 10 mPa·s. In that work, the equation proposed to calculate viscosities of aqueous PEG solutions takes into account the influences of poly(ethylene glycol) concentration and temperature in the range (277 to 313) K. The same model equation was tested by Günduz (1996) for PEG 8000 and dextran 580 000 in water at 293.15 K, with a resultant AAD of 1.9% and 1.5%, respectively. It must be stressed that in this latter case the results were obtained by adjustment of four parameters for each polymer separately. For a mixture of both polymers (PEG + dextran) in water, a Grunberg equation was used for correlating the viscosities, resulting in an AAD of 6.8% (Günduz, 1996). A subsequent work of the same author (Günduz, 2000) presented AAD-values up to 9.4% for aqueous mixtures of PEG + dextran of different molecular masses. Polymer concentrations up to 7 mass % and temperatures between (303.15 and 343.15) K were considered.

Concluding the above remarks, it can be observed that the results achieved in the present work are in good agreement with the AAD values usually presented in the literature. The advantage of the equation presented here, in comparison with other equations, is that it has a generalized form in relation to PEG molecular mass, concentration of polymer and temperature.

5.4.2 Viscosity prediction in multicomponent systems.

The predictive capacity of eq 5.3 for estimating viscosities of the ternary, quaternary and quinary aqueous PEG systems was investigated. The values of viscosity calculated by eq 5.3 were compared with the experimental data from Table 5.4. An AAD of 9.9% was obtained. It should be observed that the predicted values are in all cases lower than the experimental viscosities. Probably there is an additional effect upon viscosity attributable to the relatively high concentration of polymers with different molecular masses. This effect is not properly described by the parameters adjusted to aqueous binary mixtures containing one polymer. In spite of this, it should be noted that such AAD values obtained in this work are similar to those reported in literature for viscosity prediction of multicomponent mixtures. Cao *et al.* (1993) reported deviations in the range of (2.7 to 5.3)% for viscosity predictions by the GC-UNIMOD model. They used a large data bank, including mostly binary mixtures of alkanes, alcohols, ketones, ethers, and esters. Using the same model Rabelo *et al.* (2000) reported deviations in the range of (0.8 and 14.0)% for some multicomponent fatty mixtures. It is also mentioned in the literature predictions of the GC-UNIMOD model for mixtures of some polyethylene glycol dimethyl ethers and methanol over a wide range of temperatures. The reported average absolute deviations were around 20%. On the other hand, predictions with good accuracy were obtained by Pereira *et al.* (2001) employing the modified Kumar equation for estimating viscosities of multicomponent mixtures. However, only low molecular mass solutes (salts, glycerin, monosaccharides, etc) were employed at relatively low solute concentrations (up to 15 mass %).

In general, the results obtained in this work, either in correlation or in prediction, were satisfactory. Moreover, the obtained generalized equation based on the polymer molecular mass is an useful tool since only few parameters are required for viscosity estimations in systems containing PEGs with molecular masses between 200 and 35 000 g·mol^{-1}.

5.5 Literature Cited

Albertson P. A. *Partition of Cell Particles and Macromolecules*; Wiley: New York, 1971.

Antonsen, K. P.; Hoffman, A.S. In *Poly(ethylene glycol) Chemistry*; Harris, J. M., Ed.; Plenum Press: New York, 1992.

Bahri, H.; Guveli, D.E. Viscosity B Coefficients of Polyethylene Glycols in Water. *Colloid Polym. Sci.* **1988**, 266, 141-144.

Bieze, T.W.N.; Barnes, A.C.; Huige, C.J.M.; Enderby, J.E.; Leyte, J.C. Distribution of Water around Poly(ethylene oxide): A Neutron Diffraction Study. *J. Phys. Chem.* **1994**, 98, 6568-6576.

Bisal, S.; Bhattacharya, P.K.; Moulik, S.P. Conductivity Study of Microemulsions: Evaluation of Hydration of Oil/Water Microemulsions Applying Bruggeman Equation. *J. Phys. Chem.* **1990**, 94, 4212-4216.

Bradoo, S.; Saxena, R. K.; Gupta, R. Partitioning and Resolution of Mixture of Two Lipases from Bacillus stearothermophilus SB-1 in Aqueous Two-Phase System. *Process Biochem.* **1999,** 35, 57-62.

Cao, W.; Knudsen, K.; Fredenslund, A.; Rasmussen, P. Group-Contribution Viscosity Predictions of Liquid Mixtures Using UNIFAC-VLE Parameters. *Ind. Eng. Chem. Res.* **1993**, 32, 2088-2092.

Coimbra, J. S. R.; Thömmes, J.; Meirelles, A. J. A.; Kula, M. R. Performance of Graesser Contactor in the Continuous Extraction of Whey Proteins: Mixing, Mass Transfer and Efficiency. *Biosseparation* **1995**, 5, 259-268.

Cruz, M.S.; Chumpitaz, L.D.A.; Alves, J.G.L.F.; Meirelles, A.J.A. Kinematic Viscosities of Poly(Ethylene Glycols). *J. Chem. Eng. Data* **2000**, 45, 61-63.

Gongxi, Y.; Ziqiang, Z.; Yixin, G.; Zhaoxiong, H. Measurement of Mass Transfer Coefficients and their Modelling of Continuous Countercurrent Aqueous Two-Phase System in a Packed Extraction Column. *Chin. J. Chem. Eng.* **1999**, 7, 196-204.

González-Tello, P.; Camacho, F.; Blázquez, G. Density and Viscosity of Concentrated Aqueous Solutions of Polyethylene Glycol. *J. Chem. Eng. Data* **1994**, 39, 611-614.

Grossmann, C.; Tintinger, R.; Zhu, J. D.; Maurer, G. Partitioning of Low Molecular Combination Peptides in Aqueous Two-Phase Systems of Poly(Ethylene Glycol) and Dextran in the Presence of Small Amounts of K_2HPO_4/KH_2PO_4 Buffer at 293 K: Experimental Results and Predictions. *Biotechnol. Bioeng.* **1998**, 60, 699-711.

Gündüz, U. Evaluation of Viscosities of Polymer-Water Solutions used in Aqueous Two-Phase Systems. *J. Chromatogr. B* **1996**, 680, 263-266.

Günduz, U. Optimization of Bovine Serum Albumin Partition Coefficient in Aqueous Two-Phase Systems. *Bioseparation* **2000**, 9 , 277-281.

Gündüz, U. Viscosity Prediction of Polyethylene Glycol-Dextran-Water Solutions Used in Aqueous Two-Phase Systems. *J. Chromatogr. B* **2000**, 743, 181-185.

Harris, J. M. In *Poly(ethylene glycol) Chemistry*; Harris, J. M., Ed.; Plenum Press: New York, 1992.

Kirinčič, S.; Klofutar, C. A Volumetric Study of Aqueous Solutions of Poly(etheylene glycol)s at 298.15 K. *Fluid Phase Equilib.* **1998**, 149, 233-247.

Kirinčič, S.; Klofutar, C. Viscosity of Aqueous Solutions of Poly(Ethylene Glycol)s at 298.15 K. *Fluid Phase Equilib.* **1999**, 155, 311-325.

Kumar A. A Simple Correlation for Estimating Viscosities of Solutions of Salts in Aqueous, Non-aqueous and Mixed Solvents Applicable to High Concentration, Temperature and Pressure. *Can. J. Chem. Eng.* **1993**, 71, 948-954.

Marquardt, D.W. An Algorithm for Least-Square Estimation of Nonlinear Parameters. *J. Soc. Indust. Appl. Math.* **1963**, 11, 431-441.

Mehrotra, A. K.; Monnery, W. D.; Svrcek, W. Y. A Review of Practical Calculation Methods for the Viscosity of Liquid Hydrocarbons and their Mixtures. *Fluid Phase Equilib.* **1996**, 117, 344-355.

Mei, L.-H.; Lin, D.-Q.; Zhu, Z.-Q.; Han, Z.-X. Densities and Viscosities of Polyethylene Glycol + Salt + Water Systems at 20°C. *J. Chem. Eng. Data* **1995**, 40, 1168-1171.

Moulik, S. P.; Gupta, S. Hydration Studies on Some Polyhydroxy Non-Electrolytes and Non-Ionic Surfactants. *Can. J. Chem.* **1989**, 67, 356-363.

Ninni, L.; Meirelles, A.J.A. Water Activity, pH and Density of Aqueous Amino Acids Solutions. *Biotechnol. Progr.* **2001**, 17, 703-711.

Pereira, G.; Moreira, R.; Vázquez, M. J.; Chenlo, F. Kinematic Viscosity Prediction for Aqueous Solutions with Various Solutes. *Chem. Eng. J.* **2001**, 81, 35-40.

Persson, J.; Johansson, H-O; Tjerneld, F. Purification of Protein and Recycling of Polymers in a New Aqueous Two-Phase System Using Two Thermoseparating Polymers. *J. Chromatogr. A* **1999**, 864, 31-48.

Porto, A. L. F.; Sarubbo, L. A.; Lima, J. L.; Aires-Barros, M. R.; Cabral, J. M. S.; Tambourgi, E. B. Hydrodynamics and Mass Transfer in Aqueous Two-Phase Protein Extraction Using a Continuous Perforated Rotating Disc Contactor. *Bioprocess Eng.* **2000**, 22, 215-218.

Powell, G. M. In *Handbook of Water Soluble Gums and Resins*; Davidson, R. L., Ed.; McGraw-Hill: New York, 1980.

Rabelo, J.; Batista, E.; Cavaleri, F.W.; Meirelles, A.J.A. Viscosity Prediction for Fatty Systems. *J. Am. Oil Chem. Soc.* **2000**, 77, 1255-1261.

Silva, L. H. M.; Meirelles, A. J. A. PEG + Potassium Phosphate + Urea Aqueous Two-Phase Systems: Phase Equilibrium and Protein Partitioning. *J. Chem. Eng. Data* **2001**, 46, 251-255.

Zaslavsky, B. Y. *Aqueous Two-Phase Partitioning*; Marcell Dekker: New York, 1995.

The authors gratefully acknowledge the financial support of FAPESP (Fundação de Amparo à Pesquisa do Estado de São Paulo: 01/10137-6) and CNPq (Conselho Nacional de Desenvolvimento Científico e Tecnológico - 521011/95-7, 466680/00-7, 145941/99).

Capítulo 6

Thermodynamic properties of maltodextrin aqueous solutions

Luciana Ninni[1]*, Antonio J. A. Meirelles*[1]*,* Gerd Maurer[2]

[1]Faculdade de Engenharia de Alimentos – Universidade Estadual de Campinas (UNICAMP)

C.P. 6121 CEP 13083-970 Campinas – SP, Brazil

[2]Lehrstuhl für Technische Thermodynamic, Universität Kaiserlautern, D-67653 Kaiserslautern, Germany.

Trabalho a ser submetido na revista *Carbohydrate Polymers*.

6. Thermodynamic properties of maltodextrin aqueous solutions

6.1 Abstract

The thermodynamic properties of maltodextrins (MD) in aqueous solutions were studied by isopiestic method, laser-light scattering and calorimetry. Three different MD samples with nominal molar masses between 1000 and 3000 g mol^{-1} were investigated at various concentrations. The experimental results of water activity and light scattering were described by the osmotic virial equation. It was found in this procedure that the second and third virial coefficients depend on the molar mass of the different compounds. The VERS model was also used to correlate experimental water activity and calorimetric data for the binary mixtures and to predict water activity of some low molar mass compounds and other thermodynamic properties reported in the literature. Mean relative deviations of 0.40% were obtained in the correlations of water activities of maltodextrin solutions when the maltodextrin molecule was treated as one component, and 0.93% when it was approximated by four components.

6.2 Introduction

Water-soluble polymers have been used in a wide range of industrial products in the food and pharmaceutical areas. This group of compounds comprises molecules from natural (renewable resource raw material) to synthetic (from petrochemical base feed stocks) origin. At the present time, the need for environmental protection favors the use of biodegradable polymers, such as polysaccharides, for industrial purposes (Swift, 1998). Polysaccharides occur with a molar mass distribution, usually represented by the average molar masses: number-average (M_n) or weight average (M_w). Among the polysaccharides, maltodextrins are polymers of great interest due to their high solubility in water (Gliksmann, 1986; Marchal, 1999) and potential application in aqueous -two - phase systems (Silva and Meirelles, 2000a,b). They are starch hydrolysates consisting of α-D-glucose units bounded by (1→4) glycosidic linkages (primarily) as well as by (1→6) linkages. These polymers exhibit broad molar mass distributions (with number-average molar masses varying between ~10^3 and 10^5 gmol^{-1}) due to the process of starch hydrolysis that is carried out with enzymes and/or acids at elevated temperatures. Alpha-amylase, commonly employed in starch hydrolysis is capable of hydrolyze α-1→4 linkages but has little effect on α-1→6 linkages. Moreover, α-amylase does not readily hydrolyze α-1→4 linkages in maltose and maltotriose. Thus, maltose, maltotriose and other low molar mass saccharides can be found in the final hydrolyzates. These characteristics confer them a wide range in solubility, viscosity, and chemical stability (Kasapis *et al*., 1993; Mothé and Rao, 1999).

Thermodynamic properties of polymeric aqueous solutions have been reported in literature (Hasse *et al*., 1995; Kany *et al*., 1999; Groβmann *et al*., 1995; Gaube *et al*., 1993, Silva and Loh, 2000). Thermodynamic data determinations are important under the industry and academic research viewpoints but only few data sets for aqueous maltodextrin solutions can be found in the literature. Among some of the works available, it can be cited Cesàro *et al*. (1999), which studied thermodynamic properties of two biopolymers (maltodextrin and gelatin) by using calorimetry. Heats of dilution of the single polymers and of the mixed polymer solutions were used to evaluate the Flory interaction parameters (Flory, 1953). Radosta *et al*. (1989 a, b, c) presented a comprehensive study about physical-chemical properties of maltodextrins in aqueous solutions. In that work a gelling maltodextrin was experimentally fractionated in 6 different fractions with different average molar masses. It was then investigated the sorption and desorption isotherms and the amount of non freezable water in the fractions. Many works about maltodextrins in the literature deal with experimental investigations of gelling maltodextrins. The gelation of low DE maltodextrins and phase equilibria in gelatin/maltodextrin systems were investigated by Kasapis *et al*. (1993a, b, c, d). Schierbaum *et al*. (1992) also presented a study of the gelation process of maltodextrin-water systems using low resolution H-NMR. They observed the time required for the beginning of gelation as a function of temperature and concentration, and the influence of the addition of amylose on the gelation process.

This paper reports experimental results for aqueous maltodextrin systems involving three different techniques, isopiestic, laser-light-scattering and calorimetric methods, for determining thermodynamic properties. Moreover, the osmotic virial equation is used to describe the experimental results from isopiestic and laser-light-scattering measurements and a semi-empirical group contribution model, the VERS equation, is going to be tested in correlating and predicting the investigated thermodynamical properties for water activity and heats of dilution in maltodextrin and sugar systems.

6.3 Experimental

6.3.1 Materials

Aqueous solutions of three different maltodextrins purchased from Aldrich Chemical and designated here according to their dextrose equivalent range as MD 4 – 7, MD 13 – 17 and MD 16 – 19 were studied in the present work. The polymers were used as received and the water content of each sample was determined by Karl Fischer titration using a Methrom device. The results of titration for the maltodextrins MD 4 – 7, MD 13 – 17 and MD 16 – 19 are, respectively: 3.31±0.20; 4.42±0.22 and 3.31±0.18 mass % of water.

6.3.2 Methods

6.3.2.1 Molar mass distributions

The maltodextrins were characterized by gel permeation chromatography (GPC) with an aqueous eluent containing 0.05 M sodium nitrate. A constant flow rate of 1 $\mathrm{mL \cdot min^{-1}}$ was maintained by a HPLC pump (Spectra Physics, type P 1000). The eluent was degassed in-line (ERMA, type ERC-3512). About 100 μL of the maltodextrin solution was injected in the eluent using a Reodyne valve. A column type MCX 1000 Å (PSS Polymer Systems) was utilized for separation. Detectors were a multiangle laser-light scattering (MALLS, Wyatt Technology, type DAWN DSP) and a interferometric refractometer (Wyatt Technology, type Optilab 903). Details on the calibration of the detectors are described by Hasse *et. al.* (1995).

The results for the number-averaged molar mass (M_n), weight-averaged molar mass (M_w) and polydispersity ratio (M_w/M_n) determined in these GPC experiments are presented in Table 6.1 and the gel permeation profiles of the maltodextrins are shown in Figure 6.1. For each maltodextrin sample, the determination of molar mass distributions were performed at least three times. Mean relative deviations between different determinations varied in the range of 3 and 13%.

Tabela 6.1. Experimental data on the number- and mass-average molar mass of the maltodextrins studied in this work.

	M_n	M_w	M_w/M_n
MD 4 – 7	2683	38360	14.31
MD 13 – 17	1475	13710	8.38
MD 16 – 19	1140	8283	7.31

As can be seen in Table 6.1 and in Figure 6.1, MD 4 – 7 comprises more high molar mass saccharides while the maltodextrins MD 13 – 17 and 16 – 19 have higher content of low molar mass saccharides. This indicates that the MD 4 –7 was less converted to low saccharides in the process of starch hydrolysis. The presence of more higher molar mass components makes MD 4 –7 capable of forming thermally reversible gels in aqueous solutions. Further details on the properties of gelling maltodextrins will appear in the following items.

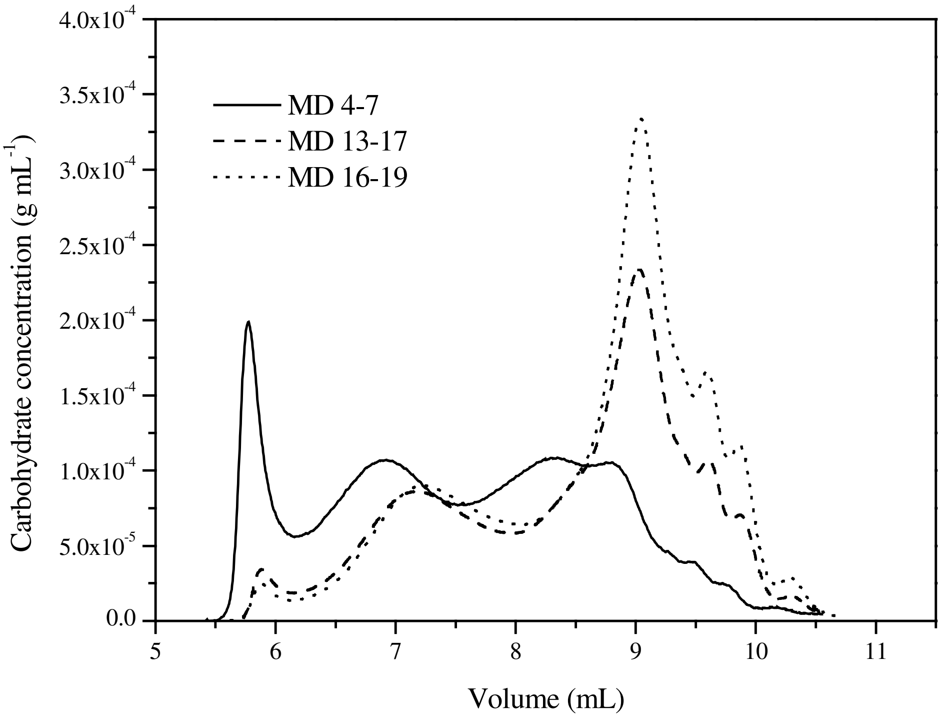

Figure 6.1. Gel permeation profiles of maltodextrins.

After the separation in the GPC columns, the light scattering from each eluted fraction of very low concentration is detected simultaneously at 16 angles between 28.7 and 143.8°. Figure 6.2 presents the experimental data of molar masses *vs.* elution volumes calculated by the software ASTRA, from the extrapolation of the light scattering to zero angle at each slice, according to the following relation:

$$\frac{Kc}{R_\theta} = \frac{1}{MP(\theta)} + 2A_2c \tag{6.1}$$

with

$$K = \frac{4\pi^2 (\mathrm{d}n/\mathrm{d}c)^2 n_0}{N_A \lambda_0^4}$$

$$\frac{1}{P(\theta)} = 1 + \left(\frac{16\pi^2 n_0^2 \sin^2(\theta/2)}{3\lambda^2} \right) \overline{R}_g^2 \qquad (6.2)$$

where K is an optical constant, c the concentration of the polymer solution, $R(\theta)$ the excess Rayleigh ratio at angle θ, M is the weight-average molar mass, $P(\theta)$ a form factor describing the angular and size dependence of the scattered light intensity, $\overline{R}_g^2$ the mean-square radius of gyration, A_2 the second virial coefficient, n_0 the refractive index of the solvent, dn/dc the differential refractive index increment of the polymer in solution (0.1486, 0.1510, 0.1522 $\mathrm{cm}^3\ \mathrm{g}^{-1}$, for MD 4 – 7, 13 –17 and 16 – 19, respectively), λ is the laser wave length (633 nm), N_A the Avogrado number, and λ_0 the wavelength of the incident light under vacuum (Huglin, 1972).

When $c\rightarrow 0$ and $\theta\rightarrow 0$, equation 6.1 becomes:

$$\frac{Kc}{R_\theta}_{c\rightarrow 0, \theta\rightarrow 0} = \frac{1}{M} \qquad (6.3)$$

In Figure 6.2, it is observed a linear dependence of the molar masses on the elution volumes. However, it can be also noted that the scattering of the data is greater in the region of low molar mass molecules. The reason is that the light scattering detector of the MALLS device is less sensitive at low molar masses. The correct slope in the obtained curves is important to calculate molar mass distributions of the polymers as shown below:

$$x(M) = \frac{dW(M)}{d(\log M)} = \frac{dW(M)}{dV} \frac{dV}{d(\log M)} = -\frac{h(V)}{f(V)} \qquad (6.4)$$

where $x(M)$ is the differential molar mass distribution also called $d\xi/d(\log M)$; $W(M)$ is the cumulative molar mass distribution; $f(V)=d(\log M)/dV$ the slope of the curve molar mass (in a logarithmic scale) vs. volume; $h(V)$ is the normalized concentration defined as: $c_i / \sum_{pico} c_i \Delta V$.

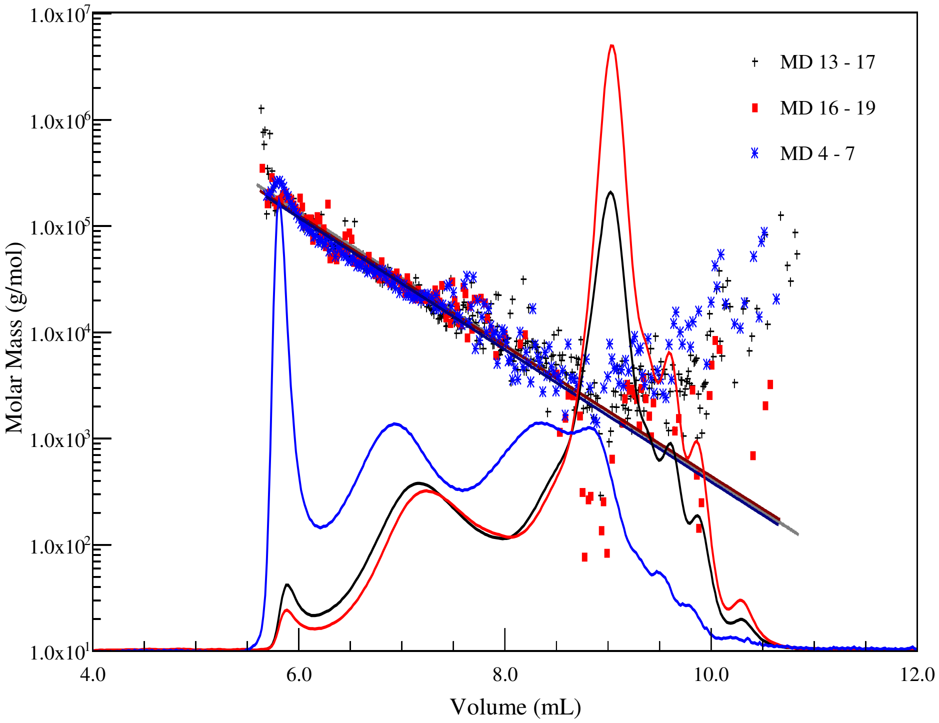

Figure 6.2. Results of the experiment GPC/MALLS for the maltodextrins studied in this work.

In order to verify whether the slope of the adjusted curve was correct, the GPC results for the molar mass distribution of each maltodextrin were approximated by the sum of Gauss-Lorentz functions. The purpose of using this method is to separate the whole distribution in more monodisperse fractions and also to evaluate if the peaks that elute later in the chromatographic runs correspond to the lower molar mass compounds: glucose, maltose and maltotriose. The Gauss-Lorentz (*G-L*) function is given by:

$$GL_i = \frac{a_i}{1 + b_i^2 (M - c_i)^2} exp\left(-d_i^2 (M - c_i)^2\right) \tag{6.5}$$

For each maltodextrin, the parameters a_i, b_i, c_i and d_i (i=1, 2, ..., N; N is the number of G-L_i functions) were fitted to the molar mass distribution. Figure 6.3 presents the adjusted G-L_i functions for MD 4 – 7. Now, for each fraction represented by a G-L_i function, it is known the correspondent elution volumes. Plotting a diagram of molar mass versus volume with data points obtained by laser-light scattering experiments up to volume of about 8 mL and assuming that the adjusted volumes by G-L_i functions for the first three fractions correspond to glucose, maltose and maltotriose, it is possible to verify if the extrapolation of the curve logarithmic of the molar mass vs. volume obtained for the higher molar mass molecules, as shown in Figure 6.2, is consistent and consequently if the slope of the straight line is correct.

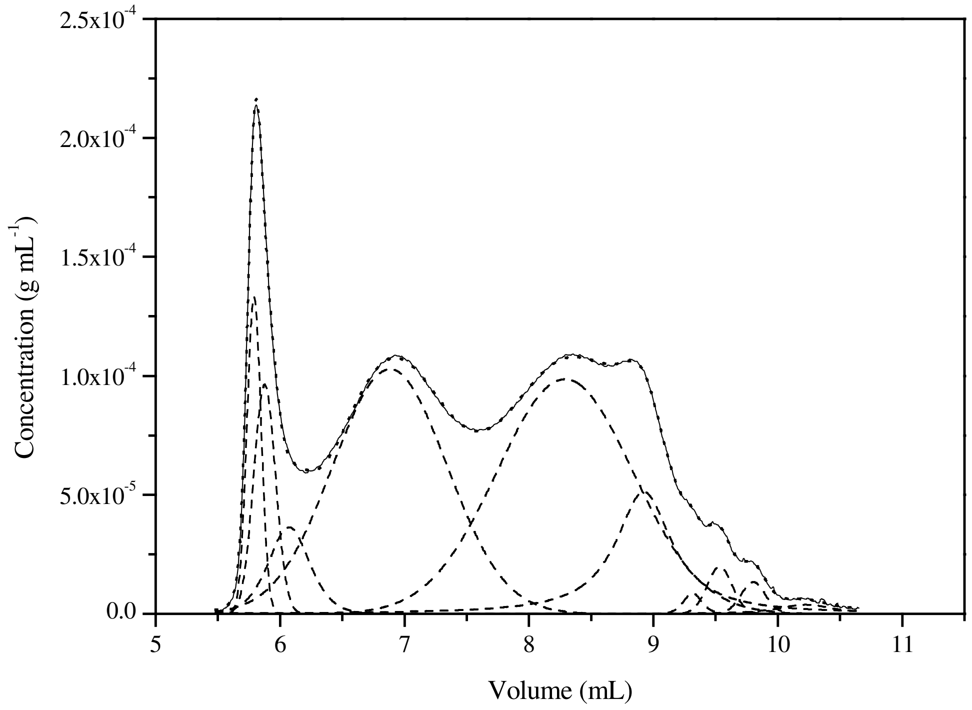

Figure 6.3. Results of Gauss-Lorentz functions for the molar mass distribution of MD 4 – 7.

This extrapolation can be seen in Figure 6.4 indicating that the previous assumption was correct and that the adjusted elution volumes (volumes on the maximal peak point) really correspond to glucose, maltose and maltotriose. The last three points in Figure 6.4 were plotted using the adjusted elution volumes and the respective molar masses for glucose, maltose and maltotriose, that are 180, 342 an 504 g mol^{-1}, respectively. Concentrations of the lower molar mass fractions estimated by the Gauss-Lorentz method were assumed to be glucose, maltose and maltotriose, and they can also be compared to values presented in literature. Values of 1.8 , 4.3 and 8.1 mass % for glucose, maltose and maltotriose, respectively are reported in literature (Defloor, 1998) for a maltodextrin with approximately 1300 g mol^{-1}, and 2.6 , 5.9 and 7.9 were found in this work for MD 16 – 19, which has a molar mass of 1140 g mol^{-1}. Therefore, it can be considered that the results from GPC/MALLS analysis are reliable and they can be used to estimate molar mass distribution of maltodextrins.

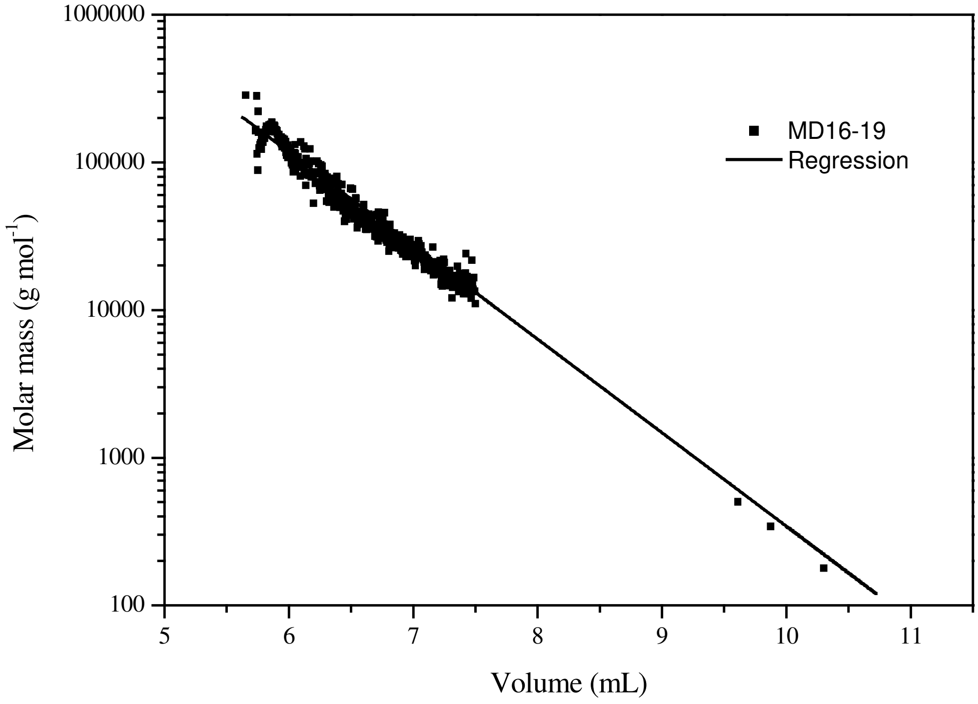

Figure 6.4. Molar mass as a function of elution volume, using the MALLS data and elution volumes for glucose, maltose and maltotriose from the Gauss-Lorenz functions.

6.3.2.2 Isopiestic Method

The water activity in aqueous solutions of maltodextrins was measured with the isopiestic method at 298.15 K for all three maltodextrins, and at 318.15 K for MD 13 –17 and 16 –19. The experimental arrangement consisted of a glass multilegged manifold with nine standard taper female ground-glass joints for the attachment of solution flasks and a high vacuum stopcock for isolation of the system after evacuation. In order to increase the mass transfer area and enhance sample mixing during the equilibration period, the glass was allowed to rotate around an axis inclined at 45°. The system was immersed in a constant temperature water bath during the equilibration times. The temperature of the thermostat fluctuated by less than ±0.1 K. In a experiment, the flasks were filled with about a gram of an aqueous solution of non volatile substance. The nine flasks of the experimental arrangement were used as follows: three flasks were filled with standard NaCl solutions in a concentration named here as NaCl(1), three flasks also with NaCl solutions but in other concentration, NaCl(2), and three for maltodextrin solutions. The two NaCl concentrations (NaCl(1) and NaCl(2)) were chosen in such a way that would be expected these concentrations were above and below the final equilibrium concentration. All the solutions were prepared with bidistilled water. In the glass, mass transfer of water between the sample and the reference solutions took place through the vapor phase, until the activity of water in the sample was the same as that in the reference solutions. The water activity of the samples was estimated from gravimetric analysis of the sample and reference solutions before and after the experiment. The water activity in the aqueous sodium chloride solutions were calculated using the correlation of Pitzer and Peiper (1984). The experimental water activity results for the three maltodextrins at 298.15 K are given in Tables 6.2 – 6.4 together with standard deviations (SD) in concentration of non volatile substance and in water activity. The w_{NaCl} values in the following Tables correspond to the average concentration between NaCl solutions (NaCl(1) and NaCl(2)) at equilibrium. These equilibrium concentrations were always the same within the experimental error. The experimental data points at 318.15 K presented in Table 6.5 were measured also by isopiestic method but with a different experimental arrangement. It consists of a stainless steel apparatus that can hold up to 30 glass cells placed in a copper block that is mounted in a thermostated chamber. In a experiment, the glass cells are filled with about 1 mL of aqueous solution, the chamber is sealed, evacuated and thermostated. The process of mass transfer and the evaluation of water activities are the same as those described above.

The apparatus and experimental procedures used for the isopiestic experiments in this work were described before by Großmann *et al.* (1995), Kany (1998), and Lammertz and Maurer (2002).

Table 6.2. Experimental results for the water activities in aqueous solutions of MD 13 – 17 at 298.15 K

w_{MD}/ g g^{-1}	SD/ g of MD	a_{w}	SD/ a_w units	w_{NaCl}/g g^{-1}	SD/ g of NaCl
0.1750	3.971e-3	0.9962	1.500e-3	0.0073	2.630e-3
0.2234	8.740e-4	0.9948	1.04e-4	0.0091	1.822e-4
0.2419	4.190e-4	0.9942	8.792e-5	0.0102	1.539e-4
0.3029	4.665e-4	0.9917	1.011e-4	0.0145	1.756e-4
0.3408	1.036e-3	0.9898	1.028e-4	0.0178	1.773e-4
0.3796	8.680e-4	0.9875	3.462e-4	0.0217	5.910e-4
0.4286	6.087e-4	0.9838	7.795e-5	0.0280	1.308e-4
0.4408	5.525e-4	0.9829	1.659e-4	0.0294	2.771e-4
0.4872	4.817e-4	0.9779	7.274e-5	0.0377	1.185e-4
0.4867	5.135e-4	0.9781	8.069e-5	0.0373	1.316e-4
0.5307	1.593e-3	0.9724	7.494e-5	0.0465	1.186e-4
0.5671	1.427e-3	0.9664	1.777e-4	0.0559	2.724e-4
0.5898	2.494e-4	0.9622	1.293e-4	0.0622	1.937e-4

Table 6.3. Experimental results for the water activities in aqueous solutions of MD 16 – 19 at 298.15 K

w_{MD}/ g g^{-1}	SD/ g of MD	a_w	SD/ a_w units	w_{NaCl}/g g^{-1}	SD/ g of NaCl
0.2598	2.386e-4	0.9928	1.050e-4	0.0086	1.827e-4
0.2743	9.011e-4	0.9922	1.116e-4	0.0134	1.943e-4
0.3434	5.117e-4	0.9886	7.555e-5	0.0198	1.296e-4
0.3887	1.541e-3	0.9854	1.060e-4	0.0254	1.797e-4
0.3844	1.310e-4	0.9860	1.497e-4	0.0243	2.538e-4
0.4197	7.735e-4	0.9831	4.272e-5	0.0292	7.143e-5
0.4492	1.565e-3	0.9802	5.450e-4	0.0339	8.977e-4
0.4559	1.183e-4	0.9797	4.126e-4	0.0348	6.782e-4
0.4824	7.963e-4	0.9763	2.426e-4	0.0403	3.920e-4
0.5357	6.175e-4	0.9689	1.228e-4	0.0521	1.909e-4
0.5850	1.036e-3	0.9594	2.296e-4	0.0664	3.390e-4

Table 6.4. Experimental results for the water activities in aqueous solutions of MD 4 – 7 at 298.15 K

w_{MD}/g g^{-1}	SD/ g of MD	a_w	SD/ a_w units	w_{NaCl}/g g^{-1}	SD/ g of NaCl
0.2859	1.546e-3	0.9967	4.286e-4	0.0048	7.518e-4
0.2644	1.026e-3	0.9970	2.842e-4	0.0052	4.984e-4
0.2914	1.310e-3	0.9966	1.028e-4	0.0059	1.803e-3
0.3167	9.982e-4	0.9960	1.620e-4	0.0069	2.843e-4
0.3365	1.822e-3	0.9953	1.789e-4	0.0081	3.138e-4
0.3399	2.520e-4	0.9957	2.031e-4	0.0075	3.563e-4
0.3379	9.311e-4	0.9957	2.306e-4	0.0075	4.046e-4
0.3488	1.992e-3	0.9956	1.877e-3	0.0077	3.291e-3
0.3802	2.348e-3	0.9945	9.010e-4	0.0099	1.496e-3
0.4099	1.111e-3	0.9939	1.906e-4	0.0106	3.333e-4
0.4590	1.367e-3	0.9919	2.373e-3	0.0140	4.125e-3
0.4615	1.097e-3	0.9922	1.393e-3	0.0136	2.424e-3

Table 6.5. Experimental results for the water activities in aqueous solutions of MD 13 – 17 and MD 16 –19 at 318.15 K.

w_{MD}/g g^{-1}	SD/ g of MD	a_w	SD/ a_w units	w_{NaCl}/g g^{-1}	SD/ g of NaCl
MD 13 – 17					
0.2767	7.206e-4	0.9927	1.390e-4	0.0128	2.421e-4
0.3284	1.498e-3	0.9903	1.148e-4	0.0169	1.984e-4
0.4452	2.126e-3	0.9821	2.200e-4	0.0308	3.681e-4
0.4968	1.820e-4	0.9767	7.011e-5	0.0396	1.135e-4
MD 16 – 19					
0.2683	2.941e-4	0.9927	1.390e-4	0.0128	2.421e-4
0.3156	2.827e-3	0.9903	1.148e-4	0.0169	1.984e-4
0.4327	1.895e-3	0.9821	2.210e-4	0.0308	3.679e-4
0.4852	4.570e-5	0.9767	7.023e-5	0.0369	1.137e-4

6.3.2.3 Calorimetric investigations

Aqueous solutions of single maltodextrins were mixed with pure water at 313.15K in a batch calorimeter (model MS 80, Setaram, Lyon, France). Specially designed cells were used to enable isothermal and isobaric mixing. In the upper compartment a small cylinder with a piston which separates the solution in the cell from compressed air allowed pressurization at 2 bar. The cells were filled with syringes in such a way that no gas bubbles were present. The cell is separated in two parts (containing the polymer solution in the upper compartment and the pure water in the lower compartment) by a Teflon seal. To start the dilution process, the seal was cut off and the heat upon dilution was determined from the integrated signal of the thermocouple of the calorimeter. To enhance mixing due to high viscosity of the maltodextrin solutions, metal balls and a rotation of the entire calorimeter was performed. To check the accuracy of the experimental data, an electrical heater was immersed in the experimental cell that was filled only with water. A constant current was sent through the resistor by a current source. The heat evolved was estimated from voltage, resistance and the time during which the current was applied. These values were compared with those from the integrated signal of the thermocouple of the calorimeter. Relative mean deviations of 1% were encountered between these two values.

The experimental results are presented in Tables 6.6 and 6.7 for the MD 13 –17 and 16 – 19. Superscripts bottom and top designate the solutions placed in the lower and upper compartment of the cells. Note that the measured heats of dilution are negative, corresponding to an exothermic behaviour upon dilution and that the heat involved in the mixing process is small. Dextran, another polysaccharide, presents the same exothermic behaviour as reported by Großmann *et al.* (1995), who in determined heats of dilution, and Silva and Loh (2000) for heats of solution. It must be stressed that for each experiment, the heat dissipated on cutting off the Teflon seal was determined after the dilution process by once again pushing and pulling the knife. The heat evolved in this procedure was lower than 1 J and its values were taken into account in the experimental values reported in Tables 6.6 and 6.7.

For the maltodextrin MD 4 –7 it was observed two different effects upon dilution: an endothermic in the beginning of the experiment, and another one exothermic about 90 minutes after the cutting off the Teflon seal. In this case, it can be supposed that in the beginning an endotermic effect takes place due to dilution of the polymer solution, that is a mixture of gel and solution, in pure water, and the second, due to the rearrangement of the molecules to build a new gel network. Some authors studied the formation of thermally reversible potato starch maltodextrin gels by H-NMR, viscometry and electronic microscopy (Schierbaum *et al.*, 1984, 1992). The main characteristic of these maltodextrins in aqueous solutions is that the progress of the gelling process is time-dependent and the transition takes place from a homogeneous structureless solution to a two-phase system. The last one consists of the solid aggregation network and the liquid solution of non-structured MD low molar mass components. A rapid increase in the gelling process is encountered at high concentrations and low temperatures. Due to difficulties in analysing the experimental data, because of the errors on pushing the pushing knife of the cells and the mixing itself involving a gel system, it was decided that these systems are deserving of much experimental work that are not to be considered in the present paper. Therefore, the experimental heats of dilution are presented only for the other two maltodextrins that do not form gel. The capacity of gel formation is enabled by the presence of enough long chains in solution, as in the case of MD 4 – 7, which has a significant high molar mass fraction as pointed out in Figure 6.1. According to Schierbaum et al. (1984), products with dextrose equivalent (DE) up to 5 – 8 are able to form thermally reversible gels at concentration above 10 mass %.

Table 6.6. Experimental heats of dilution of maltodextrin 13 – 17 at 313.15 K[a]

m_w^{top}/g	m_w^{bottom}/g	w_{MD}^{top}/g g^{-1}	Q/J
20.480	15.938	0.290	-1.193
19.416	15.857	0.290	-1.234
20.161	15.902	0.300	-1.220
17.911	15.916	0.398	-1.682
18.230	15.855	0.404	-2.051
17.970	15.905	0.398	-1.825
19.618	14.805	0.508	-3.157
20.492	14.976	0.481	-2.805
18.277	14.783	0.548	-3.640
18.335	14.822	0.548	-3.662
17.405	14.979	0.579	-4.490
17.479	15.000	0.579	-4.492
14.686	14.866	0.638	-5.887
14.592	14.772	0.638	-5.464
12.904	14.854	0.694	-6.686
13.173	14.855	0.694	-6.773

[a] w_{MD}^{bottom}/g g^{-1} was zero for all experiments.

Table 6.7. Experimental heats of dilution of maltodextrin 16 – 19 at 313.15 K[a]

m_w^{top}/g	m_w^{bottom}/g	w_{MD}^{top}/g	Q/J
22.939	15.014	0.404	-3.502
22.867	14.953	0.393	-2.616
19.857	14.779	0.501	-4.487
18.863	15.472	0.511	-3.899
18.259	15.057	0.548	-6.432
18.406	15.030	0.543	-6.026
16.432	15.038	0.608	-8.938
16.195	15.039	0.608	-8.478
14.924	14.871	0.649	-10.340
15.312	14.953	0.637	-9.610
12.543	14.801	0.700	-12.210
12.818	15.021	0.700	-12.189

[a] w_{MD}^{bottom}/g g^{-1} was zero for all experiments.

6.3.2.4 Densimetric data

In order to convert polymer mass fractions (w in g g^{-1}) into concentrations (c in g cm^{-3}), the specific densities (ρ^* in g cm^{-3}) of the maltodextrin solutions were determined at 298.15 K. Density measurements were carried out in triplicate using a digital densimeter (DMA 58, Anton Paar) which was calibrated with water and air as standards at the corresponding working temperature. The accuracy of the density measurements was estimated as 3×10^{-5} g cm^{-3}. The experimental results for MD 13 – 17 and MD 16 – 19 are shown in Table 6.8 below.

Table 6.8. Specific density of aqueous MD 13 –17 and MD 16 – 19 solutions at 298.15 K

MD 13 –17		MD 16 –19	
w_{MD}/g g^{-1}	ρ^*/ g cm^{-3}	w_{MD}/g g^{-1}	ρ^*/ g cm^{-3}
0.0499	1.01573	0.0500	1.01591
0.0999	1.03516	0.0995	1.03525
0.1487	1.05472	0.1416	1.05224
0.2004	1.07628	0.1988	1.07614
0.2497	1.09761	0.2506	1.09869
0.2996	1.11995	0.2878	1.11537
0.3512	1.14387	0.3489	1.14380
0.4025	1.16867	0.3980	1.16776
0.4992	1.21786	0.4507	1.19390
0.5491	1.24457	0.4938	1.21650
		0.5392	1.24056
		0.5941	1.27196

No significant difference between the two sets of experimental data of specific density was observed for both maltodextrins at the studied temperature.

6.3.2.5 Laser-light scattering experiments

The multiangle laser-light scattering device utilized for the determinations of the light scattering from maltodextrin solutions was the same as that in the GPC experiments. The difference is that multiple concentrations of the same non-fractionated polymer sample are pumped in the optical cell to find how the scattering intensity varies with concentration. A flow rate of 0.5 cm^3·min^{-1} was employed using a syringe pump (Infors, type Predicor). Filters (Sartorius) with pore size 0.20 μm were used in the line between the syringe and the flow cell to remove dust from the aqueous solutions and avoid great noises in the measurements. The experiments were performed at 298.15 ±0.2 K and at least 6 different concentrations were pumped into the optical cell. The results of the laser-light scattering experiments are presented in Tables 6.9 and 6.10 for the maltodextrins MD 13 –17 and 16 –19, respectively.

Table 6.9. Excess Rayleigh ratios of MD 13 – 17 in water at 298.15 K

100 c_s/g cm^{-3}		0.720	1.438	2.183	3.001	3.617	4.341	5.076	5.805
	θ/°								
$10^5 K\ c_s(R^E_\theta)^{-1}$ mol g^{-1}	28.71	8.117	8.444	8.847	9.268	9.605	10.030	10.340	10.700
		7.909	8.227	8.882	9.177	9.547	9.951	10.160	10.530
	36.2	8.155	8.387	8.860	9.212	9.600	9.959	10.320	10.690
		7.903	8.252	8.878	9.093	9.503	9.918	10.250	10.670
	44.5	8.088	8.375	8.846	9.234	9.597	10.010	10.340	10.710
		7.99	8.294	8.858	9.153	9.529	9.926	10.240	10.590
	54.0	8.038	8.313	8.759	9.141	9.506	9.863	10.230	10.590
		7.976	8.296	8.777	9.055	9.430	9.835	10.180	10.550
	64.9	8.135	8.436	8.890	9.278	9.632	10.020	10.380	10.750
		8.137	8.429	8.909	9.230	9.578	9.983	10.330	10.680
	77.1	8.077	8.354	8.785	9.158	9.511	9.869	10.240	10.610
		8.092	8.396	8.817	9.108	9.464	9.865	10.220	10.610
	90.0	8.313	8.591	9.021	9.416	9.742	10.130	10.500	10.870
		8.355	8.629	9.048	9.381	9.725	10.120	10.480	10.840
	115.1	8.242	8.520	8.922	9.294	9.618	9.991	10.360	10.740
		8.304	8.577	8.951	9.289	9.615	10.000	10.360	10.730
	125.4	8.170	8.445	8.842	9.208	9.535	9.883	10.270	10.640
		8.234	8.534	8.890	9.209	9.537	9.924	10.290	10.680
	135.5	8.220	8.509	8.909	9.281	9.593	9.968	10.330	10.720
		8.336	8.611	8.969	9.298	9.626	10.020	10.360	10.740
	143.8	8.068	8.388	8.793	9.150	9.467	9.826	10.210	10.600
		8.202	8.512	8.896	9.199	9.544	9.939	10.250	10.670

Table 6.10. Excess Rayleigh ratios of MD 16 – 19 in water at 298.15 K

100 c_s/g cm^{-3}		1.408	2.111	2.823	3.530	4.230	4.919	5.644
	θ/°							
$10^5 K c_s (R^E_\theta)^{-1}$ mol g^{-1}	36.2	1.051	1.073	1.124	1.188	1.243	1.295	1.379
		1.043	1.107	1.199	1.214	1.285	1.344	1.382
	44.5	1.061	1.087	1.133	1.191	1.245	1.312	1.359
		1.068	1.102	1.196	1.222	1.279	1.329	1.354
	54.0	1.058	1.083	1.128	1.198	1.244	1.298	1.374
		1.079	1.116	1.200	1.224	1.283	1.342	1.375
	64.9	1.083	1.111	1.153	1.217	1.265	1.332	1.382
		1.116	1.124	1.210	1.244	1.295	1.345	1.375
	77.1	1.079	1.107	1.151	1.217	1.262	1.319	1.387
		1.115	1.135	1.214	1.244	1.297	1.352	1.388
	90.0	1.118	1.149	1.189	1.253	1.298	1.361	1.413
		1.159	1.162	1.243	1.280	1.329	1.379	1.411
	102.9	1.087	1.117	1.158	1.223	1.265	1.321	1.387
		1.131	1.138	1.216	1.251	1.298	1.352	1.389
	115.1	1.118	1.148	1.185	1.249	1.292	1.354	1.403
		1.156	1.155	1.233	1.274	1.317	1.367	1.400
	125.4	1.112	1.14	1.179	1.246	1.288	1.341	1.405
		1.151	1.158	1.233	1.269	1.316	1.368	1.407
	135.5	1.121	1.152	1.188	1.250	1.294	1.354	1.400
		1.160	1.152	1.234	1.273	1.318	1.366	1.400
	143.8	1.108	1.138	1.176	1.242	1.285	1.337	1.401
		1.149	1.148	1.230	1.264	1.315	1.366	1.409

6.4 Modeling

6.4.1 Osmotic virial equation

The thermodynamic data of aqueous maltodextrin and mono-, di- and trisaccharides were correlated by the osmotic virial equation:

$$\ln a_1 = -\frac{c_s}{\rho_1}\left(\frac{1}{M_\mathrm{n}} + A_2^{\mathrm{osm}} c_s + A_3^{\mathrm{osm}} c_s^2 + \ldots\right) \tag{6.6}$$

where a_1 is the water activity, c_s is the concentration of solute in mass/volume, ρ_1 is the molar density of pure water, M_n is the molar mass of the solute and A_2^{osm} and A_3^{osm} are the second and third osmotic virial coefficients of the solute in the solvent, respectively. If the experimental reduced water activity ($-\rho_1 \ln a_1/c_\mathrm{s}$) is plotted over c_s, it is possible to evaluate at $c_\mathrm{s}=0$ the number average molar mass M_n and the second and third virial coefficients. For polydisperse polymer samples the second and third virial coefficients are given by (Kurata, 1982):

$$A_2^{\mathrm{osm}} = \sum_{i=2}^{N}\sum_{j=2}^{N} w_i w_j A_{ij} \tag{6.7}$$

$$A_3^{\mathrm{osm}} = \sum_{i=2}^{N}\sum_{j=2}^{N}\sum_{k=2}^{N} w_i w_j w_k A_{ijk} \tag{6.8}$$

and $$c_s = \sum_{i=2}^{N} c_i$$

where N is the number of components in a polydisperse sample, c_i is the concentration of component i, w_i is the weight fraction of component i, and A_{ij} and A_{ijk} are the second and third mixed virial coefficients.

In a solution of a polydisperse sample it is possible that the virial coefficients are molar mass dependent, and in this case, it is necessary to consider the polydispersity of the sample in the osmotic virial equation. The description of polydispersity can be performed by a molar mass distribution function or by splitting the distribution in more monodiperse components named pseudocomponents. This procedure was employed to polydisperse dextran samples in the work of Kany *et al.* (1999), assuming that the molar mass distributions of these polymers were approximated by 8 pseudocomponents. The results of such evaluation showed that the virial coefficients do not depend on the molar masses of the polymer components. In this case, the molar masses varied between 3000 and 1.5×10^5 g mol^{-1}. The same observation was found by Hasse *et al.* (1995) for the virial coefficients of poly(ethylene glycol)s, that are much more narrowly distributed than dextrans.

As it was seen before, the studied maltodextrins are very polydisperse samples containing components varying from mono-, di- and trisaccharides such as glucose, maltose and maltotriose to oligo- and polysaccharides. The great polydispersity can confer the maltodextrins varied properties in aqueous solutions and this is the objective here: the study of thermodynamic properties of low molar mass saccharides and maltodextrins in diluted (laser-light scattering) and concentrated (isopiestic method) solutions.

Thus, it was assumed that the maltodextrins in this work consist of glucose (G), maltose (M), maltotriose (MT) and a polydisperse fraction (PF) which was splitted in 8 components, as shown in Figure 6.3. The weight fractions and number- and weight average molar masses of these components are given in Table 6.11[a].

Table 6.11. Division of components in the maltodextrin samples

Component	w_i/g g^{-1}	M_n (von GPC)	M_w (von GPC)
MD 13 –17			
Glucose (G)	0.0184	180.1	180.1
Maltose (M)	0.0606	342.2	342.2
Maltotriose (MT)	0.0449	504.4	504.4
Polydisperse fraction (PF)	0.8760	2552.0	1.4098×10^4
MD 16 –19			
Glucose (G)	0.0266	180.1	180.1
Maltose (M)	0.0594	342.2	342.2
Maltotriose (MT)	0.0792	504.4	504.4
Polydisperse fraction (PF)	0.8348	1909.2	9.161×10^3

---

[a] as frações mássicas dos oito componentes da fração polidispersa, bem como suas massas molares são apresentadas na Tabela 6.15 no final deste capítulo.

Equation 6.6 is used in the correlation of water activity data. For the laser-light scattering data the evaluation is based on the following equation:

$$\frac{Kc_s}{R_\theta^E} = -\frac{\rho_1}{RT}\frac{\partial \mu_1}{\partial c_s} \tag{6.9}$$

where the terms on the left side are experimental and are given in Tables 6.9 and 6.10, and the derivative in the right side can be evaluated based on equation 6.6 as follows:

$$\frac{\mu_1}{RT} = \frac{\mu_{1,\mathrm{pure}}}{RT} + \ln a_1 \tag{6.10}$$

$$\frac{Kc_s}{R_\theta^E} = \frac{1}{M_\mathrm{w}} + 2A_2^{\mathrm{LS}} c_s + 3A_3^{\mathrm{LS}} c_s^2 + \ldots \tag{6.11}$$

M_w is the weight averaged molar mass; and A_2^{LS} and A_3^{LS} are second and third virial coefficients, respectively given by (Kurata, 1982):

$$A_2^{\mathrm{LS}} = \frac{1}{M_\mathrm{w}^2}\sum_{i=2}^{N}\sum_{j=2}^{N} w_i w_j M_i M_j A_{ij} \tag{6.12}$$

$$\begin{aligned} A_3^{\mathrm{LS}} = {} & \frac{1}{M_\mathrm{w}^2}\sum_{i=2}^{N}\sum_{j=2}^{N}\sum_{k=2} w_i w_j w_k M_i M_j A_{ijk} - \\ & \frac{4}{3M_\mathrm{w}^3}\sum_{i=2}^{N}\sum_{j=2}^{N}\sum_{k=2}^{N}\sum_{l=2}^{N} w_i w_j w_k w_l M_i M_j M_k M_l (A_{ij}A_{jk} - A_{ik}A_{jl}) \end{aligned} \tag{6.13}$$

The mixed virial coefficients A_{ij} and A_{ijk} in equations 6.7-6.8 and 6.12-6.13 were approximated by geometric mixing rules as given below:

$$A_{ij} = (A_{ii}A_{jj})^{1/2} \tag{6.14}$$

$$A_{ijk} = (A_{iii}A_{jjj}A_{kkk})^{1/3} \tag{6.15}$$

It can be noted from equations 6.7-6.8 and 6.12-6.13 that, for polydisperse polymers, the light-scattering virial coefficients A_2^{LS} and A_3^{LS} differ from osmotic virial coefficients A_2^{osm} and A_2^{osm}, whereas for monodisperse polymers there is no difference between osmotic and light-scattering virial coefficients.

A simultaneous evaluation of laser-light scattering and isopiestic data was performed using a data bank comprising experimental water activity and light scattering data for maltodextrins determined in this work, and experimental water activity data for glucose, maltose and maltotriose at 298.15 K obtained from the literature (Taylor, 1955; Uedaira, 1969; Myiajima, 1983a, b; Cooke, 2002). The assumption that the second and third virial coefficients do not depend on the molar mass of the solute components did not result in a good agreement between experimental and correlated values. Thus it was assumed that the second virial coefficients for glucose (A_{GG}), maltose (A_{MM}), maltotriose (A_{MTMT}) and polydisperse fraction (A_{PFPF}) would be a function of the molar mass of these components and that the third virial coefficient was the same for all components, i.e., $A_{GGG} = A_{MMM} = A_{MTMTMT} = A_{PFPFPF}$. The results of such correlation are given in Figure 6.5 for reduced water activities vs. c_s. Note that in this figure, the results are getting worse at high solute concentrations of the low molar mass compounds and that the model underestimate the reduced water activities of the maltodextrins.

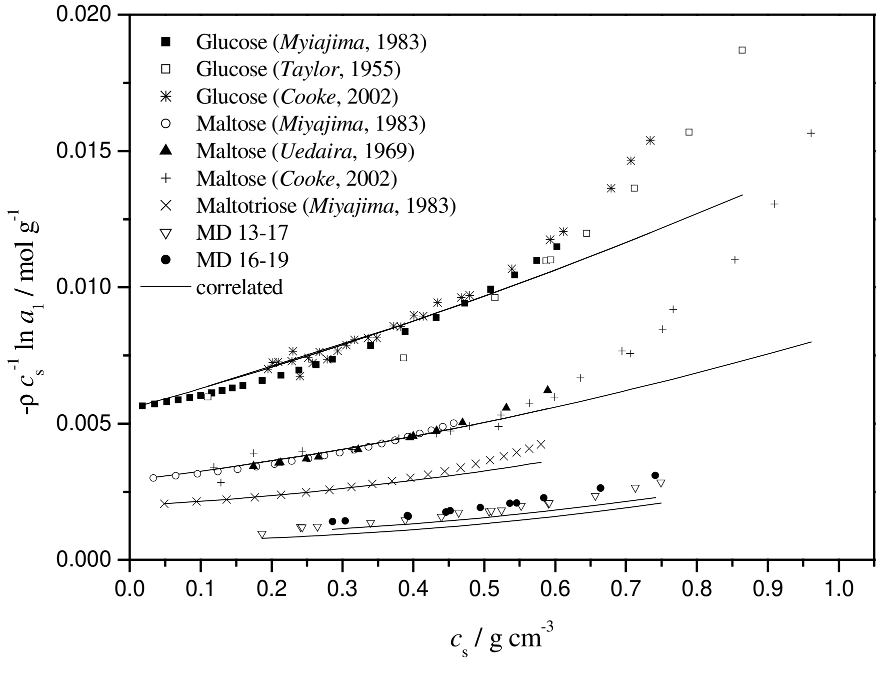

Figure 6.5. Reduced water activity in aqueous solutions of saccharides at 298.15 K.

Another attempt to improve the correlation results was to consider the dependence of the third virial coefficient on the molar mass of the different components ($A_{GGG} \neq A_{MMM} \neq A_{MTMTMT} \neq A_{PFPFPF}$). The obtained results showed that this dependency is clearly verified for the low molar mass saccharides glucose, maltose and maltotriose and that for the defined polydisperse fraction the values assume a constant value, as shown in Figure 6.6 and Table 6.12. It is also noteworthy to observe that the considered dependency leads to better agreement between experimental and correlated values of reduced water activity of the studied systems, as presented in Figure 6.7. To evaluate the light scattering data of maltodextrin systems, which were simultaneously correlated with reduced water activity data, the low molar mass fractions of these polymers corresponding to the components glucose, maltose and maltotriose were not considered in the calculations. This means that both concentration and molar mass of such compounds were discounted from raw data in the calculation of light scattering. This assumption, as it was commented before, is supported by the fact that the signal provided by the device MALLS for low molar mass compounds is almost null. Thus, it is assumed that the Kc_s/R_θ^E data corresponds to the scattering of the higher molar mass molecules. Besides virial coefficients, the weight molar masses (M_w) of the maltodextrins were also simultaneously correlated. The correlation provided values of M_w within the experimental error of the GPC determinations. The results can be seen in Figure 6.8.

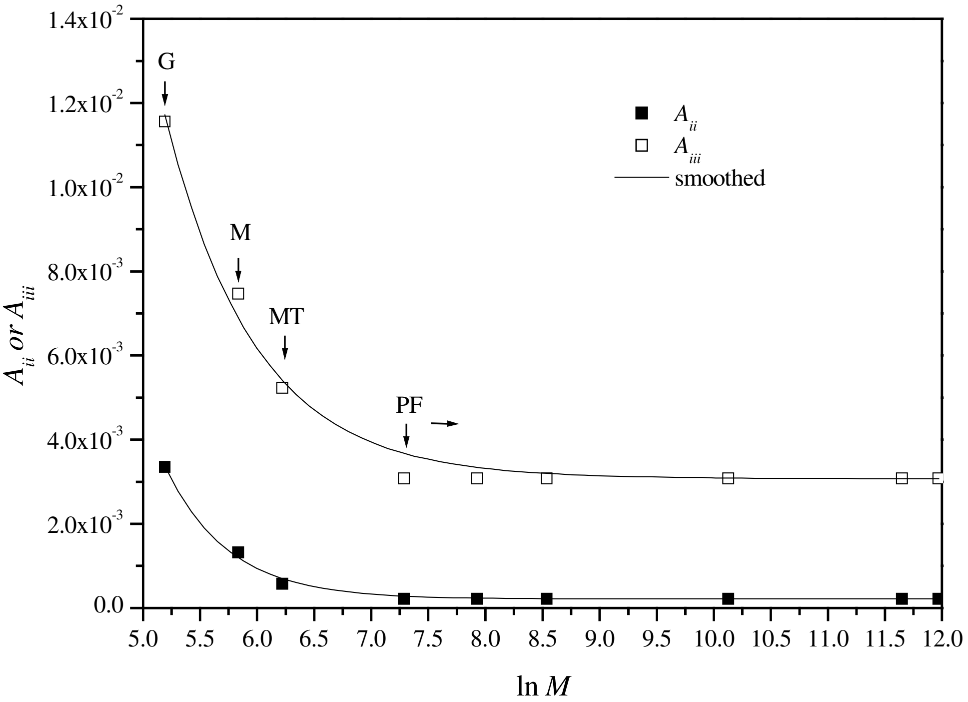

Figure 6.6. Dependence of second and third virial coefficients on the molar mass.

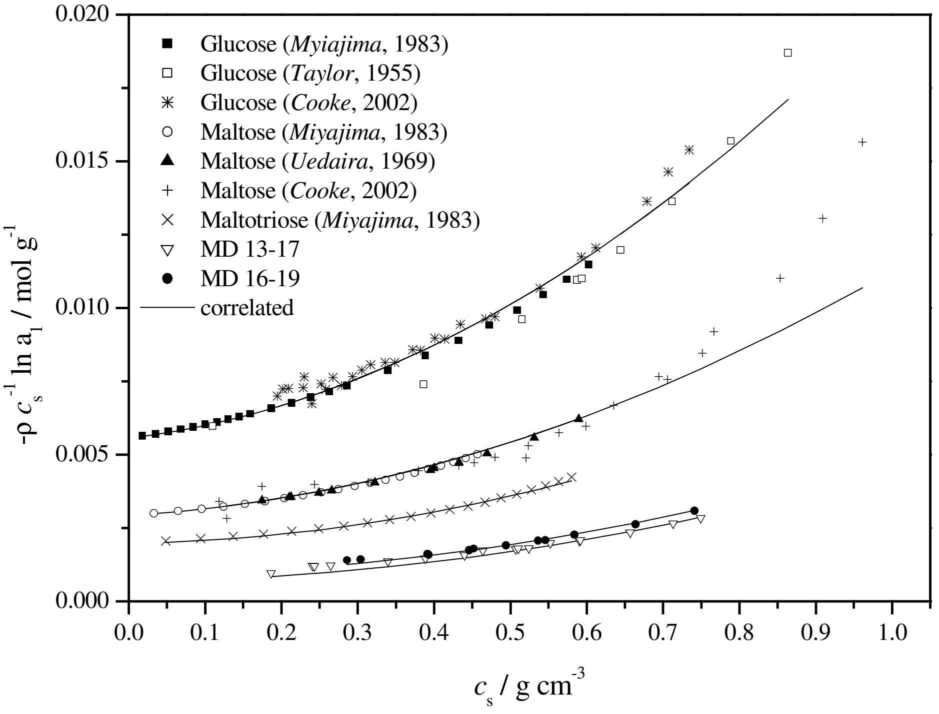

Figure 6.7. Reduced water activity in aqueous solutions of saccharides at 298.15 K.

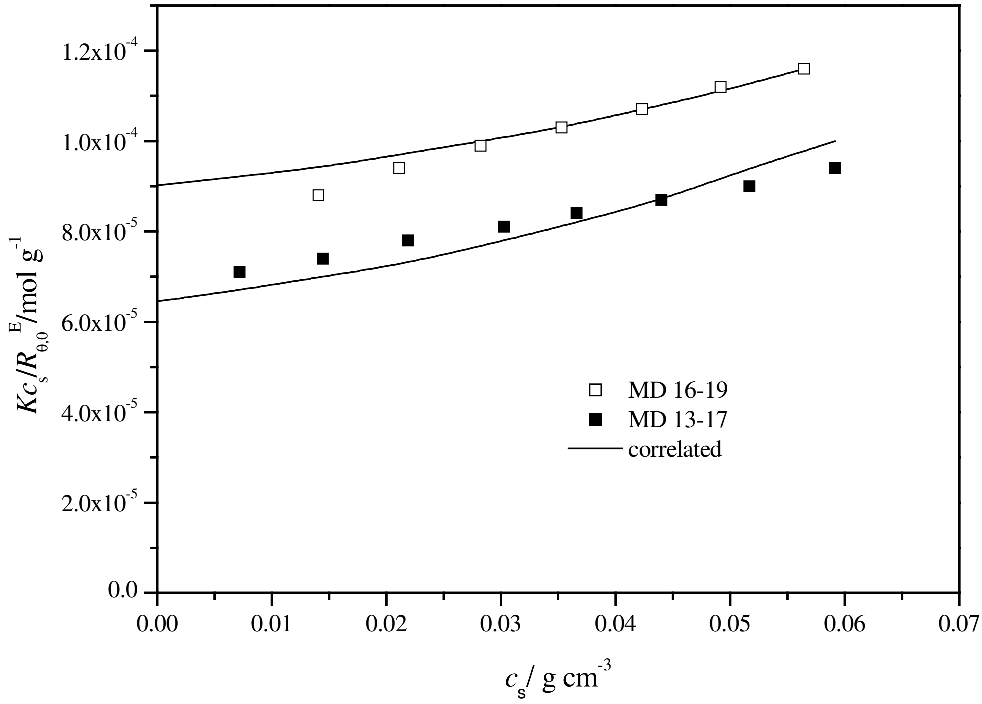

Figure 6.8. Laser-light scattering data of aqueous maltodextrin solutions.

Table 6.12. Second and third virial coefficients of the saccharides and polydisperse fraction studied in this work

$A_{GG} = 0.003353$	$A_{GGG} = 0.011556$
$A_{MM} = 0.001315$	$A_{MMM} = 0.007468$
$A_{MTMT} = 0.000572$	$A_{MTMTMT} = 0.005230$
$A_{PFPF} = 0.000213$	$A_{PFPFPF} = 0.003075$

6.4.2 VERS Model

Another equation used in this work to evaluate experimental data of water activities and enthalpies of dilution of the maltodextrins and low molar mass saccharides is the VERS model.

The VERS model (Virial Equation with Relative Surface Fractions), developed by Grossmann *et al.* (1995) and used successfully to correlate and predict some thermodynamic properties of aqueous PEG and dextran solutions, was used in the modelling of the systems in this work. This equation is based on a semi-empirical group contribution approach for the excess Gibbs energy with a structure similar to Pitzer's virial equation for electrolyte solutions (Pitzer, 1991). The activity coefficients are normalized according to the asymmetric convention: for water the standard state follows Raoul's law and for the other components it follows Henry's law. In this model, the solute concentration is expressed by its surface fraction per 1000 g of water normalized by the surface fraction of water. The equations for the activities of water (a_w) and solute ($a^*_{i,m}$) are given below:

$$\ln a_1 = -\frac{M_1}{1000}\sum_i m_i - \frac{1000}{M_1}\sum_{i\neq 1}\sum_{j\neq 1}\frac{\Theta_i}{\Theta_1}\frac{\Theta_j}{\Theta_1}A_{ij} - 2\left(\frac{1000}{M_1}\right)^2\sum_{i\neq 1}\sum_{j\neq 1}\sum_{k\neq 1}\frac{\Theta_i}{\Theta_1}\frac{\Theta_j}{\Theta_1}\frac{\Theta_k}{\Theta_1}B_{ijk} \quad (6.16)$$

$$\ln a^*_{i,m} = \ln m_i + 2\left(\frac{1000}{M_1}\right)\frac{q_i}{q_1}\sum_{j\neq 1}\frac{\Theta_j}{\Theta_1}A_{ij} + 3\left(\frac{1000}{M_1}\right)^2\frac{q_i}{q_1}\sum_{j\neq 1}\sum_{k\neq 1}\frac{\Theta_j}{\Theta_1}\frac{\Theta_k}{\Theta_1}B_{ijk} \quad (6.17)$$

$$\Theta_i = \frac{m_i q_i}{\sum\limits_{\substack{\text{all components}\\ j}} m_j q_j} \quad (6.18)$$

$$q_i = \sum_{\substack{\text{allcomponents}\\ l}} v_l^{(i)} Q_l \tag{6.19}$$

where, Θ_1 and Θ_i are, respectively, the surface fractions of water and component i, m_i is the molality of component i, Q_l the group l surface parameter, $v_l^{(i)}$ the number of groups l in component i, and q_i the surface parameter of component i. The interaction parameters A_{ij} and B_{ijk} are given by:

$$A_{ij} = \sum_{\substack{\text{all groups}\\ l}} \sum_{\substack{\text{all groups}\\ m}} \Theta_l^{(i)} \Theta_m^{(j)} a_{lm} \tag{6.20}$$

$$B_{ijk} = \sum_{\substack{\text{all groups}\\ l}} \sum_{\substack{\text{all groups}\\ m}} \sum_{\substack{\text{all groups}\\ n}} \Theta_l^{(i)} \Theta_m^{(j)} \Theta_n^{(k)} b_{lmn} \tag{6.21}$$

$$\Theta_l^{(i)} = \nu_l^{(i)} \frac{Q_l}{q_i} \tag{6.22}$$

for the partial molar excess enthalpies of water (h_1^E) and solute i (h_i^E) the equations are:

$$h_1^E = -T^2 \left(\frac{\partial(\mu_i^E / T)}{\partial T} \right)_{p,n_j} \tag{6.23}$$

$$\frac{h_1^E}{RT} = T \left(\frac{1000}{M_1} \right) \sum_{i \neq 1} \sum_{j \neq 1} \frac{\Theta_i}{\Theta_1} \frac{\Theta_j}{\Theta_1} \frac{\partial A_{ij}}{\partial T} \tag{6.24}$$

$$\frac{h_{i \neq 1}^E}{RT} = -2T \left(\frac{1000}{M_1} \right) \frac{q_i}{q_1} \sum_{j \neq 1} \frac{\Theta_j}{\Theta_1} \frac{\partial A_{ij}}{\partial T} \tag{6.25}$$

$$\frac{\partial A_{ij}}{\partial T} = \sum_{\substack{\text{all groups}\\ \text{l}}} \sum_{\substack{\text{all groups}\\ \text{m}}} \Theta_l^{(i)} \Theta_m^{(j)} \left(\beta_{lm}^{(1)} + \frac{\beta_{lm}^{(2)}}{T} \right) \tag{6.26}$$

To account for the influence of temperature on the equilibrium, the following empirical expression was used:

$$a_{lm} = \beta_{lm}^{(0)} + \beta_{lm}^{(1)}(T/\mathrm{K})(1-(T_0/T)) + \beta_{lm}^{(2)} \ln(T/T_0) \tag{6.27}$$

where, a_{lm} is a binary group site interaction parameter and T_0=298.15 K is a reference temperature. All parameters are assumed to be symmetric, i.e. $\beta_{lm}^{(j)} = \beta_{ml}^{(j)}$.

For the assignment of groups, water is treated as a single group and the maltodextrins consist of four structural groups: *n* pyranose rings, *n*-1 osidic bonds (—O—), *n* alkane (CH_2) and (3*n*+2) hydroxyl groups. This division of groups was proposed by Catté *et al.* (1995) to describe carbohydrate molecules. Here, *n* is calculated as: $n = \dfrac{M_n - 18.0152}{162.142}$, where M_n is the number average molar mass of the solute that is subtracted from the molar mass of one molecule of water and divided by the molar mass of one molecule of glucose minus one water. The group surface parameters of the structural groups are estimated by the method of Bondi (1964) and equal to: 1.5620 for the pyranose rings; 0.442 for osidic bonds; 0.540 for CH_2 and 1.200 for hydroxyl groups. The molecules of the maltodextrins studied in the present work were treated in the modelling in two different ways: one, considers the maltodextrin as only one component i.e., the polydispersity is neglected and the low and high molecular mass compounds are considered together in a same fraction (method 1); another one, considers the polydispersity of these polymers assuming that the maltodextrins consist of four different components: glucose, maltose, maltotriose and a polydisperse fraction (method 2). The concentration of the low cited molar mass components were estimated by the Gauss-Lorentz functions as presented in Figure 6.3. The polydisperse fraction is the fourth component called in this work as PF, which concentration and molar mass is estimated from the subtraction of concentrations and molar masses of the low compounds. The concentrations and molar masses used in method 2 were already presented in Table 6.11. Number-average molar masses for method 1 are the same as those presented in Table 6.1.

The estimation of the model parameters presented in equation 6.21 was performed as following: the coefficient $\beta_{lm}^{(0)} = \beta_{\text{pyr-pyr}}^{(0)}$ or $\beta_{\text{pyr-o}}^{(0)}$ or $\beta_{\text{pyr-CH}_2}^{(0)}$ or $\beta_{\text{pyr-OH}}^{(0)}$ were fitted to experimental results for the water activities of saccharides and maltodextrin solutions at 298.15

K; the parameters $\beta_{lm}^{(1)}$ and $\beta_{lm}^{(2)}$ with l or m=pyr, —O—, CH$_2$— and HO— were fitted to the experimental results for the heat of dilution of aqueous maltodextrin solutions in pure water at 313.15 K. These parameters were estimated by minimizing the sum of squares as follows:

$$\mathrm{SSQ} = \sum_{N\mathrm{exp}} (a_w^{\mathrm{exp}} - a_w^{\mathrm{calc}})^2 \tag{6.28}$$

$$\mathrm{SSQ} = \sum_{N\mathrm{exp}} (Q^{\mathrm{exp}} - Q^{\mathrm{calc}})^2 \tag{6.29}$$

The values of the estimated parameters for both methods are given in Table 6.13 below and the results of correlation in Table 6.14.

Figure 6.9 shows the results of correlation obtained for water activity in water – maltodextrin solutions by method 1 as well as the prediction results for the water activities of mono-, di-, and trisaccharides in aqueous solutions reported in literature. The predictive capabilities of the VERS model were also tested using other two kinds of experimental data for glucose and maltose: freezing point depression and boiling point elevation.

A data base including experimental water activities of glucose, maltose, maltotriose and maltodextrins was used in the correlation for the determination of interaction parameters. As can be seen in Figure 6.9, the calculated values are in close agreement with experimental data even at high polymer concentrations. The same occurred to the predictions of other thermodynamic properties for these carbohydrate systems except for very high solute concentrations, where the predictions fail (see Figures 6.10 and 6.11, for method 1). The studied maltodextrins reduce the activity of water by only about 4 % at 60% mass fraction, which is not so much in comparison with glucose that, at the same concentration, reduces the a_w by 16%.

Table 6.13. Interaction parameters of VERS model for both methods

Binary interaction parameters	Method 1	Method 2
$\beta^{(0)}_{pyr-pyr}$	6.53039×10^{-1}	3.0352×10^{-1}
$\beta^{(0)}_{pyr\text{-}O}$	-8.85105×10^{-1}	-3.1716×10^{-1}
$\beta^{(0)}_{pyr\text{-}CH_2}$	8.64279×10^{-1}	2.7212×10^{-1}
$\beta^{(0)}_{pyr\text{-}OH}$	-1.60260×10^{-1}	-6.2193×10^{-2}
$\beta^{(1)}_{pyr\text{-}pyr}$	7.2612×10^{-5}	2.6464×10^{-3}
$\beta^{(1)}_{pyr\text{-}O}$	-1.1812×10^{-4}	-1.8649×10^{-2}
$\beta^{(1)}_{pyr\text{-}CH_2}$	3.5878×10^{-4}	3.2687×10^{-4}
$\beta^{(1)}_{pyr\text{-}OH}$	-5.3399×10^{-5}	-3.6652×10^{-3}
$\beta^{(2)}_{pyr\text{-}pyr}$	9.7974×10^{-4}	9.9689×10^{-2}

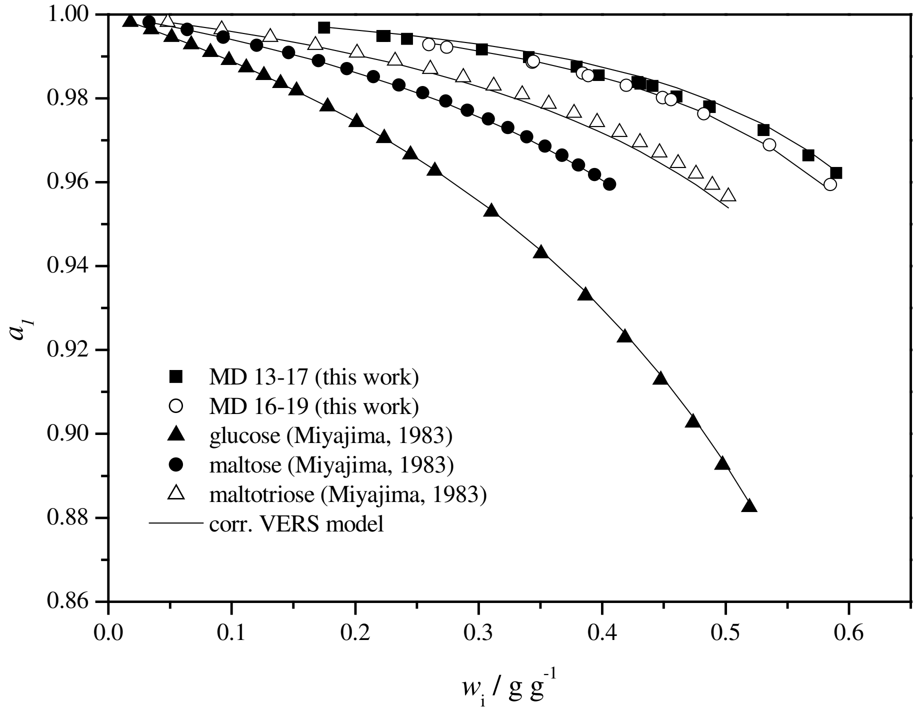

Figure 6.9. Experimental and calculated water activities of water – maltodextrin and some mono- and oligosaccharides at 298.15 K (method 1).

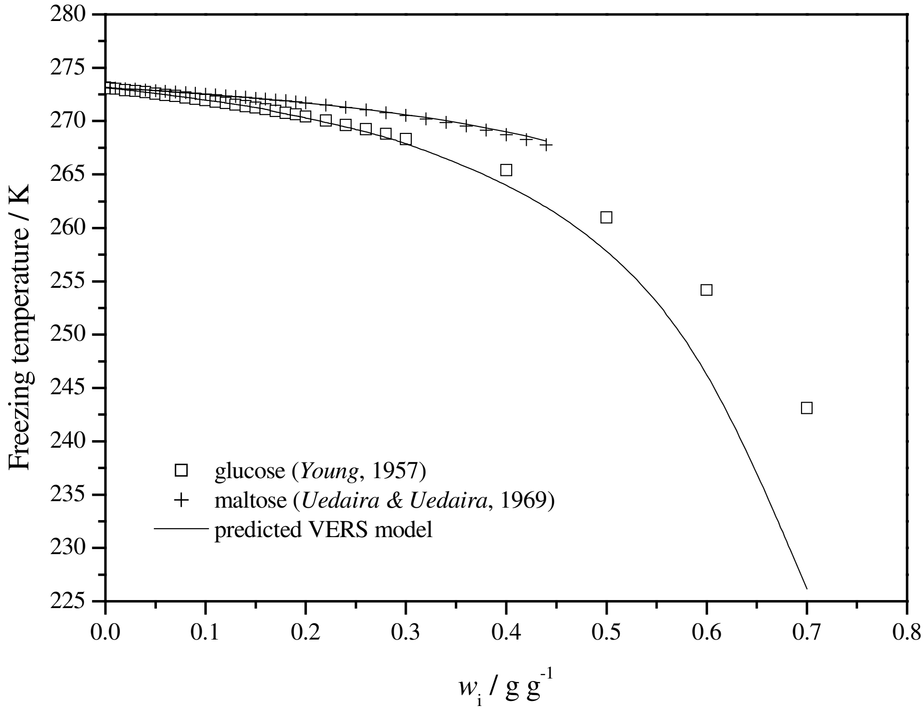

Figure 6.10. Experimental and predicted freezing temperatures for glucose and maltose at various concentrations (method 1).

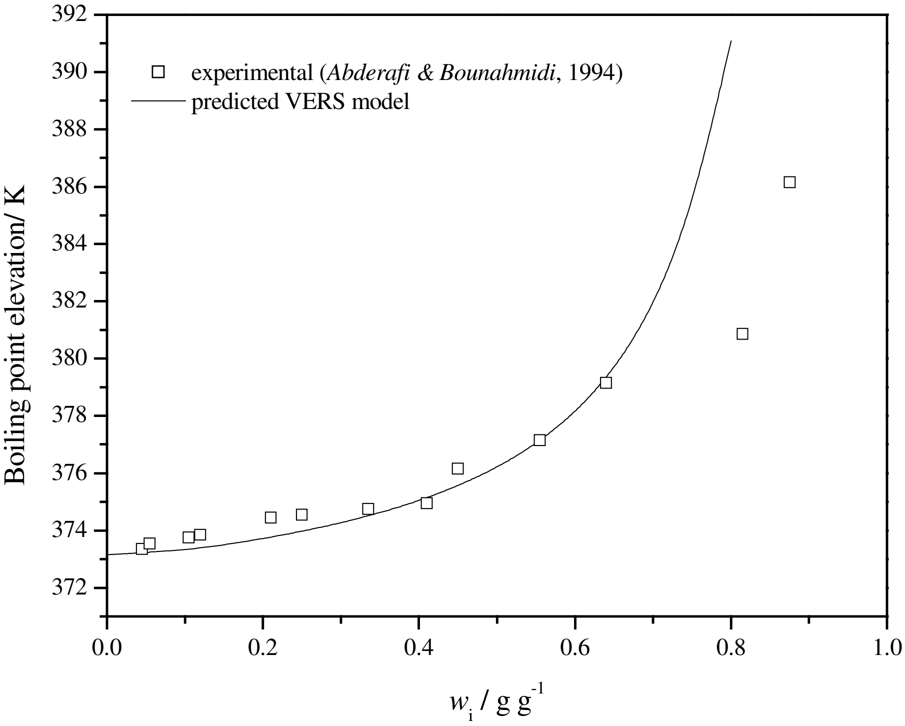

Figure 6.11. Experimental and predicted boiling temperatures for glucose (method 1).

The influence of temperature on the activity of water is almost negligible i.e., the water activity remains nearly unchanged when temperature is increased from 298.15 to 318.15 K. This fact is confirmed by the calorimetric measurements – the heats of dilution for the aqueous maltodextrin solutions are very small – and also by experimental data on water activity at 318.15K. The heat on diluting an aqueous solution of maltodextrin in pure water measured in the present work were also correlated by the VERS model. Figure 6.12 shows the calculated and experimental results for MD 13 – 17 and 16 –19. As can be seen in this figure, the experimental enthalpies of dilution for both maltodextrins have a slightly dependency on the molar mass and the heat effects involved are small. Even so, the model can distinguish between the maltodextrins in calculating the enthalpies involved in the process of dilution. Small values for heats of dilution were also observed in experiments with dextran solutions, as reported by Großmann *et al.* (1995).

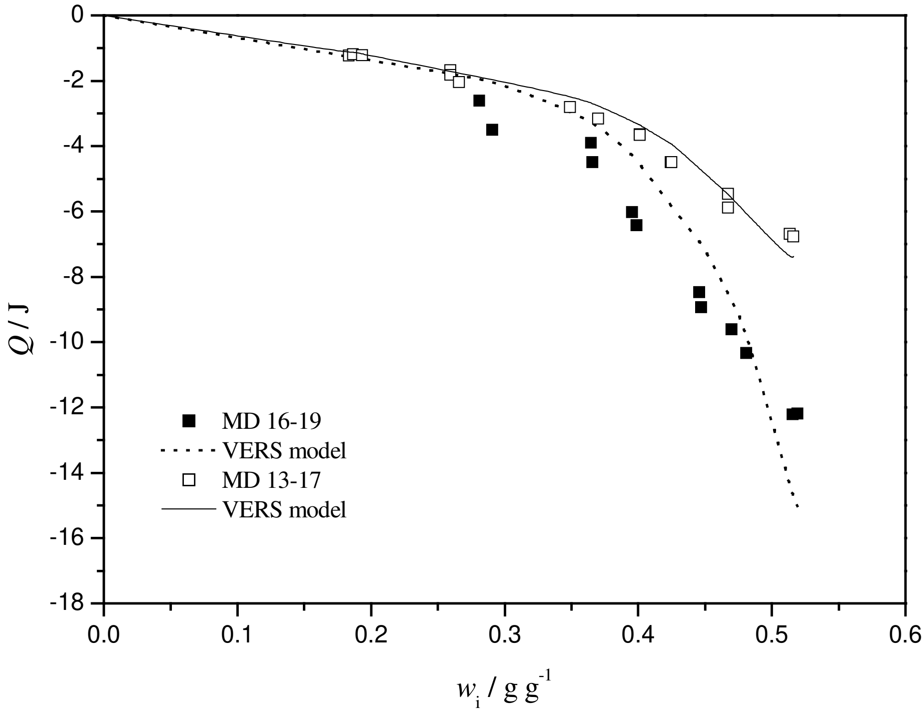

Figure 6.12. Experimental and calculated heat of dilution in aqueous solutions of MD 13–17 and MD 16–19 at 313.15 K. (method 1).

The average absolute deviations (%AAD) between experimental and estimated values for all thermodynamic properties and methods 1 and 2 are presented in Table 6.14.

As can be seen in Table 6.14, the lower global AAD result is provided by method 1, which does not consider the polydispersity of the maltodextrins, but the difference between both methods is not so large. To verify the applicability of the adjusted parameters by both methods to predict water activities of solutions containing high and low molar mass compounds, the experimental data from Radosta *et al.* (1989) for different fractions of a maltodextrin sample was compared with calculated a_w from VERS model. The predictions show that the model was able to distinguish the a_w lowering behaviour even in the systems with very high molar mass components (n=120 indicates a molar mass of approximately 19 500 g mol^{-1}). The calculation of these water activities by VERS model with the parameter adjusted by method 1 is slightly better than that adjusted by method 2. The predictions resulted from method 1 are shown in Figure 6.13. The AAD% for the two attempts are 0.05 and 0.09 % for methods 1 and 2, respectively.

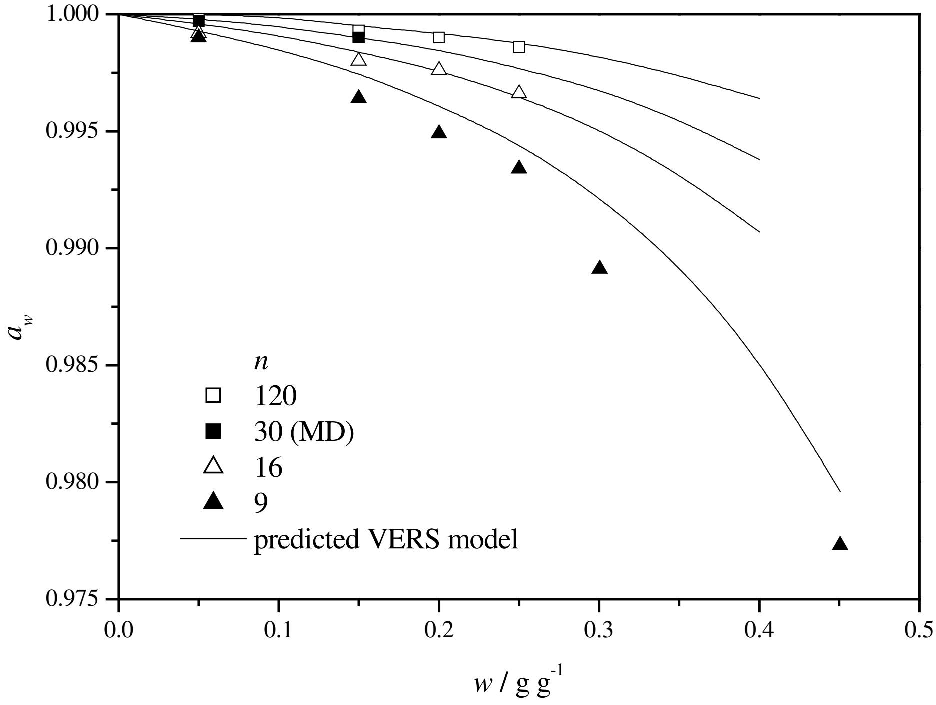

Figure 6.13. Results of the predictions (method 1) for a_w of maltodextrin fractions (n is the polymerisation number). Experimental data from Radosta *et al.* (1989).

Table 6.14. Average relative deviations between experimental and calculated data by VERS model

Saccharide	Conc. Range/ g g^{-1}	Temperature/K	%AAD (method 1)	%AAD (method 2)	References
		Water activity			
glucose	0.0177-0.7478	298.15 – 317.99	0.65	0.80	1, 2, 3, 4
maltose	0.0331-0.8372	298.15 – 317.99	0.63	3.42	1, 3, 5
maltotriose	0.0218-0.6567	298.15 – 317.99	0.14	0.37	1, 3
maltotetraose	0.0904-0.7952	317.99	0.44	2.30	3
maltopentaose	0.1382-0.7750	317.99	1.55	1.72	3
MD 16 – 19	0.2598-0.5850	298.15 – 318.15	0.04	0.09	this work
MD 13 –17	0.1750-0.5898	298.15 – 318.15	0.13	0.13	this work
MD 4 –7	0.2859-0.4615	298.15	0.19	0.61	this work
		Freezing point depression			
glucose	0.005-0.7		0.38	0.55	6
maltose	0.005-0.44		0.02	0.01	7
		Boiling point elevation			
glucose			0.23	0.22	8
global AAD			0.40	0.93	

[1] Miyajima *et al.*, 1983; [2] Taylor, 1955; [3] Cooke, 2002; [4] Velezmoro *et al.*, 2000, [5] Uedaira and Uedaira, 1969; [6] Young, 1957; [7] Weast, 1973; [8] Abderafi and Bounahmidi, 1994.

At the beginning, it was expected that the results for the method 2 would provide better results for calculating the thermodynamic properties. The results show, on the contrary, that method 1 was better to estimate the studied properties. Probably the reason for this behaviour is the low concentration of the low molecular saccharides in the maltodextrin samples possibly the influence of those saccharides on the thermodynamic properties of maltodextrins measured in the present work is small and to consider their influence as an independent factor do not bring any improvement to the correlation of the properties.

6.5 Conclusions

The water activity, light scattering and heats of dilution of aqueous solutions of three different maltodextrins were investigated and evaluated by a osmotic virial equation and a semi-empirical group contribution model. This data covered a wide concentration range from diluted to concentrated solutions. Therefore it was possible to evaluate the virial coefficients in the systems containing molecules varying from saccharides to polysaccharides. It was found that the second and third virial coefficients were molar mass dependent up to maltotriose with (*n*=3) and that they are constant for higher molar mass components. For the VERS model a good agreement between experimental and correlated values of water activities was found for maltodextrins and low molar mass saccharides systems. The model was also able to predict other thermodynamic properties for glucose and maltose such as freezing point depression and boiling point elevation.

6.6 Acknowledgments

The authors gratefully acknowledge the financial support of CNPq (Conselho Nacional de Desenvolvimento Científico e Tecnológico - 290011/01-9 + 46668/00-7 + 521011/95-7) and DAAD (Deutsche Akademische Austauschdienst).

6.7 References

Abderafi, S.; Bounahmidi, T. Measurement and Modeling of Atmospheric Pressure Vapor-Liquid Equilibrium Data for Binary, Ternary and Quaternary Mixtures of Sucrose, Glucose, Fructose and Water Components. *Fluid Phase Equilibria* 93 (**1994**) 337-351.

Bondi, A. Van der Waals volumes and Radii. *J. Phys. Chem.* 68 (**1964**) 441-451.

Catté, M; Dussap, C-G; Gros, J-B. A Physical Chemical UNIFAC Model for Aqueous Solutions of Sugars. *Fluid Phase Equilibria* 105 (**1995**) 1-25.

Cesàro, A.; Cuppo, F.; Fabri, D.; Sussich, F. Thermodynamic Behavior of Mixed Biopolymers in solution and in Gel Phase. *Thermochimica Acta* 328 (**1999**) 143-153.

Cooke, S. A.; Jónsdóttir, S. Ó; Westh, P. A Thermodynamic Study of Glucose and Related Oligomers in Aqueous solution: Vapor Pressures and Enthalpies of Mixing. *J. Chem. Eng. Data* 47 **(2002)** 1185-1192.

Defloor, I.; Vandenreyken, V.; Grobet, P. J.; Delcour, J. A. Fractionation of Maltodextrins by Ethanol. *J. Chromatography* 803 (**1998**) 103-109.

Flory, P. J. *Principles of Polymer Chemistry*, Cornell University Press, Ithaca, **1953**.

Gaube, J., Pfennig, A., Stumpf, M. Vapor-Liquid Equilibrium in Binary and Ternary Aqueous Solutions of Poly(ethylene glycol) and Dextran. *J. Chem. Eng. Data* 38 (**1993**) 163-166.

Glicksman, M. *Food Hydrocolloids* v III, CRC Press Inc., New York, **1986**.

Groβmann, C., Tintinger, R., Zhu, J., Maurer, G. Aqueous Two-Phase Systems of Poly(ethylene glycol) and Dextran – Experimental Results and Modeling of Thermodynamics. *Fluid Phase Equilibria* 106 (**1995**) 111-138.

Hasse, H., Kany, H-P, Tintinger, R., Maurer, G. Osmotic Virial coefficients of Aqueous Poly(ethylene glycol) from Laser-light Scattering and Isopiestic Measurements. *Macromolecules* 28 (**1995**) 3540-3552.

Huglin, M. B. *Light Scattering from Polymer Solutions*. Academic Press, London, **1972**.

Kany, H-P, Hasse, H., Maurer, G. Thermodynamic Properties of Aqueous Dextran Solutions from Laser-light Scattering, Membrane Osmometry, and Isopiestic Measurements. *J. of Chem. Eng. Data* 44 (**1999**) 230-242.

Kany, H-P. *Thermodynamische Eigenschaften Wässriger Polymer-Lösungen*. Ph Thesis, University of Kaiserslautern, Germany, **1998**.

Kasapis, S., Morris, E. R., Norton, I. T., Clark, A. H. Phase Equilibria and Gelation in gelatin/maltodextrin Systems – Part I: Gelation of Individual Components. *Carbohydrate Polymers* 21 (**1993a**) 243-248.

Kasapis, S., Morris, E. R., Norton, I. T., Clark, A. H. Phase Equilibria and Gelation in gelatin/maltodextrin Systems – Part II: Polymer Incompatibility in Solution. *Carbohydrate Polymers* 21 (**1993b**) 249-259.

Kasapis, S., Morris, E. R., Norton, I. T., Clark, A. H. Phase Equilibria and Gelation in gelatin/maltodextrin Systems – Part III: Phase Separation in Mixed Gels. *Carbohydrate Polymers* 21 (**1993c**) 261-268.

Kasapis, S., Morris, E. R., Norton, I. T., Clark, A. H. Phase Equilibria and Gelation in gelatin/maltodextrin Systems – Part IV: Composition-Dependence of Mixed-Gel Moduli. *Carbohydrate Polymers* 21 (**1993d**) 269-276.

Lammertz, S.; Maurer, G. Thermodynamic Properties of Aqueous solutions of Polyelectrolytes and an Inorganic Salt. *ESAT* Congress, Greek, **2002**.

Marchal, L. M.; Beeftink, H. H.; Tramper, J. Towards a Rational Design of Commercial Maltodextrins. *Trends in Food Science & Technology* 10 (**1999**) 345-355.

Miyajima, K., Sawada, M., Nakagaki, M. Studies on Aqueous Solutions of Saccharides. I. Activity Coefficients of Mmonosaccharides in Aqueous Solutions at 25 °C. *Bull. Chem. Soc. Jpn.* 56 (**1983a**) 1620-1623.

Miyajima, K., Sawada, M., Nakagaki, M. Studies on Aqueous Solutions of Saccharides. II. Viscosity B-Coefficients, Apparent Molar Volumes, and Activity Coefficients of D-Glucose, Maltose, and Maltotriose in Aqueous Solutions. *Bull. Chem. Soc. Jpn.* 56 (**1983b**) 1954-1957.

Mothé, C. G., Rao, M. A. Rheological Behavior of Aqueous Dispersions of Cashew Gum and Gum Arabic: Effect of Concentration and Blending. *Food Hydrocolloids* 13 (**1999**) 501-506.

Pitzer, K. S. Activity Coefficients in Electrolyte Solutions. CRC Press, Boca Raton, **1991**.

Pitzer, K. S.; Peiper, C. Thermodynamic Properties of Aqueous sodium Chloride Solutions. *J. Phys. Chem. Ref. Data* 13 (**1984**) 1-102.

Radosta, S.; Schierbaum, F. H. Polymer-water Interaction of Maltodextrins. Part III: Non-Freezable Water in Maltodextrin solutions and Gels. *Starch* 41 **(1990a)** 142-147.

Radosta, S.; Schierbaum, F.; Reuther, F.; Anger, H. Polymer-water Interaction of Maltodextrins. Part I: Water Vapour Sorption and Desorption of Maltodextrin Powders. *Starch* 41 **(1989b)** 395-401.

Radosta, S.; Schierbaum, F.; Yuriev, W. P. Polymer-water Interaction of Maltodextrins. Part II: NMR Study of Bound Water in Liquid Maltodextrin-Water Systems. *Starch* 41 **(1989c)** 428-430.

Schierbaum, F., Kettlitz, B., Radosta, Reuther, F., Richter, M., Vorweg,W. *Acta Alimentaria Polonica* 10 (**1984**) 69-99.

Schierbaum, F., Kettlitz, B., Radosta, S., Reuther, F., Richter, M., Vorweg, W. Zum Stand der Kenntnisse über Struktur-Eigenschaftsbeziehungen von Maltodextrinen. *Acta Alimentaria Polonica* 10 (**1984**) 69-99.

Schierbaum, F., Radosta, S., Vorweg, W., Ynriev, V. P., Brando, E. E., German, M. L. Formation of thermally reversible maltodextrin gels as revealed by low resolution H-NMR. *Carbohydrate Polymers* 18 (**1992**) 155-163.

Silva, L. H. M., Meirelles, A. J. A. Phase Equilibrium and Protein Partitioning in Aqueous Mixtures of Maltodextrin with Polypropylene Glycol. *Carbohydrate Polymers* 46 (**2001**), 267-274.

Silva, L. H. M., Meirelles, A. J. A. Phase equilibrium in polyethylene glycol/maltodextrin aqueous two-phase systems. *Carbohydrate Polymers* 42 (**2000**) 273-278.

Silva, L. H. M.; Loh, W. Calorimetric Investigation of the Formation of Aqueous Two-Phase Systems in Ternary Mixtures of Water, Poly(ethylene oxide) and Electrolytes (or Dextran). *J. Phys. Chem. B* 104 (**2000c**) 10069-10073.

Swift, G. Requirements for Biodegradable Water-Soluble Polymers. *Polymer Degradation and Stability* 59 (**1998**) 19-24.

Taylor, J. B.; Rowlinson, J. S. The Thermodynamic Properties of Aqueous Solutions of Glucose. *Trans. Faraday Soc.* 51 **(1955)** 1183-1192.

Uedaira, H.; Uedaira, H. Miyajima, K., Sawada, M., Nakagaki, M. Activity Coefficients of Aqueous Xylose and Maltose Solutions. *Bull. Chem. Soc. Jpn.* 42 (**1969**) 2137-2140.

Velezmoro, C. E.; Oliveira, A. L.; Cabral, F. A.; Meirelles, A. J. A. Prediction of Water Activity in Sugar Solutions using Models of Group Contribution and Equation of State. *J. Chem. Eng. Jpn.* 33 **(2000)** 645-653.

Weast, R. C. *CRC Handbook of Chemistry and Physics*, 53rd. edn., The Chemical Rubber, Cleveland, **1973**.

Young, F. E. D-Glucose-Water Diagram. *J. Phys. Chem.* 61 **(1957)** 616-619.

Table 6.15. Components of the polydisperse fraction (PF) of maltodextrins MD 13 – 17 and MD 16 – 19.

MD 13 – 17		MD 16 – 19	
w / g g^{-1}	M / g mol^{-1}	w / g g^{-1}	M / g mol^{-1}
0.0539	780.83	0.1400	809.31
0.1146	1239.40	0.1504	1221.18
0.1575	1457.61	0.1190	1632.33
0.1085	2773.14	0.1484	2864.48
0.1146	5107.10	0.0290	6990.53
0.3009	25062.33	0.2304	19197.2
0.1415	114665.5	0.0097	102304.5
0.0120	157650.2	0.0078	141695.5

A. Anexo 1

Neste anexo são apresentados os resultados da correlação dos dados de viscosidade dos sistemas PEG-água pelo modelo GC-UNIMOD. Apresentamos esses resultados adicionalmete, já que o objetivo primeiro deste trabalho é empregar modelos de contribuição de grupos para modelagem e predição de propriedades físico-químicas de sistemas aquosos. Entretanto, como visto no capítulo 5, os dados de viscosidade de sistemas contendo PEG foram tratados por uma equação empírica que não considerou contribuição de grupos, mas tratou da modelagem da hidratação das moléculas desses polímeros de forma a comparar esses resultados com dados experimentais de hidratação de vários métodos reportados na literatura.

Na tentativa de emprego do modelo GC-UNIMOD para correlacionar e predizer dados de viscosidade dos sistemas PEG – água foram utilizados os seguintes procedimentos:

1) (Opção 1) Primeiramente, os valores de parâmetros de interação de grupos das tabelas de equilíbrio líquido-vapor do modelo UNIFAC (Skjold-Jorgensen et al., 1979) foram empregados na predição da viscosidade dos sistemas PEG – água;

2) (Opção 2) Dado que a predição com o procedimento do item 1 não foi suficiente para descrever bem as viscosidades dos sistemas e que parâmetros para sistemas PEG – PEG foram ajustados neste trabalho (vide Capítulo 4), optou-se por empregá-los no cálculo das viscosidades. Os parâmetros restantes entre grupos da molécula de PEG e água foram ajustados empregando uma base de dados experimentais deste trabalho e dados reportados na literatura (Mei *et al.*, 1995; Kirinčič and Klofutar, 1999);

3) (Opção 3) Uma outra tentativa, alternativa àquela apresentada no item 2 acima, foi de ajustar todos os parâmetros envolvidos nos sistemas PEG – água com o propósito de diminuir ainda mais os desvios entre valores de viscosidade experimentais e calculados, já que para altas concentrações e massas molares, a proposta do item 2 não foi satisfatória;

Os resultados das tentativas acima descritas são apresentados no texto, gráficos e tabelas a seguir.

Viscosidade dos polímeros puros

Como visto no Capítulo 4, para a estimativa das viscosidades cinemáticas das misturas aquosas contendo PEGs pelo modelo GC-UNIMOD é necessário o conhecimento da viscosidade dos componentes puros. Para a água esses dados são facilmente obtidos da literatura a várias temperaturas e para os PEGs esses dados foram calculados – para PEGs com massas molares entre 200 e 4000 g mol^{-1} – por uma equação generalizada proposta por Cruz *et al.* (2000) baseada no número de átomos de carbono das moléculas de PEG. Como existem dados de viscosidade para misturas de PEG em água, tanto neste trabalho como na literatura, para polímeros com massas molares maiores que 4000 g mol^{-1} e, considerando que a extrapolação de valores feita pela equação generalizada de Cruz *et al.* não é recomendada pois fornece desvios entre viscosidades calculada e experimental muito altos, resolveu-se então fazer mais algumas medidas de viscosidades para os PEGs 8000 e 10 000 puros entre as temperaturas de 333,15 e 363,15 K (vide Tabela A.1). O mais alto desvio padrão observado experimentalmente foi de 9.833×10^{-7} m^2 s^{-1} e o mais baixo de 1.057×10^{-7}.

Tabela A.1. Viscosidades cinemáticas experimentais dos PEGs 8000 e 10 000

	$\nu/\ 10^6\ m^2\ s^{-1}$	
T/K	PEG 8000	PEG 10 000
333,15	2171,8	4513,2
338,15	1831,2	3903,2
343,15	1536,7	3248,9
348,15	1359,7	3028,2
353,15	1157,4	2667,1
358,15	1013,6	2307,3
363,15	830,17	2053,0

Primeiramente a intenção era usar a mesma equação proposta por Cruz *et al.* (2000) e ajustar novos parâmetros estendendo a faixa de emprego da equação que descreveria também a viscosidade de PEGs puros de mais alta massa molar. Os dados de viscosidade foram correlacionados empregando a seguinte equação:

$$\ln \nu/10^{-6}\mathrm{m}^2\mathrm{s}^{-1} = A + B/(T/\mathrm{K} - C) \qquad \text{(A.1)}$$

em que T é a temperatura absoluta. Os valores dos parâmetros A, B e C foram determinados por regressão e são apresentados na Tabela A.2 juntamente com os desvios relativos médios para cada PEG.

Tabela A.2. Parâmetros da equação A.1

PEG	*A*	*B*	*C*	*N*	%Desvio
200	-3,796	1183	142,3	8	2,62
400	-3,426	1216	142,2	18	2,86
600	-3,232	1254	142,2	28	2,07
1000	-2,320	1178	142,0	44	0,94
1500	-2,198	1240	142,5	68	1,88
3350	-0,650	1167	142,4	152	0,46
8000	1,173	1173	149,8	362	1,58
10 000	2,696	1091	142,3	476	1,45

N= número de átomos de carbono real baseado na massa molar média determinada por GPC.

%Desvio=$\left[\left(\sum_{i=1}^{n}\left(\frac{\left|\nu_{\exp,i}-\nu_{\mathrm{calc},i}\right|}{\nu_{\exp,i}}\right)\right)\right]\times\frac{100}{n}$, em que n é o número de pontos experimentais, $\nu_{\exp,i}$ e $\nu_{\mathrm{calc},i}$ são os valores de viscosidade cinemática experimental e calculado, respectivamente.

Seguindo o trabalho de Cruz *et al.* (2000), elaborou-se uma correlação generalizada baseada no número de átomos de carbonos reais (N) presentes na amostra. Dessa forma, encontrou-se que os parâmetros A e B são dependentes de N da seguinte forma:

$$A=(a_0-a_1)/\{1+\exp[(N-a_2)/a_3]\}+a_1 \qquad \text{(A.2)}$$

$$B=b_0+[b_1\exp(-N/b_2)] \qquad \text{e } C\text{=c0=constante} \qquad \text{(A.3),(A.4)}$$

As constantes das equações A.2 a A.4 foram obtidas por regressão de todos os dados experimentais disponíveis e são apresentadas na Tabela A.3, a seguir.

Tabela A.3. Parâmetros das equações A.2 – A.4

a_0=-186,374	b_0=1121,725
a_1=4,7428	b_1=91,539
a_2=-1149,507	b_2=490,798
a_3=367,940	c_0=138,823

Nessa tentativa não conseguiu-se bom ajuste dos dados de viscosidade experimentais envolvendo PEGs com massas molares entre 200 e 10 000 g mol^{-1}. O desvio relativo médio entre os 57 pontos experimentais e calculados empregados no ajuste foi de 27%, sendo que os maiores desvios foram observados para os PEGs de menor massa molar. Por essa razão, optou-se por trabalhar com duas diferentes equações para o cálculo das viscosidades dos PEGs puros para o emprego na equação do modelo GC-UNIMOD. A correlação de Cruz *et al.* foi utilizada para o cálculo das viscosidades de PEGs puros até massa molar 4000 g mol^{-1} e a correlação apresentada acima (equações A.1 – A.4, e parâmetros da Tabela A.3) foi empregada para PEGs acima de 4000 g mol^{-1} já que forneceu desvios de 4,1 e 1,6% para os PEGs 8000 e 10 000, respectivamente e, uma extrapolação para PEG 6000 e outros de maior massa molar parece ser razoável como visto na Figura A.1 abaixo.

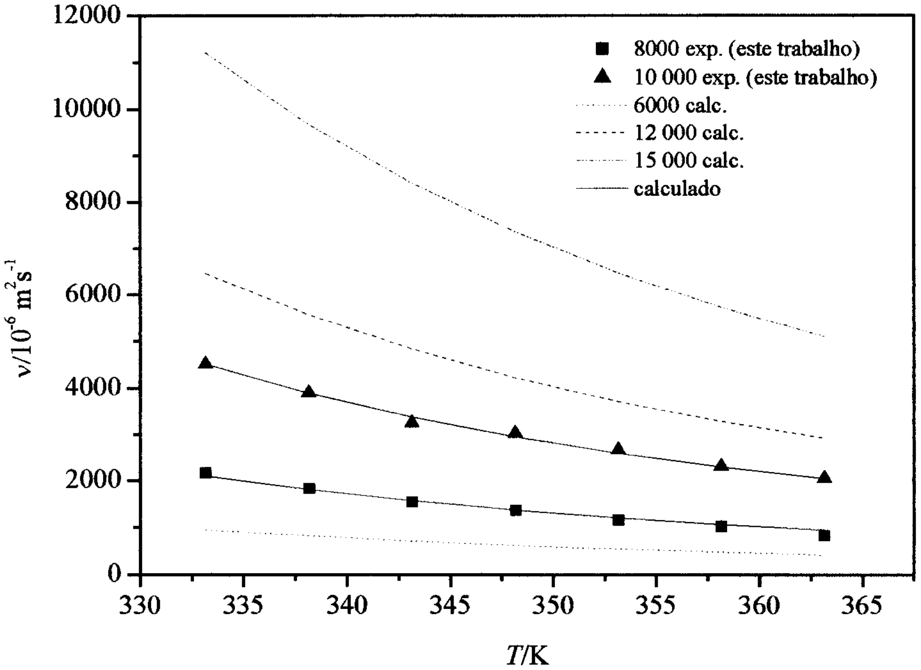

Figura A.1. Viscosidades cinemáticas experimentais e calculadas para os PEGs 8000 e 10 000 e simulação de viscosidades calculadas para PEGs 6000, 12 000 e 15 000.

Na verdade, os PEGs acima de 1000 g mol^{-1} apresentam-se sólidos nas temperaturas nas quais as medidas experimentais das viscosidades desses polímeros em água foram determinadas. Por essa razão, as duas equações citadas acima para o cálculo de viscosidade de PEGs puros serão extrapoladas na temperatura, já que as medidas de viscosidade dos puros foram determinadas apenas em temperaturas maiores que a temperatura de fusão dos PEGs a qual varia com a massa molar dos mesmos.

Modelo GC-UNIMOD

Para as predições e correlações apresentadas neste anexo, as moléculas de PEG foram divididas em três grupos funcionais: CH_2, OH and CH_2O. Os parâmetros de volume e área dos grupos bem como os parâmetros de interação entre grupos para as três diferentes tentativas são apresentados nas Tabelas A.4 – A.7, a seguir.

Tabela A.4. Parâmetros para o modelo UNIMOD

Grupos	Q_k	R_k	v_k^{i*}
CH_2	0,540	0,6744	n+2
OH	1,200	1,000	2
CH_2O	0,780	0,9183	n
H_2O	1,400	0,9200	1

* v_k^i é o número de vezes (n) que um determinado grupo aparece na molécula. n pode ser calculado como: $n = \frac{MM - 62}{44}$, em que MM é a massa molar nominal da molécula de PEG em g mol^{-1}.

Tabela A.5. Parâmetros de interação binários para o modelo UNIMOD (Opção 1)

	CH_2	OH	CH_2O	H_2O
CH_2	-	986,5	251,5	1318,0
OH	156,4	-	28,06	353,5
CH_2O	83,36	237,7	-	-314,7
H_2O	300,0	-229,1	540,5	-

Tabela A.6. Parâmetros de interação binários para o modelo UNIMOD (Opção 2)

	CH_2	OH	CH_2O	H_2O
CH_2	-	273,8	-382,4	320,6
OH	147,2	-	-49,8426	331,9
CH_2O	34,6421	-262,6	-	322,1
H_2O	11,7141	420,5	-271,3	-

Tabela A.7. Parâmetros de interação binários para o modelo UNIMOD (Opção 3)

	CH_2	OH	CH_2O	H_2O
CH_2	-	305,1	-67,1474	318,5
OH	-485,2	-	-171,4	316,7
CH_2O	-34,6427	395,8	-	-52,0670
H_2O	-137,2	322,9	43,1083	-

Resultados com relação à Opção 1: nessa tentativa, apenas a predição com parâmetros da literatura foi averiguada. Como no caso das misturas de PEGs no capítulo A.4, as predições não foram satisfatórias para decrever as viscosidades dos sistemas aquosos contendo PEGs. Em comparação aos resultados do Capítulo A.4, os desvios obtidos na predição foram significativamente maiores e também aumentaram com o aumento da massa molar e concentração dos polímeros na mistura. Para os PEGs de menor massa molar (PEGs 200 a 600) por exemplo, os desvios relativos médios entre as viscosidades calculadas e experimentais foram iguais a 19,7% para 62 pontos.

Resultados semelhantes na predição de viscosidades cinemáticas de sistemas contendo metanol e polietileno glicol dimetil éter (CH_3O – $(CH_2CH_2O)_nCH_3$) foram também observados por Herraiz *et al.* (1999). Esses autores reportam que as predições da viscosidade das misturas pelo modelo GC-UNIMOD tornam-se piores à medida que a massa molar dos polímeros aumenta. A mais alta massa molar testada foi de aproximadamente 250 g mol^{-1} ou n=5. Os desvios relativos médios obtidos pelos autores foi aproximadamente igual a 20% para as misturas estudadas, sendo o sistema metanol etileno glicol dimetil éter uma excessão, para o qual o desvio foi de 10%. Mesmo assim, esses desvios bem como aqueles observados neste trabalho são visivelmente maiores que os desvios reportados por Cao *et al.* (1993) para todo banco de dados que foi utilizado para testar o modelo GC-UNIMOD. Cao *et al.* obteve desvio global de 4,1% para as predições de viscosidades de diferentes tipos de sistemas.

Além disso, outra possível fonte de erros é que as massas molares empregadas no modelo foram os valores nominais dados pela denominação dos PEGs, ou seja, PEG 1000, PEG 3350, etc. Mesmo para as amostras de PEGs deste trabalho que foram analisadas por GPC e portanto possuíam valor real de masssa molar,empregou-se o valor nominal já que para os dados da literatura não havia informações das massas molares reais nos artigos. O trabalho de Cruz *et al.*

(2000) relata desvios absolutos aproximadamente iguais a 6,6% para o caso de massas molares reais não informadas, enquanto que para os polímeros analisados no trabalho daqueles autores o erro foi de 1,22% empregando número de carbono real baseado na massa molar média determinada por GPC.

A extrapolação da viscosidade dos polímeros puros com relação à temperatura também pode ser causa de erro. Como dito anteriormente, os dados empregados no ajuste das equações para o cálculo das viscosidades cinemáticas dos compostos puros foram determinados somente em temperaturas maiores que o ponto de fusão dos mesmos. Assim, uma extrapolação para temperaturas mais baixas (a extrapolação pode chegar a até 70°C) das equações ajustadas pode não representar o caso real. Para os PEGs 200 a 600 os erros devido a extrapolação podem ser descartados já que eles são líquidos à temperaturas mais baixas como a ambiente.

Resultados com relação à Opção 2: O emprego de parâmetros de interação de grupos ajustados a sistemas PEG-PEG (Capítulo 4) apresenta-se como uma alternativa à predição com parâmetros da literatura (item 1) já que os parâmetros possuem mais especificidade. Assim, parâmetros entre os gupos OH, CH_2 e CH_2O foram mantidos iguais àqueles utilizados no capítulo 4 e o restante, entre esses grupos e a água, foram ajustados aos dados experimentais de viscosidades cinemáticas dos sistemas PEG-água (Tabela A.6). Os resultados alcançados nesse procedimento foram, como esperado, melhores que os do item 1. O desvio relativo médio para todo o banco de dados incluindo sistemas com PEGs de massas molares variando de 200 a 35 000 g mol^{-1} foi de aproximadamente 25 %.

Resultados com relação à Opção 3: O ajuste de todos os parâmetros entre grupos do PEG e a água foi uma última alternativa para se obter resultados melhores no cálculo das viscosidades e também para a predição de misturas mais complexas. Os desvios para cada um dos PEGs estudados em soluções aquosas são apresentados na Tabela A.8 abaixo. Como se observa nessa tabela , o desvio global foi ainda menor que no item 2, mas mesmo assim o modelo proposto no capítulo 5, que não considera contribuição de grupos, mas também é generalizado na massa molar dos polímeros e considera hidratação e interação entre moléculas, fornece menores desvios entre viscosidades cinemáticas calculadas e experimentais.

Tabela A.8. Resultados do ajuste de parâmetros de acordo com o item ? para o cálculo de viscosidades de PEGs em solução aquosa

PEG	AAD%	PEG	AAD%
200	15,6	3350	10,9
300	7,0	4000	4,5
400	10,7	6000	7,7
600	19,7	8000	12,1
900	7,7	10 000	9,9
1000	20,9	12 000	4,7
1500	14,2	15 000	1,8
2000	5,4	20 000	11,4
3000	3,7	35 000	1,6
global	11,3		

Nas Figuras A.2 e A.3 estão representados graficamente os resultados referentes à opção 3 do cálculo das viscosidades pelo modelo GC-UNIMOD. A Figura A.3 abaixo mostra a variação, com a concentração, da viscosidade cinemática para vários sistemas PEG-água em que os dados experimentais são reportados por Kirinčič & Klofutar (1999). Como se observa, os valores de viscosidade calculadas pelo modelo GC – UNIMOD são sempre menores que os valores experimentais, e os maiores desvios aparecem para os pontos mais concentrados e com PEGs de maior massa molar. Os resultados, mesmo ajustando todos os parâmetros envolvidos nesses sistemas, não foram satisfatórios. Isso significa que o comportamento da viscosidade dinâmica das misturas estudadas é bastante complicado e o modelo empregado não foi capaz de representá-lo.

Além do ajuste de parâmetros na correlação de dados experimentais e calculados, a predição de viscosidades de misturas contendo mais de um PEG foi também realizada (ver dados experimentais Capítulo 5). Como trata-se de sistemas concentrados ($w \approx 0,2$; 0,3 e 0,4) as predições também não forneceram bons resultados, além dos pontos calculados estarem sempre subestimando as viscosidades dos sistemas. Um exemplo de tais resultados é apresentado na Figura A.4 abaixo.

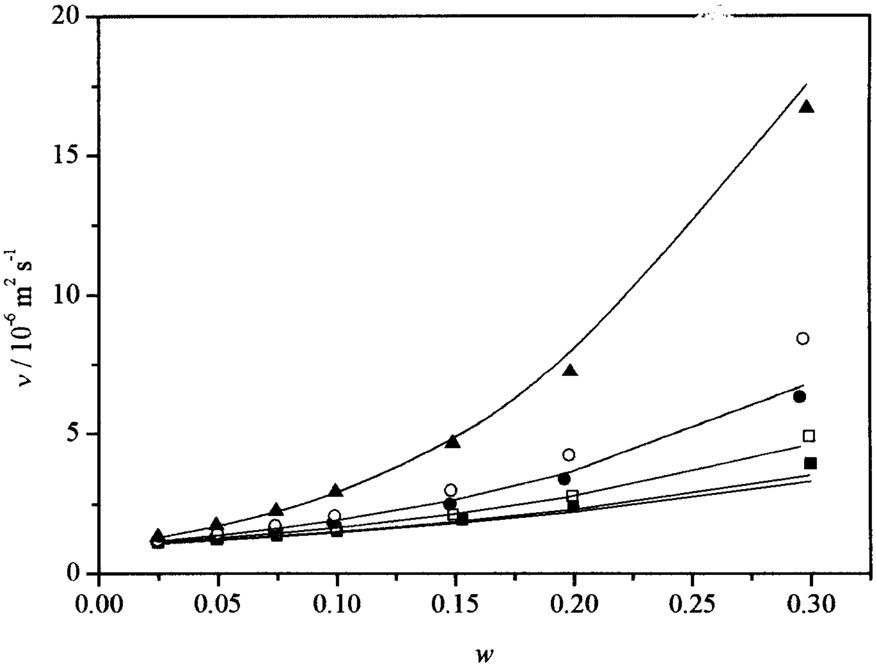

Figure A.2. Viscosidades calculadas e experimentais a 293,15 K e várias concentrações: ■, PEG 400; □, PEG 600; ●, PEG 1000; ○, PEG 1500; ▲, PEG 3350; —, valores calculados.

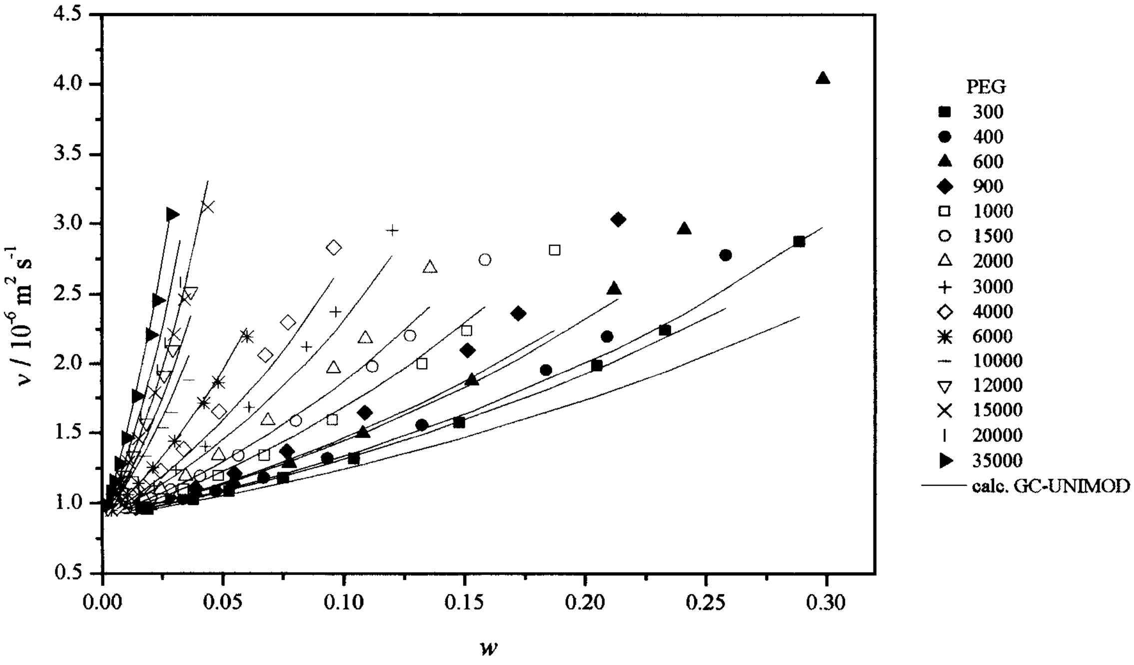

Figura A.3. Viscosidades calculadas pelo modelo GC-UNIMOD e experimentais a 298,15 K e várias concentrações.

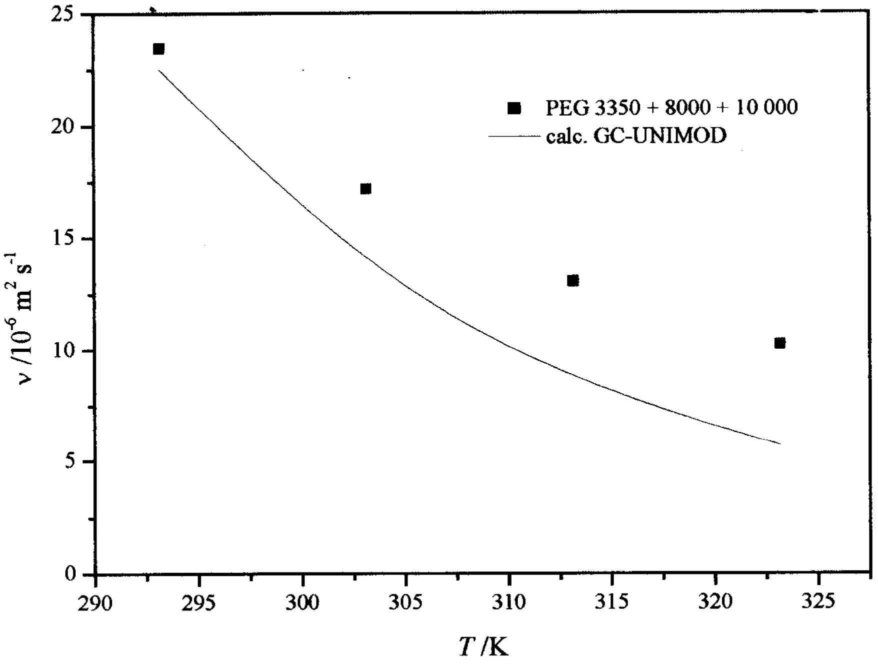

Figura A.4. Predição das viscosidades de uma mistura quaternária.

Referências bibliográficas

Cao, W.; Knudsen, K.; Fredenslund, A.; Rasmussen, P. Group-Contribution Viscosity Predictions of Liquid Mixtures Using UNIFAC-VLE Parameters. *Ind. Eng. Chem. Res.* **1993**, 32, 2088-2092.

Cruz, M. S.; Chumpitaz, L. D. A.; Alves, J. G. L. F.; Meirelles, A. J. A. Kinematic Viscosities of Poly(Ethylene Glycols). *J. Chem. Eng. Data* **2000**, 45, 61-63.

Kirinčič, S.; Klofutar, C. Viscosity of Aqueous Solutions of Poly(Ethylene Glycol)s at 298.15 K. *Fluid Phase Equilib.* **1999**, *155*, 311-325.

Mei, L.-H.; Lin, D.-Q.; Zhu, Z.-Q.; Han, Z.-X. Densities and Viscosities of Polyethylene Glycol + Salt + Water Systems at 20°C. *J. Chem. Eng. Data* **1995**, *40*, 1168-1171.

Skjold-Jorgensen, S.; Kolbe, B.; Gmehling, J.; Rasmussen, P. Vapor-Liquid Equilibria by UNIFAC Group-Contribution. Revision and extension. *Ind. Eng. Chem. Process Des. Dev.* **1979**, 18, 714-722.

Conclusões Gerais

A seguir, são apresentadas conclusões gerais a respeito de cada capítulo apresentado neste trabalho.

1) Soluções aquosas contendo diferentes polióis (D-sorbitol, D-manitol, xylitol, eritritol e glicerol) foram estudadas, como apresentado no capítulo 2, determinando-se suas atividades de água com o emprego de um higrômetro elétrico nas temperaturas entre 10 e 35 °C a várias concentrações. Os dados referentes às determinações de a_w, bem como dados de solubilidades desses compostos em água, foram empregados na predição e correlação com os modelos de contribuição de grupos ASOG e UNIFAC. O emprego dos valores dos parâmetros de interação dos modelos disponíveis na literatura resultou em predições ruins, principalmente a altas concentrações. Por essa razão, optou-se por um reajuste de parâmetros considerando que um grupo hidroxila presente, por exemplo, numa molécula de algum álcool, tem um outro comportamento em comparação aos grupos hidroxilas que estão presentes nas moléculas dos polióis. No polióis, os grupos hidroxilas estão ligados a carbonos consecutivos na molécula, e por isso, pode haver um efeito de proximidade intramolecular. O reajuste, baseado nesse efeito de proximidade, e também realizado com um banco de dados abrangendo altas concentrações dos solutos em solução e diferentes moléculas de polióis (com número de carbonos variando de 3 a 6), forneceu bons resultados nas correlações e também nas predições de a_w em sistemas multicomponentes, depressão do ponto de congelamento e ponto eutético quando o modelo UNIFAC-Larsen foi utilizado.

2) O emprego do método de contribuição de grupos UNIFAC combinado ao termo de Debye-Hückel mostrou-se uma ferramenta útil no cálculo da atividade de água, pH e solubilidade de aminoácidos em soluções aquosas considerando a dissociação parcial desses compostos em água. Como mostrado no Capítulo 3, o modelo forneceu praticamente os mesmos desvios para os pH reais e ideais das soluções de aminoácidos estudadas em três diferentes condições de pH: em tampão ácido, básico e em água. Mas foi também verificado que, apesar da diferença não ser tão significativa para o pH, para as concentrações a diferença entre o caso real e o ideal é mais significativa (como se vê na Figura 7). Nos cálculos de

solubilidade dos aminoácidos em água e em soluções contendo sais ou ácidos, notou-se também que o modelo foi capaz de fornecer melhores resultados em comparação aos resultados calculados no caso ideal. O que reforça essa afimação é que, para os aminoácidos valina e glicina, os valores de Δs e Δh requeridos para o cálculo de solubilidade não foram ajustados neste trabalho e sim retirados da literatura.

3) As viscosidades de misturas de polietileno glicóis foram determinadas e correlacionadas pelo método de contribuição de grupos GC-UNIMOD. O reajuste de parâmetros da literatura mais uma vez foi necessário, a fim de melhorar os resultados do cálculo da viscosidade pelo modelo, assim como a predição em sistemas multicomponentes. Foi observado que, especialmente para misturas binárias que continham polímeros muito diferentes com relação à massa molar, os resultados de predição com valores de parâmetros da literatura eram ruins. Isso poder ser o resultado do ajuste desses parâmetros a um banco de dados que continham moléculas semelhantes entre si. Com o reajuste dos parâmetros de interação foi também melhorada a capacidade preditiva do modelo para o cálculo de viscosidades de sistemas contendo PEGs.

4) O emprego de um banco de dados abragendo soluções aquosas de polietileno glicóis com massas molares entre 200 e 10 000 g mol^{-1} tornou possível ajustar parâmetros de uma equação semi-empírica para a viscosidade de soluções (equação de Kumar) e relacioná-los ao grau de hidratação desses polímeros, comparando-os, dentro do possível, com dados disponíveis na literatura. Os resultados da correlação e das predições são bastante razoáveis, o que sugere o uso dessa equação para a estimativa de viscosidades de soluções aquosas contendo PEGs. Já o modelo de contribuição de grupos GC-UNIMOD não foi capaz de descrever bem os dados experimentais, mesmo quando todos os parâmetros de interação de grupos foram reajustados. Tem-se duas suposições para tal resultado: 1) extrapolação das viscosidades dos componentes puros (PEGs que se apresentam sólidos nas temperaturas de estudo); 2) maior complexidade da viscosidade dinâmica dos sistemas estudados, não corretamente descrita pelo modelo.

5) No estudo de propriedades termodinâmicas de sistemas contendo maltodextrinas foram realizadas determinações experimentais e avaliação e cálculo das propriedades pela equação osmótica virial e o método de contribuição de grupos VERS. A avaliação dos coeficientes

viriais pela equação osmótica (que foram ajustados simultâneamente a dados de atividade de água e espalhamento de luz e, portanto, soluções concentradas e diluídas) mostrou a dependência desses coeficientes com a massa molar de glicose, maltose e maltotriose, atingindo valor constante para moléculas acima de massa molar 504 g mol^{-1}. O modelo VERS, que tem estrutura similar à equação virial de Pitzer para eletrólitos, foi empregado com sucesso no cálculo de atividade de água e outras propriedades em misturas contendo maltodextrinas e açúcares.

Assim, pode-se concluir que os métodos de contribuição de grupos podem ser uma ferramenta útil no cálculo de propriedades físico-químicas em sistemas contendo alguns compostos presentes em produtos alimentícios, como os estudados neste trabalho, assim como de polímeros empregados em separações de biomoléculas. O que deve ser ressaltado é que, muitas vezes, os valores dos parâmetros de interação binários já disponíveis na literatura não são capazes de oferecer uma boa predição de propriedades, e que um reajuste de tais parâmetros torna-se necessário para sistemas contendo moléculas muito diferentes dos compostos orgânicos mais tradicionais ou que apresentem determinadas características na molécula, como por exemplo, as hidroxilas no caso dos polióis.